VIBRATION EFFECTS ON UNDERGROUND CONCRETE STRUCTURES

by

Frederick B. Kuhnow

A thesis submitted to the faculty of
The University of Utah
in partial fulfillment of the requirements for the degree of

Master of Science

Department of Mining Engineering

The University of Utah

May 2013

The University of Utah Graduate School

STATEMENT OF THESIS APPROVAL

The thesis of **Frederick B. Kuhnow**

has been approved by the following supervisory committee members:

Michael G. Nelson	, Chair	**March 27, 2013** Date Approved
Michael K. McCarter	, Member	**March 27, 2013** Date Approved
Chris P. Pantelides	, Member	**March 27, 2013** Date Approved

and by **Michael G. Nelson** , Chair of

the Department of **Mining Engineering**

and by Donna M. White, Interim Dean of The Graduate School.

ABSTRACT

When performing blasting operations in open pit settings, energy is released and transmitted through the geological structure. Some negative effects can significantly impact mining operations and can adversely affect mine production. This thesis presents recommendations for blast design to prevent damage on adjacent concrete structures of underground operations due to ground motion resulting from blasting. The work includes a summary covering currently accepted views of blasting vibration measurements, human response to blasting, and criteria for wall damage control as background information. This is followed by sections on vibration level estimation and blasting techniques to control vibration, a section on structural dynamics of reinforced concrete structures subject to ground motion, and a case study describing a problem regarding an open pit mine expansion and whether production blasting will damage the concrete shaft structure due to blast-induced ground motion.

Based on the results, a set of criteria is provided to implement in current and future surface mining operations that involve blasting near underground concrete structures. A set of techniques on how to improve vibration levels for safe operations is presented. Knowledge of particle velocity and wave propagation for site-specific circumstances to determine a safe level of vibration is recommended. A set of criteria to implement a monitoring plan to prevent structural damage of underground concrete structures near surface mining operations is provided. Emphasis is placed in making use of electronic detonators and early delay detonators to achieve successful levels of vibration. A dynamic analysis is necessary to determine if vibration from blasting can damage the concrete shaft structure. Determining the vibration frequency is key to analyzing the response of the structure, not only to static loading but also dynamic loading.

Dedicated to my wonderful mother, whose support has made all my achievements possible.

TABLE OF CONTENTS

LIST OF FIGURES

Figure Page

LIST OF TABLES

Table Page

1. INTRODUCTION

When performing blasting operations in an open pit setting, energy is released and transmitted through the structural geology. Some of the effects can significantly impact mining operations and can adversely affect mine production. When expanding the limits of a surface operation, generally there are no geometric constraints as long as the slope design, operability, and ore to waste ratios allow a safe and economically feasible operation. However, some mining operations have a surface and underground operation adjacent to each other and the combined effect of expansion and proximity of the two operations can be impacted by one another.

This thesis will focus on a set of safety considerations to prevent underground concrete structures and highwall damage from blasting through techniques that can help improve vibration levels. Knowledge of particle velocity propagation for site-specific circumstances is presented to determine safe levels of vibration. Five wall control methods to prevent slope damage from blasting are presented and finally, a set of criteria to prevent damage of concrete structures due to blast loading is presented. Emphasis will be placed in making use of electronic detonators and early delay detonators to achieve successful levels of vibration.

Accepted industry guidelines to evaluate existing conditions and current blasting practices such as vibration characterization, wall damage control, pattern design, and charge weight/delay timing in an open pit mine operation is also presented. However, the response of concrete structures to blast-induced ground motion and the interaction of structure-rock are complicated. Therefore, several factors must be considered in order to achieve reasonable conclusions.

1.1 Objectives

The objectives of this work are:

- Analyzing effects of vibration on concrete underground structures from production blasting on a surface mine expansion (push back) and determining whether the vibration created by this blasting will have adverse effects on such structures.
- Predicting and preventing damage to slopes and highwalls due to vibration from blasting.
- Providing design specifications used in the civil engineering industry on concrete structures subject to earthquake-induced ground motion.
- Providing a set of recommendations to predict slope damage.
- Providing a set of criteria to predict and prevent concrete failure from high strain loading (blast).

1.2 Scope

This work will consist of the analysis of vibrations from blasting by using a case study on a surface mine operation that will undergo an expansion (push back). This push back will situate the proposed new crest at a distance of approximately 50 m (150 ft) from an existing concrete ventilation shaft. The analysis will involve recording, measuring, and analyzing blasting data generated by both a production blast and a signature blast (single-charge test blast detonated within the project or area of concern). Furthermore, this thesis will present industry required design specifications presented in the Uniform Building Code (1997) and the American Concrete Institute (ACI 2008) as they relate to structural dynamic design. The results will then be evaluated using research conducted by the U.S. Bureau of Mines, industry research groups, and this research to provide a set of recommendations based on these findings.

2. LITERATURE REVIEW

2.1 Reducing Blasting Damage by Expanding Delay Timing

Rein and Thomas (1985) worked at the Henderson mine on a study of blasting operation effects on underground mining. At the mine, production drifts (3.6 m by 3.7 m) are spaced 24 m apart center to center and have undercut drifts (3.4 m by 3.8 m) 17 m directly above them. The production drifts are inter-connected with drawpoint crosscuts (4 m by 4.3 m) driven on 12 m centers. Drawpoint crosscuts receive substantial brow steel and concrete support prior to undercutting. The brow steel is a 15-cm by 46-cm-wide flange beam with a 2.5-m wear plate to box in the 'cave' side of the beam. The concrete is a minimum of 0.3-m-thick and the batch design results in 27.5-Mpa-strength. The finished drawpoint opening is 3.7-m by 3.2-m with a choke area of 3.7-m by 2.4-m. Undercutting and belt formation are accomplished by blasting rings of 7.6-cm holes drilled from the undercut drifts. The rings have a burden of 2.0-m and six rings develop one complete bell. Prior to production, a bell is formed above the drawpoint crosscut to deliver caved rock to the drawpoints. After bell formation is complete, undercutting proceeds across the bell in two-three-ring-shots. Approximately 30 m behind the 'cave face' production begins. This 30 m zone is maintained to provide relative stability at the undercut levels 'cave face' where blasting activities are occurring. During undercut and bell development, the concrete drawpoints develop severe cracking and often need repair before they are placed into production. Drawpoint cementing cannot be postponed until after undercutting because the drawpoint brows are needed to restrain rock during the bell and undercut blasting operations.

Although caving is normal in this type of operation, significant damage can be observed after blasting takes place. A study was started in 1984 to investigate the cause and to develop mitigation techniques. The major observations were as follows:

- One to three cracks develop during concrete curing.

- Two to four additional cracks occur where the undercut area is large enough to cause abutment loading.
- Ten or more additional cracks and concrete slabbing occur during blasting.
- Cold joints have no influence on the location, orientation, or formation of new cracks.

Cursory examination indicated that when the peak particle velocity (PPV) was about 760 mm/sec (29.92 in./sec), structural damaged was developed. The original timing scheme using long period delays was altered so that instead of shooting the center hole followed by both sides in a sequence, the south side was shot last because it was closer to the cave and more highly stressed; it was determined this would reduce the confinement of the charge and therefore the PPV. Similarly, bell development timing on the first and second shots was modified to a center, north side, and south side sequence.

In conclusion, mapping cracks yielded semiquantitative data to assess blast damage. Detail of location, orientation, and dilatation did not seem to be of value. Reducing blast energy by introducing more delay timing proved to be an effective mechanism to reduce drawpoint damage and associated costs in repairs. Furthermore, reducing hole size was also effective in reducing damage because reduces loads per delay.

2.2 Seismic Soil-Tunnel-Structure Interaction Analysis and Retrofit of the Posey-Webster Street Tunnels

Shamshabadi, Sedarat, and Kozak (2001) describe the soil-tunnel structure interaction performed for the Possey and Webster Street Tunnels located between two major faults. This analysis provided important information on potential impact on the tunnel structure due to the proximity to the faults. Based on the study, a dynamic analysis was performed and a major earthquake event of 7.25-magnitude was simulated. This event was capable of generating a peak horizontal rock outcrop acceleration of 0.76 g and a vertical acceleration of 0.80 g.

Based on the findings, retrofit was necessary to reduce stresses at soil regions surrounding the tunnel. The retrofit consisted of installing jet grout columns and stone columns

along both sides of the Posey and Webster Street tunnels. The main objective of the retrofit was to prevent flotation of the tunnels due to liquefaction of the sandy soils beneath the tunnels. The structural retrofit consisted of providing expansion joints and a significant reduction in forces applied to tunnel segments.

It was concluded that the interaction between the soils surrounding the tunnel and the tunnel structure is a significant factor in the response of the tunnel structure to seismic excitations. In addition, the retrofit to the tunnel structure provided flexibility to the structure, prevented flotation of the surrounding sandy soils, and reduced the forces applied to the tunnel segments.

2.3 Dynamic Analysis of Buildings for Earthquake Resistant Design

Staatciouglu and Humar (2002) discussed the dynamic analysis of buildings for earthquake resistant design as both linear (elastic) and nonlinear (inelastic). The latter requires additional considerations for proper simulation of hysteretic response. In the linear dynamic analysis, the modal response spectrum or numerical integration linear time history method is used to conduct analysis. Spectral analysis is intended for the computation of maximum structural response. The spectral analysis is conducted for a single-degree of freedom structure or for a building that can be approximated to behave in its first mode response by selecting the value corresponding to its period, directly from the design response spectrum. Correct assessment of the fundamental period becomes important in obtaining spectral values, and the design response spectrum is based on the Uniform Hazard Spectrum (UHS) for the site as adjusted for the ground condition (Humar and Mahgoub 2003). A UHS provides the maximum spectral acceleration that a single degree-of-freedom system with 5% damping is likely to experience with a given probability of exceedance and reflects the seismicity of the region.

Nonlinear (inelastic) response history analysis involves the computation of dynamic response at each time increment with due consideration given to the inelasticity in members. Nonlinear analysis allows for flexural yielding (or other inelastic actions) and accounts for subsequent changes in strength and stiffness. The most important distinction between linear and

nonlinear time history analyses is the inelastic hysteretic behavior of elements that make up the structure. A nonlinear time history analysis provides a maximum ductility demands in members and the maximum deflections experienced by the structure. If the ductility demands are less than the ductility capacities and the deflections are within acceptable limits, the design is satisfactory.

In conclusion, dynamic analysis of building requires careful structural modeling, appropriate selection of ground motion records, and thorough knowledge and familiarity of the analyst with computer software employed. It is possible to attain reasonably accurate assessment of the inelastic seismic response of buildings though dynamic analysis, which can be used in earthquake resistant design of buildings. Design and detailing provision of current building codes often ensure elimination of undesirables features of response that translate to premature decay in strength. This is particularly true for flexural-dominant buildings where well rounded stable hysteresis loops dominate the response of the structure.

2.4 Effects of Blasting on Infrastructure

Moore and Richards (2007) described observations made as part of investigations into the effects of blasting in open pit coal mines on adjacent infrastructure. The methodology for assessing the damage potential of ground vibration on structures was established in a previous investigation funded by Australian Coal Association Research Project (ACARP), Project No C9040, entitled “Structure Response to Vibration” (Moore and Richards 2002). The infrastructure types included conveyors, power transmission towers, wooden power poles, electrical substations, pipelines, bridges, public access roads and underground workings.

This project established that the dynamic strains in a structure induced by ground vibration could be predicted using sine wave approximations, plane wave strain theory and structure response/frequency criteria. The induced strains could then be compared to the strength of materials using allowable stress or other stress limit criteria. Where possible, direct strain measurements were used to validate the theoretical predictions and justify the conclusions reached. The dynamic stresses resulting from blast vibration were compared to stresses from nonblasting causes.

The effect of open pit blasting on adjacent underground workings was determined by a prior investigation in the Hunter Valley, in the region of South Wales, Australia. The investigation measured ground vibration and strain resulting in the roof of a main entry heading, and related these to the strength of the underground structure. The methodology allows determination of the stress resulting in the underground structure to be determined from PPV measurements, relates this stress to the failure stress of the underground structure, and using an appropriate factor of safety, permits a rational blast vibration limit to be determined. This methodology has since been used successfully at underground mines in the Hunter Valley and Queensland.

2.5 Seismic Response of Soft-First-Story Buildings Supported by Yielding Foundations

Nagae and Hayashi (2004) investigated the 1995 Hyougoken Nanbu Earthquake in Tokyo. Soft-first-story buildings suffered significant damage because the buildings had to consume most of energy in their soft-first-story columns. As a preventive measure of this type of failure, it is well-known that making the soft-first-story stronger (i.e., increasing the column size) is efficient. But, in this case, the strength of super structure becomes large and the inertial force from it significantly influences the design of the foundations, especially in soft-soil sites.

In the traditional design, it is thought that the foundation should be stronger than the super structure, so that does not suffer damages during great earthquakes. Nagae and Hayashi (2004) proposed an alternative that reduces the reinforcement of foundation members and forces yielding in the foundation. To consider the effect of the yielding foundation on the seismic response of the super structure, soft-first-story buildings supported by pile foundations were analyzed. The yielding of grade beams and piles were defined as the yielding of foundation, and the strengths of grade beams and piles were changed as the parameters. For model analysis, a two-dimensional (2D) frame structure model was connected with a free ground column by nonlinear soil (p-y) springs. The results from the dynamic analyses showed that the yielding of grade beams and the yielding of piles can reduce the seismic response of the soft-first-story during a great earthquake. It was also indicated that the energy consumption of the soil in the

vicinity of piles decreases the total energy consumption of the structure, and that the yielding of the foundation derives not just from the energy consumption by the foundation members, but also from the extra energy consumption by the soil in the vicinity of the piles.

In this research, the influence of the yielding foundation on the super structure during the great earthquake was analyzed on 12-story buildings supported by pile foundations. The yielding of the grade beams and the yielding of piles were defined as the yielding of foundation, and the strengths of the grade beam and pile were changed as parameters. The buildings were modeled as 2D frame structures that have multistory wall over the first-story columns. The site was located in Daiba, and area of Tokyo were the soil is very soft; where the free-ground and p-y springs exhibited nonlinear behaviors under the great earthquake. The results from the dynamic analyses under the conditions mentioned above showed that the yielding of grade beams and the yielding of piles can reduce the seismic response of soft-first-story during the great earthquake. Also, it was concluded the energy consumption of the structure and the yielding of foundation derive from not just the energy consumption of the foundation members, but also the extra energy consumption of the soil in the vicinity of the pile.

2.6 Computation of Dynamic Seismic Responses to Viscous Fluid of Digitized Three-Dimensional Berea Sandstones with a Coupled Finite-Difference Method

In Zhang and Toksoz (2012), the seismic response of saturated porous rocks was studied numerically and in the lab. A stress-strain calculation was implemented to calculate velocities and attenuation of rock samples whose sizes are much smaller than the seismic wavelength of interest. To compensate for the contribution of small cracks losses in the imaging process to velocity and attenuation, a hybrid method to recover the crack distribution was developed in which the differential effective medium theory, the Kuster-Toksoz model, and a modified squirt-flow model were utilized in a two-step Monte Carlo inversion. The inversion model showed that P- and S- waves measured for the dry and water-saturated cases, the measured attenuation of P-

waves for different fluids, and the velocities were predicted accurately when compared to laboratory data. The hybrid method was a practical way to model numerically the seismic properties of saturated porous rock before very high resolution digital data-acquisition equipment was available. Crack losses in saturated porous rocks are critical for accurately predicting velocities and attenuations of such rocks. The viscosity and attenuation depend on at least three mechanisms: friction, viscous fluid, and scattering. The significant impact of small cracks losses during the imaging process and the Monte Carlo approach to account for such losses offered an adequate methodology.

Compared to traditional methods using only theoretical models, such as the BISQ model (Dvorkin and Nur 1993, Dvorkin et al. 1994, and Marketos and Best 2010), the digitized method offered by Zhang and Nafi Toksoz provides much more information about microstructures of the rock. Therefore, numerical models applied to digitized rock images have many advantages over those studies using theoretical models alone. These numerical models complement the rapidly advancing three-dimensional (3D) digital imaging, for better understanding of and predicting elastic and inelastic properties of porous rocks.

2.7 A New Approach for Loads Moving on Infinite Beams Resting on Elastic Foundations

Raftoyiannis, Tassos, and Michaltsos (2011) presented work that deals with the problem of infinite beams resting on an elastic foundation. Moving loads along such beams is of great theoretical and practical significance. It is clear that the main factor is validating the foundation model. The soils (or rock) can be modeled by foundation models such as Winkler's model or others with two parameters that include the shear parameter influence of some secondary parameters. It has been proven that the effect of various models on the foundation behavior is insignificant, except in the case of a semi-infinite elastic medium, where the wave field including surface waves does affect the response of the beam. The transverse vibration of a beam is governed by Equation 2.1.

$$EIw'''' + c\dot{w} + m\ddot{w} + kw = P\,\delta(x - \upsilon t) \qquad \text{(Equation 2.1)}$$

where

EI = flexural rigidity, N m^2 (lbf ft^2)

c = the damping coefficient,

k = Winkler's foundation coefficient, N/m (lbf/ft)

υ *= speed of the load, km/h, (mph)*

δ *= Dirac delta function*

P = Load, N (lbf)

The static problem of an infinite beam can be studied through observing that of a semi-infinite beam with half the load *P*. The static problem is governed by Equation 2.2.

$$EIw'''' + kw = 0 \qquad \text{(Equation 2.2)}$$

The importance of this approach is that it includes the interaction of the structural member with the properties of the underlying soil. The Winkler's foundation coefficient *k* can be obtained by Equation 2.3.

$$k = H\,E_s / (1+\upsilon_s)(1-2\upsilon_s) \qquad \text{(Equation 2.3)}$$

where

k = Winkler's foundation coefficient, N/m (lbf/ft)

H = soil layer thickness, m (ft)

E_s *= Young's modulus of the soil, N/m^2 (lbf/ft^2)*

υ_s *= Poisson's ratio*

It was concluded that is not possible to achieve the critical speed of a beam on an elastic foundation because that speed is significantly higher than the corresponding for a free single-span supported beam, even on cohesionless soils. However, the proposed formulae provided in this study are accurate for subcritical speeds either with or without damping. This accuracy is significant for normal and well-designed beams even when they are founded on cohesionless soils, but it decreases for feeble beams on cohesionless soils as the critical speed is approached. The Fybra formulae and diagrams provided in the report show that a point does not continue to

oscillate as the moving load passes beyond half the equivalent distance, whereas it can be seen that the same point continues to oscillate with rather significant free vibration response for a range of subcritical speeds when beam is resting on an elastic foundation.

3. WALL CONTROL TECHNIQUES

When performing blasting operations in an open pit setting, energy is released and transmitted through the geological structure. Some of the effects can significantly impact mining operations and can adversely affect mine production. This chapter describes and analyses the effects of rock blasting on slopes and highwalls. It provides a set of recommendations to predict slope damage and provides a set of criteria to prevent slope damage from blasting. Use of particle velocity propagation is presented to determine safe levels of vibration through blasting techniques, and five wall control methods to prevent slope damage from blasting are presented. Wall control blasting is important in surface operations. However, for the purpose of this research, its importance is secondary since rockmass structures behave different that manmade concrete structures when subject to vibration from blasting.

3.1 Wall Control Blasting

Efficient wall control blast design can be defined as achieving a safe and stable slope at the most economical cost. Basically, the time and effort spent in developing and implementing efficient design are insurance against future wall failure. The question is, “How much insurance is needed?” The answer is not always clear, but is related to site factors that include geology and water conditions, slope design, life of slope, and value of excavation.

From a production point of view, the goal of wall control blasting is to make the transition from a well fragmented rockmass to an undamaged slope in as short an area as possible. This can be quite challenging because of the many factors that influence wall damage. To develop efficient designs one must have a basic understanding of wall failure mechanisms as well as the

limitations of the various wall control procedures. In addition, it is imperative that the design be precisely implemented, evaluated and refined in a continuous basis.

3.2 Factors That Influence Wall Stability

There are four major factors that control wall stability (ISEE 2012):

- Geology
- Slope design
- Blast design
- Operational control over design implementation or value of excavation

Obvioulsy the geology of the site will influence both slope and blast designs. It is important that close attention be paid to the geological conditions of the wall at the blast site to develop blasts that will limit damage.The strength of the rockmass under shear, tensile, and compressional loading will also dictate the overall stability of the slope.

In most cases the final slope design is modified during the excavation process as the site conditions become more understood. In addition, mine plan changes can alter the slope design. Key parameters of slope design include overall height, bench height, batter angle, berm width, and inter ramp angle. These parameters are ilustrated in Figure 3-1.

An important collection of data on excavated slopes was compiled by Hoek and Bray (1981) and is illustrated in Figure 3-2. The information refers to slopes in open pit mines, quarries, dam foundation excavations, and highway cuts. The slope heights and corresponding slope angles for slopes of materials classified as hard rock were plotted, which included stable and unstable slopes. The data suggests that the highest and steepest slopes from this data collection fall along a fairly clear line as illustrated in Figure 3-2. This illustration also shows that while slopes are stable at steep angles and at heights of hundreds of meters, many flat slopes fail at heights of only a few meters. This difference is due to the fact that stability of slopes varies with inclination of faults or discontinuity surfaces. Hence, the importance of geological characteristics of slope as an important factor in slope stability.

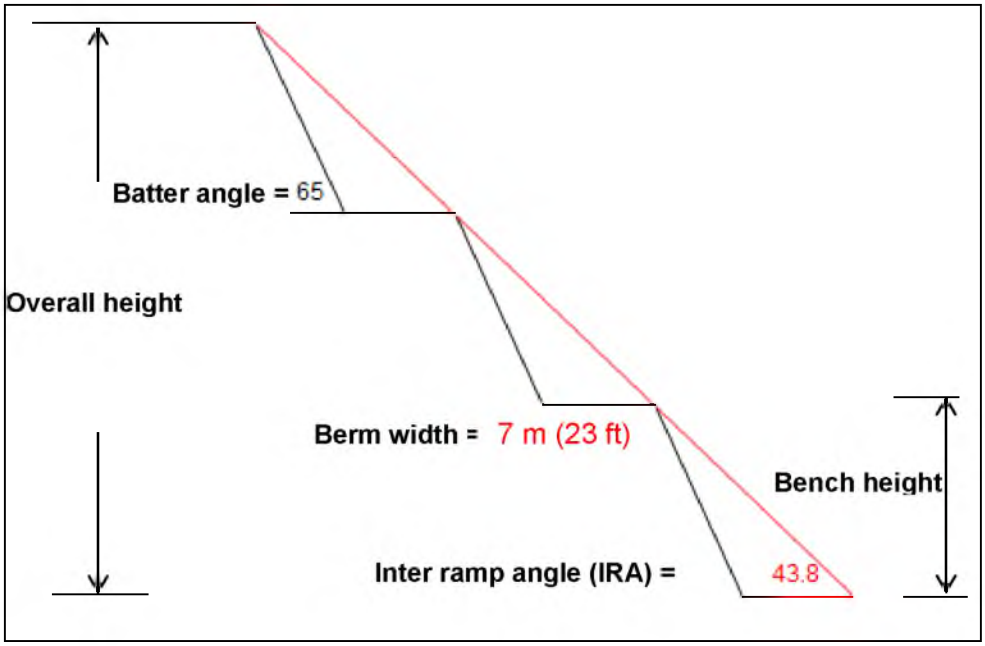

Figure 3-1 Typical slope parameters

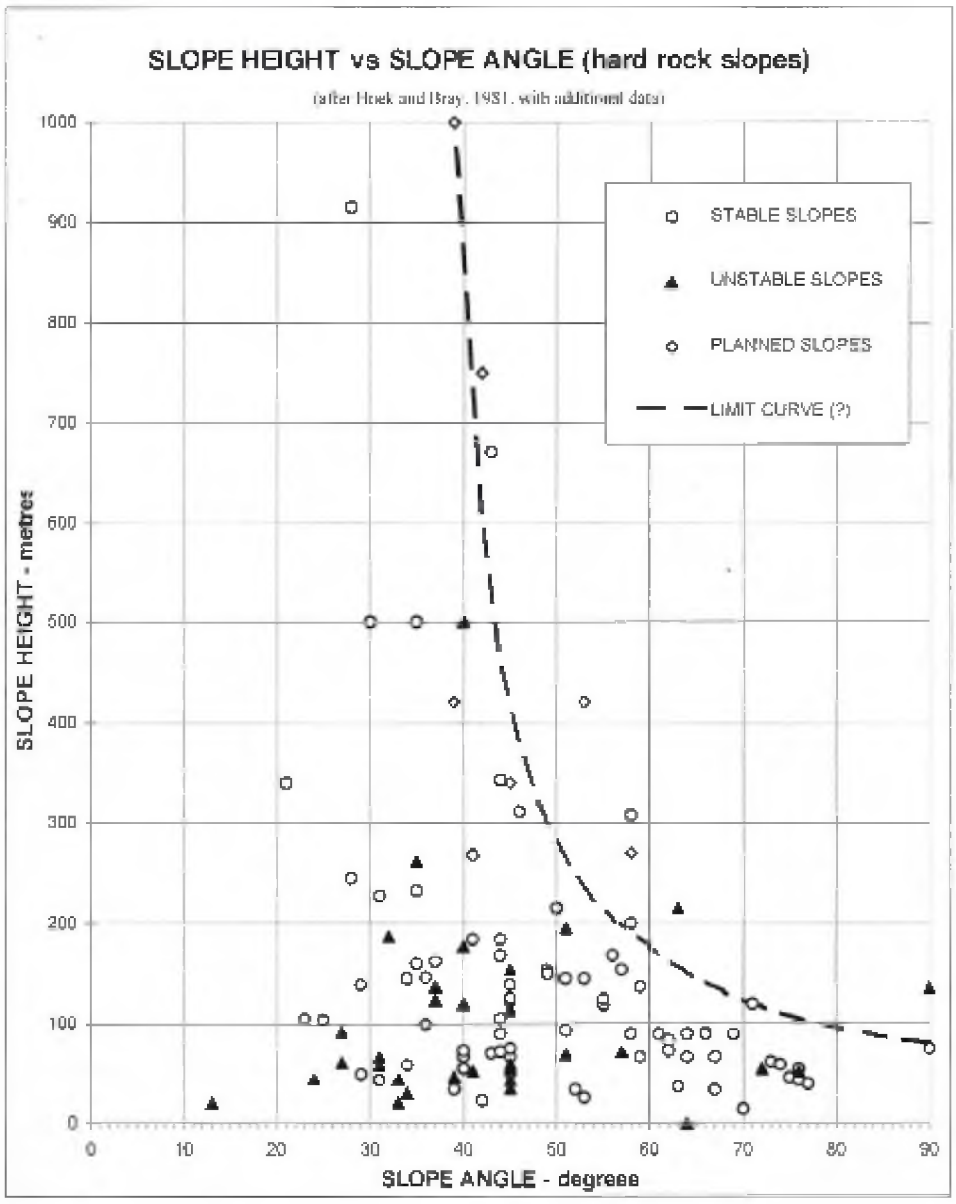

***Source*: Hoek and Bray 1981**
Reprinted with Permission from *Rock Slope Engineering.* 1981, Institution of Mining and Metallurgy, London. Page 20.
Figure 3-2 Slope height versus slope angle relationships for hard rock slope

3.3 Blast-Induced Vibration

During the detonation process of a blast, the explosives are quickly converted into a high-temperature, high-pressure gas. Immediately around the blasthole, the high reaction pressures propagate a shock wave into the rockmass. The initial pressure of the shockwave created by the blast is much greater than the rock's strength, as a result, the rock around the blasthole is crushed. This crushing and expansion of the blasthole reduces the pressure to the point where the shockwave is reduced to a strain pulse. As the strain pulse propagates through the rockmass at a rate equal to the P-wave (seismic velocity), it compresses the rock radially which results in tangential tension or hoop stress. If the tangential tension is greater than the tensile strength of the rock, fractures are created (typically 20 to 30 charge diameters) that extend in all directions. When the strain pulse reaches a rock/air interface (such as a join or discontinuity) the pulse is reflected back in tension, and if the tension is greater than the tensile strength of the rock spalling occurs. This fracturing relieves the stress to the point where new fractures from shock are not created. This process is called stress failure and can be estimated by determining the vibration levels within the rockmass using the near field vibration prediction equation (McKenzie 1999).

$$V = K W^{\alpha} / R^{\beta} \qquad \textit{(Equation 3.1)}$$

w*here*

V = peak particle velocity or PPV, mm/sec (in./sec)

K = site constant

W = instantaneous charge, kg (lb)

R = distance, m (ft)

α *=site constant*

β *= site constant*

Typical vibration attenuation parameters based on rock type are listed in Table 3-1.

Table 3-1 Typical attenuation parameters

Rock Type	K	α	β	Max PPV (mm/sec)
Massive Granite	700	0.7	1.5	711-736
Andesite	200	0.9	1.8	610
Strong Sandstone	400	0.78	1.56	457
Strong Shale	175	1.25	2.5	356
Jointed Granite	190	0.86	1.72	889

Adapted from McKenzie 1999.

3.4 Vibration Damage Levels

The peak particle velocity required to damage rock varies greatly depending on the strength and structure of the rockmass. Typical damage thresholds are classified as follows (McKEnzie 1999).

- 50-100 mm/sec Loose structure falls
- 127-508 mm/sec Damage to weak rock
- 381-1016 mm/sec Damage to hard fresh rock

Frequency should also be considered as well as PPV. (see also “Vibrations from Blasting” , Chapter 4).

Example 3.1

At what distance would the vibrations from a 45-kg charge blasthole attenuate to 25.4 mm/sec in jointed granite? ***Ans*: From Figure 3-3, for a PPV = 254 (mm/sec), 45-kg charge, and jointed granite, distance = 5.9 m.**

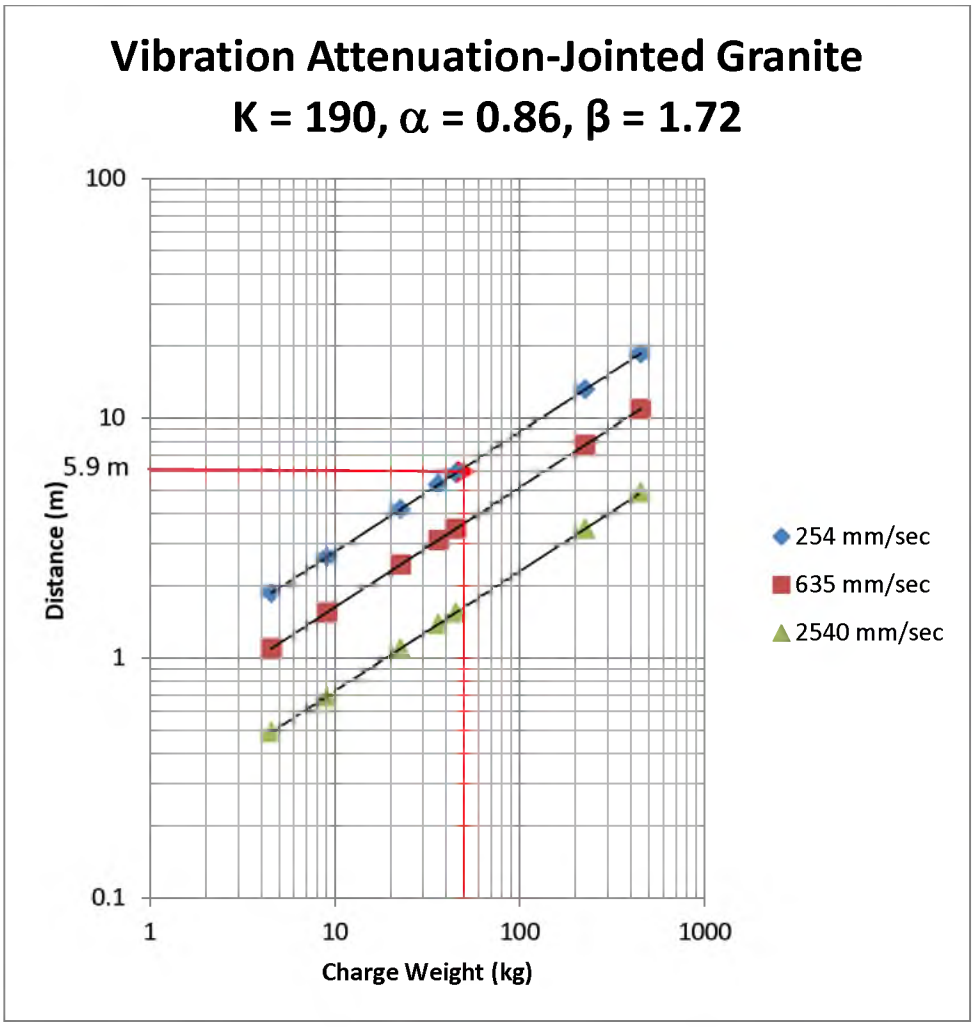

Adapted from McKenzie 1999
Figure 3-3 Near-field vibration attenuation for jointed granite

Obviously, excessive ground vibration levels can damage the structural integrity of the wall. It is recommended that a vibration monitoring program be developed to evaluate the intensity, frequency and duration of blast-induced vibrations. This program should include a number of data points to determine the relationship between distance and nature of the vibrations produced. If the slope is saturated with water it may be appropriate to include pore pressure gauges to measure what influence of blast vibrations have on in-situ pressures.

3.5 Controlled Blasting to Increase Wall Stability

Several blast design factors influence stability of the wall but can be summarized in four main factors that need to be considered to increase wall stability when blasting (ISEE 2012):

1. Horizontal relief away from wall
    a) The explosive energy's paths of least resistance for displacement must be away from the wall
    b) Plan narrow blasts with four rows maximum
    c) Establish clean free faces
    d) Use proper timing configurations
2. Dispersed energy concentration in back rows
    a) Disperse energy by using more holes and less charge
    b) Air deck to reduce borehole pressures and excessive heave
    c) Use buffer rows to protect final row
3. Blast size
    a) The number of holes per delay interval influences the vibration levels produced
    b) Long duration events may cause pit walls to resonate and produce more damage
4. Drill control
    a) Proper depth is critical above berms or catch benches
    b) Maintain the correct angle and azimuth of the blastholes
    c) Plan and layout accurate patterns.

3.6 Wall Control Methods

In the industry five wall control blasting methods are generally used that depend on rockmass structure, drill bit diameter, and site sensitivity (ISEE 2012):

1. Modified production or trim blasting
2. Cushion or buffer blasting

3. Pre- or midsplit blasting
4. Postsplit blasting (smooth blasting)
5. Line drilling or any combination of the above

1. Modified production or trim blasting involves the change of one or more parameters throughout the design to reduce wall damage (reducing the number of rows, changing the delay sequence, providing a free face, etc.). The charging of the row nearest to the wall is reduced by 30% to 60 %.The last row of blastholes is located in front of the final wall separated by the standoff distance. This offset controls both the wall stability and the ease of excavation. The standoff distance must be optimized to limit overbreak without adversely affecting productivity.
2. Cushion or buffer blasting typically involves reducing the loading and pattern of one or two rows next to the final wall. Charge weight in the toe is reduced by 45%, the toe's burden and spacing is reduced by 25%. Spacing on the toe row should be less than the burden to promote breakage parallel to the wall. Only minimal stemming is used in the toe tow.
3. Pre- or midsplit blasting utilizes a row of closely spaced, lightly charged blastholes that are placed along the final limits. Presplit holes are detonated prior to the detonation of all adjacent blastholes to create a fracture line to impede the extension of blast-induced cracks and prevent gas penetration into the final wall. Midsplit holes are fired in the middle of the timing sequence before the holes immediately adjacent detonate. While presplitting or midsplitting can produce excellent results in favorable geology, they are also expensive and labor intensive. A cost / benefit analysis should be performed before adopting strict presplitting design requirements. Jointed material or complex geology requires closer hole spacing and may hinder the desired split between holes.
4. Postsplit blasting (often known as smooth blasting) involves the detonation of a closely spaced lightly loaded row of holes after adjacent production or cushion holes have fired. By initiating instantaneously or with minimum delay between the holes, a shearing action is obtained which gives smooth walls with minimum overbreak. Postsplitting will generally

provide better results than presplitting when blasting highly jointed rockmasses. Postsplitting is also used when conventional presplitting will displace and cutoff adjacent production or cushion holes.

5. Line drilling consists of a line of unloaded holes drilled along the final limit to provide a weak plane to break to. It is used where no detonation along the perimeter of the blast can be tolerated (vibration predictions, weak ground). The spacing of the line drilling is typically 12 times the hole diameter, but in hard massive rock it is 3 to 6 hole diameters. The buffer row is typically offset about 50% to 75% of the normal production burden. This technique is the most cost effective in soft ground such as weakly cemented alluvium.

3.7 Timing Configurations to Protect Wall

Timing also plays an important role in wall damage control. Delay configurations can significantly help to reduce wall damage while protecting the integrity of the wall. Timing will be discussed in "Vibration Control Techniques," Chapter 9.

3.7.1 Basic Considerations

If two faces exist, detonate a minimum number of holes per delay for both production and wall control blasts, with the exception of the presplit row, to reduce overbreak and minimize vibration levels placing the point of initiation (POI) at the corner as shown in Figure 3-4.

It is important to time the blast in sequence. If not timed correctly, excessive overbreak may occur as illustrated in Figure 3-5. When one free face exists, proper configuration of blasting can help reduce excessive overbreak. The point of initiation should be placed in the middle and the adjacent holes fired as shown in Figure 3-6. Otherwise, poor blasting configurations on one free face setting can have negative consequences when holes adjacent to the point of initiation are not fired simultaneously as shown on Figure 3-7.

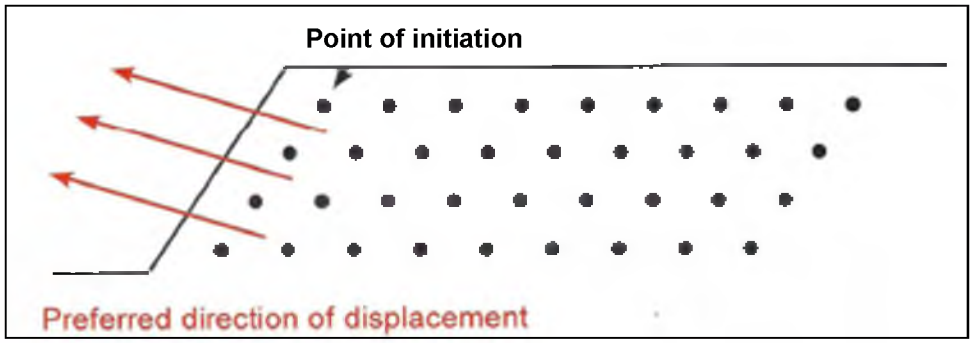

Figure 3-4 Two-face point of initiation

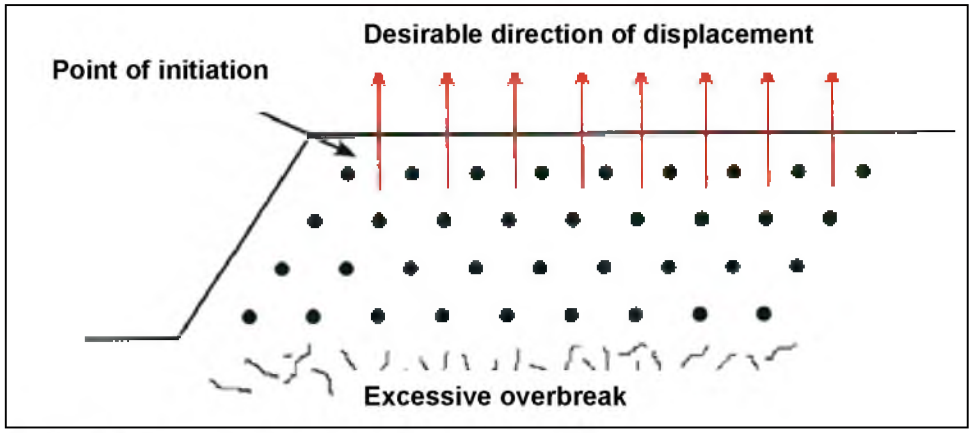

Figure 3-5 Excessive overbreak

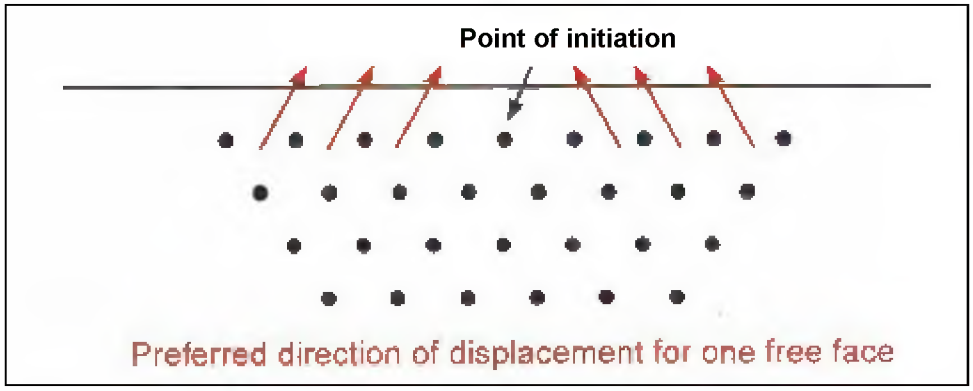

Figure 3-6 One-face point of initiation

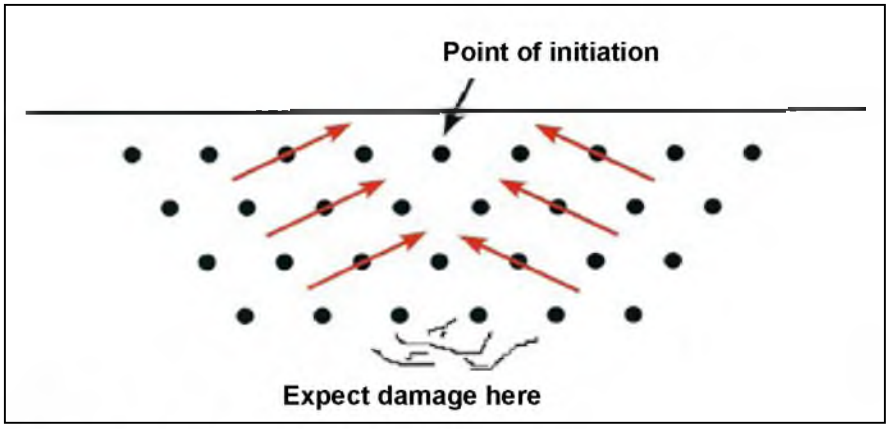

Figure 3-7 Poorly designed sequence

3.8 Presplit Blasting

Presplit holes should also be detonated before drilling and loading adjacent cushion holes to make prep work easier and avoid cutoffs. If this is not possible, the presplit (midsplit) is fired at least 50-ms before adjacent cushion holes. It is recommended to detonate the cushion blast and the next presplit together to optimize crew productivity as shown in Figure 3-8.

Presplit holes should be fired instantaneously (connected with detonating cord with no delays between holes or in holes) if possible. If vibration level is a major concern, fire groups of holes together with 17 or 25 ms between groups. Expect higher relative vibration levels when firing presplit holes because of their high degree of confinement. Shorter periods (<500 ms) in-hole delays should be used on modified production and cushion blasts to protect against cutoffs while minimizing the adverse effects of scatter.

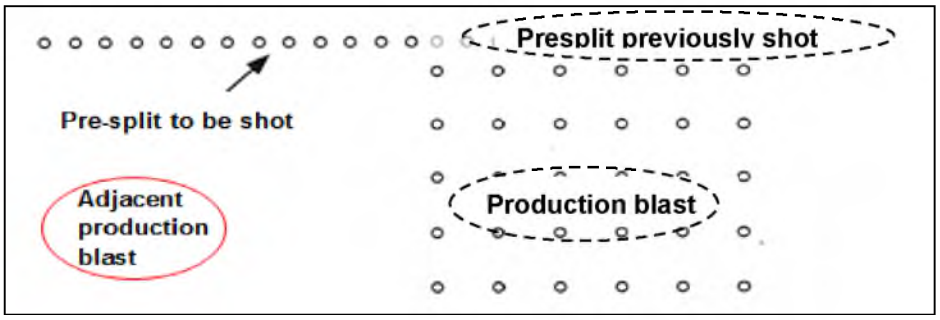

Figure 3-8 Presplit blasting

Special attention should be placed on dominant frequencies of vibrations produced in wall control blasting. The dominant frequencies should not match the natural frequency of the pit slope to avoid resonance. The natural frequency of a pit slope can be obtained by monitoring techniques that include robotic total stations, slope radar, and other seismic-monitor measuring devices. If possible, use delay sequences that minimize the production of unwanted frequencies. This requires very accurate delays and a good understanding of the vibration attenuation characteristics of the site. It may be beneficial to limit the blast's duration if the vibrations are causing the wall to resonate.

The effectiveness of any surface excavation relies on slope stability. Slope stability can be accomplished by establishing a wall control program that includes the implementation of a vibration control plan, the implementation of wall control methods, and the optimization of timing configuration in the blast design.

Blast vibration control is an important part of the optimization of blast designs for slope protection. The amplitude and frequency of vibrations are directly influenced by the blast design and timing configurations used. Both factors contribute to the particle displacement within the slope. In the far field, the displacement must be minimized to reduce the potential for blast-induced failures. One method successfully used to minimize displacement is increasing the frequency content of blast vibrations. All slopes have certain natural frequencies at which they resonate. If the slope's natural frequency is similar to the dominant frequency of the blast, the blast energy will be amplified, causing higher displacement levels. However, if the dominant blast frequency is higher than the slope's resonant frequency, less displacement will occur. Obviously, the key to the success of this method is the characterization of the slope's response to blast-induced vibration. This can be accomplished by implementing an extensive monitoring program of the production blasting and also the use of single-charge blasthole detonations (signature hole). Chapter 9 discusses methods to implement these techniques and results are explained in following subsections.

Implementation of the five methods described in this chapter will help minimize wall damage. Although some are more labor intensive and cost effective than others, the results are

far more economical than pit slope failures and the proper familiarization of the personnel with these techniques allows the company to optimize the process and apply it at different settings within the same mine layout or implement similar procedures at other mining operations within the same company or organization.

4. VIBRATIONS FROM BLASTING

When explosive charges are detonated, a large amount of energy is released. The energy released around the charge creates rock fragmentation and displaces the rockmass within a radial area around the blast creating a crater or inelastic zone. Outside this inelastic zone the energy creates an elastic or nonpermanent movement of the rockmass mostly due to the vibration created by the detonation. The blast energy beyond the crater zone takes form of ground elastic vibration. The speed at which the vibration travels through the ground is known as the wave propagation velocity or seismic wave velocity and depends on the density and elasticity of the rockmass.

4.1 Waves

There are two types of elastic waves, body waves and surface waves. Body waves travel through the interior of the material and surface waves travel along the surface of the material (Hardy 1974)

Body waves are progressive excitations of ground volume that involve elastic dilatations and distortions. There are two types of body waves: compressional or P-waves and shear or S-waves. In compressional or P-waves the particle motion is in the direction of motion, whereas in shear waves or S- waves the particle motion is perpendicular to the motion. The compressional or P-wave travels approximately between 1800 m/sec (6000 ft/sec) and 6000 m /sec (20,000 ft/sec) depending on the geology. The shear or S-wave travels approximately at 0.6 times the velocity of the compressional or P-waves.

Surface waves, however, are much slower. They travel approximately at 0.9 times the velocity of shear or S-waves. There are two types of surface waves, Rayleigh or R-waves and

Love or L-waves. Surfaces waves are of particular importance in blasting. They are of significantly larger amplitudes than body waves and therefore, capable of causing more damage on a structure.

4.2 Elastic Ground Particle Motion

As the vibration travels through earth, the ground moves in all directions and then it returns to its original location. It is possible to record this movement by measuring the motion in three dimensions, or directions, (radial, vertical, and transverse), as illustrated in Figure 4-1. The amplitude represents the velocity (or particle velocity) of the blast waveform but can also represent acceleration or displacement.

The maximum speed at which the particle moves when the vibration wave passes by is called peak particle velocity (PPV) and is commonly used to determine the potential for damage.

Acceleration is known as the rate of change of the velocity and is measured in g's where g is the acceleration due to gravity near the earth's surface, 9,810 mm/sec^2 (386 in./sec^2). Although acceleration is commonly used in earthquake engineering to determine the potential for damage, its use in blasting engineering is limited due to the fact that vibration waves from blasting are significantly lower amplitude and much higher dominant frequencies than earthquake waves.

Finally, displacement is the distance a particle moves with respect to its resting position as the wave travels through and is measured in mm (in). Blast waves can be approximated as simple harmonic motion having sinusoidal shape.

4.3 Frequency of Vibration

A vibrating particle will start to move from its resting position to a positive peak, then to a negative peak, to finally return to zero to complete one cycle. Therefore, frequency is the number of cycles a particle completes per second and is reported in hertz (Hz), Equation 4.1. The time

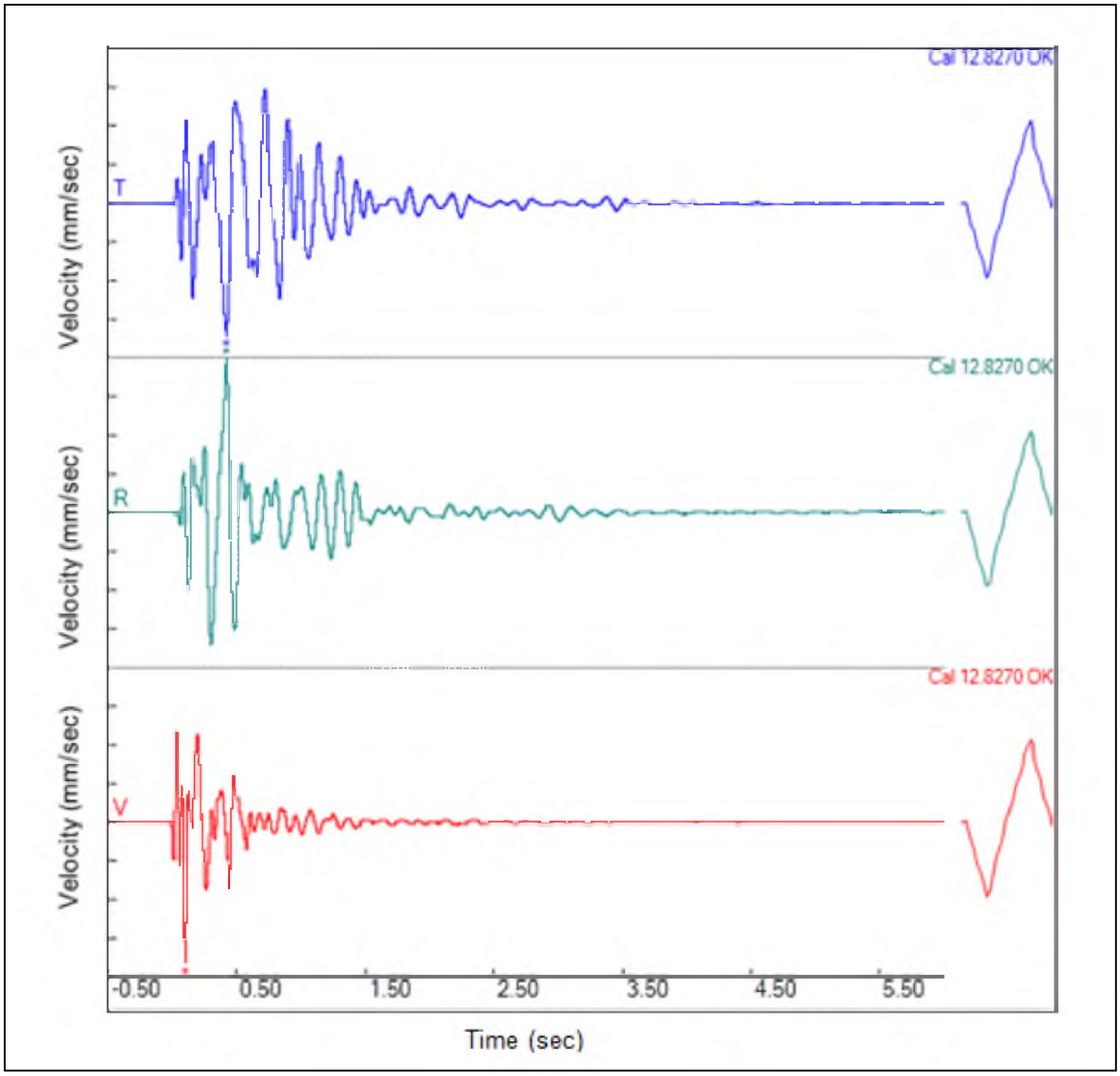

Figure 4-1 Typical blast vibration waveform

Interval of one complete cycle is called period *T* and is measured in seconds. In blasting, frequency is of particular importance because it can result in potential damage to structures. The U.S. Bureau of Mines has conducted a number of studies to recommend safe levels of vibration to minimize effects on residential structures. Figure 4-2 suggests recommended vibration level criteria presented in RI 8507 (Siskind et al. 1980).

$$f = 1/T \qquad \textit{(Equation 4.1)}$$

where

f = frequency (Hz)

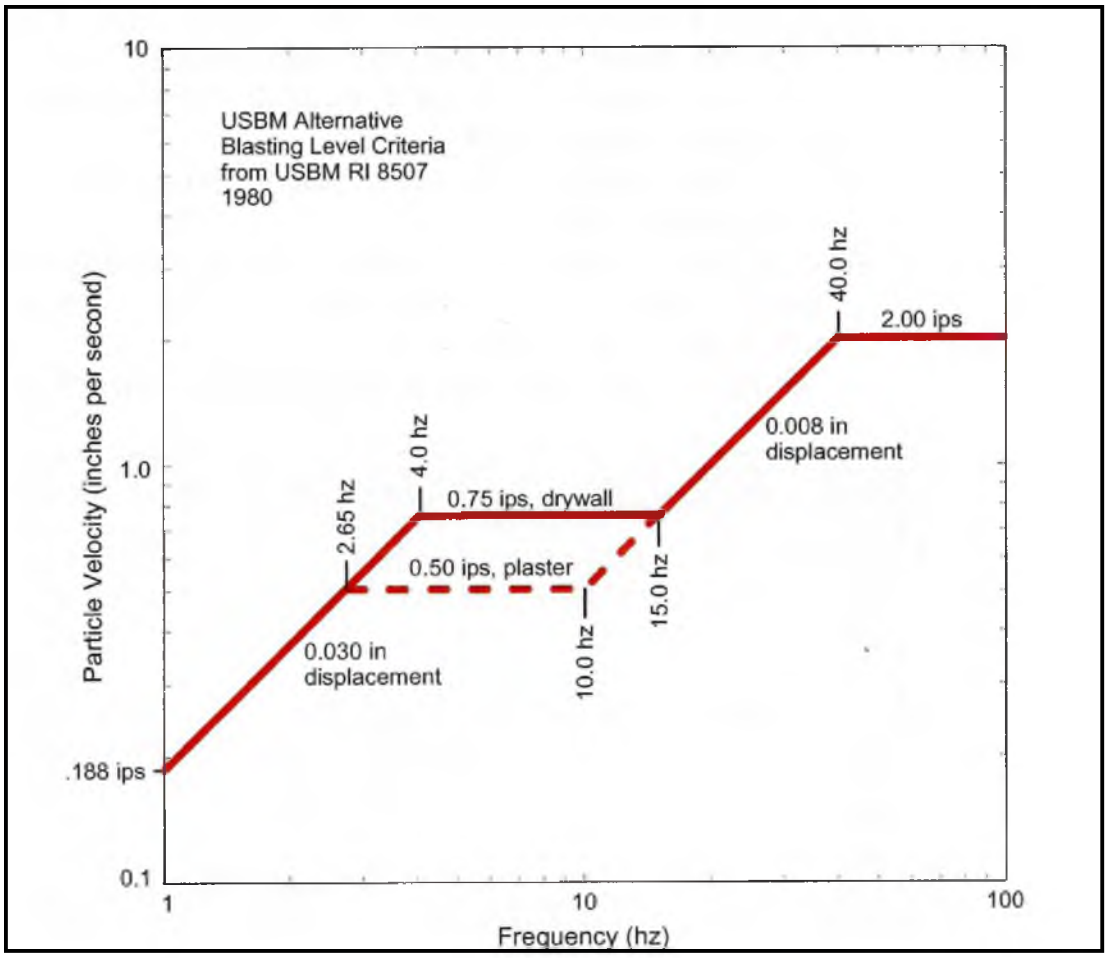

Source: **ISEE 2012**
Figure 4-2 RI 8507 Courtesy of the U.S. Bureau of Mines

T = period (seconds)

The specific frequency components of a complex wave are difficult to interpret. Mathematical models are necessary to evaluate the component frequencies. One of the most common analyses is the Fast Fourier Transform (FFT), where the analysis simply breaks a complex wave into its single frequency components and weights the relative energy in each frequency in graphical form using the general trigonometric form of Equation 4.2.

$$f(x)=a_0+\sum_{n=1}^{\infty}\left(a_n \cos\frac{n\pi x}{L}+b_n \sin\frac{n\pi x}{L}\right) \qquad \textit{(Equation 4.2)}$$

It is also important to mention that, when assessing damage on structures from vibration, there is a potential for resonance to occur. Simplistically, resonance occurs when the blast wave

or seismic wave frequency matches the natural frequency of a site (or structure). Resonance in a structure can significantly amplify the amplitudes of the ground wave. Thus, if a building is hit by a vibration wave with a frequency of equal magnitude than its natural frequency, the response of the structure is magnified. This magnification can lead to serious consequences in the integrity of the structure. Therefore, natural frequency of a structure must be known when analyzing a structure's response to vibration. Furthermore, since the frequency is the reciprocal of period of vibration, when the natural frequency of a structure is known, so is its natural period. Determining natural period of structures, however, is not as straightforward as one would like. How to determine a structure's period of vibration is discussed in "Seismic Design," Chapter 6.

Ground vibrations from blasting will tend to have much lower amplitudes and higher dominant frequencies than earthquake vibrations. This is primarily due to a blast's lower initial energies and shorter propagation distances. Propagation velocities, amplitudes, and frequencies of both blasting and earthquakes waves are related to the elastic properties of the rock, soils, and other materials through which they travel. Propagation velocity is the speed at which the energy travels and is dependent on the stiffness of the medium. For hard rock, it can be up to 6,100 m/sec (20,000 ft/sec) and for packed soil as low as 610 m/sec (2,000 ft/sec).

The amplitudes and frequency characteristics of ground vibrations change as they travel from the blast site to measurement location. They dissipate as vibration energy fills an increasing volume of earth as it travels outwards in all directions away from the blast. The relationship between PPV and distance is nonlinear. As a result, the vibration decreases exponentially with increasing distance as illustrated in Figure 4-3.

Since vibrations attenuate with increasing distance, it is possible to predict or estimate the attenuation within an acceptable level of accuracy by mathematical expressions. The two most influential factors on vibration amplitude are the weight of the charge and the distance from the charge. In any direction, vibrations generally decay in a predictable manner (directly proportional to distance and inversely proportional to charge weight).

Distance and charge weight are used to define the concept of square root scaled distance or SD_2. The U.S. Bureau of Mines recommends using the concept of scaled distance as

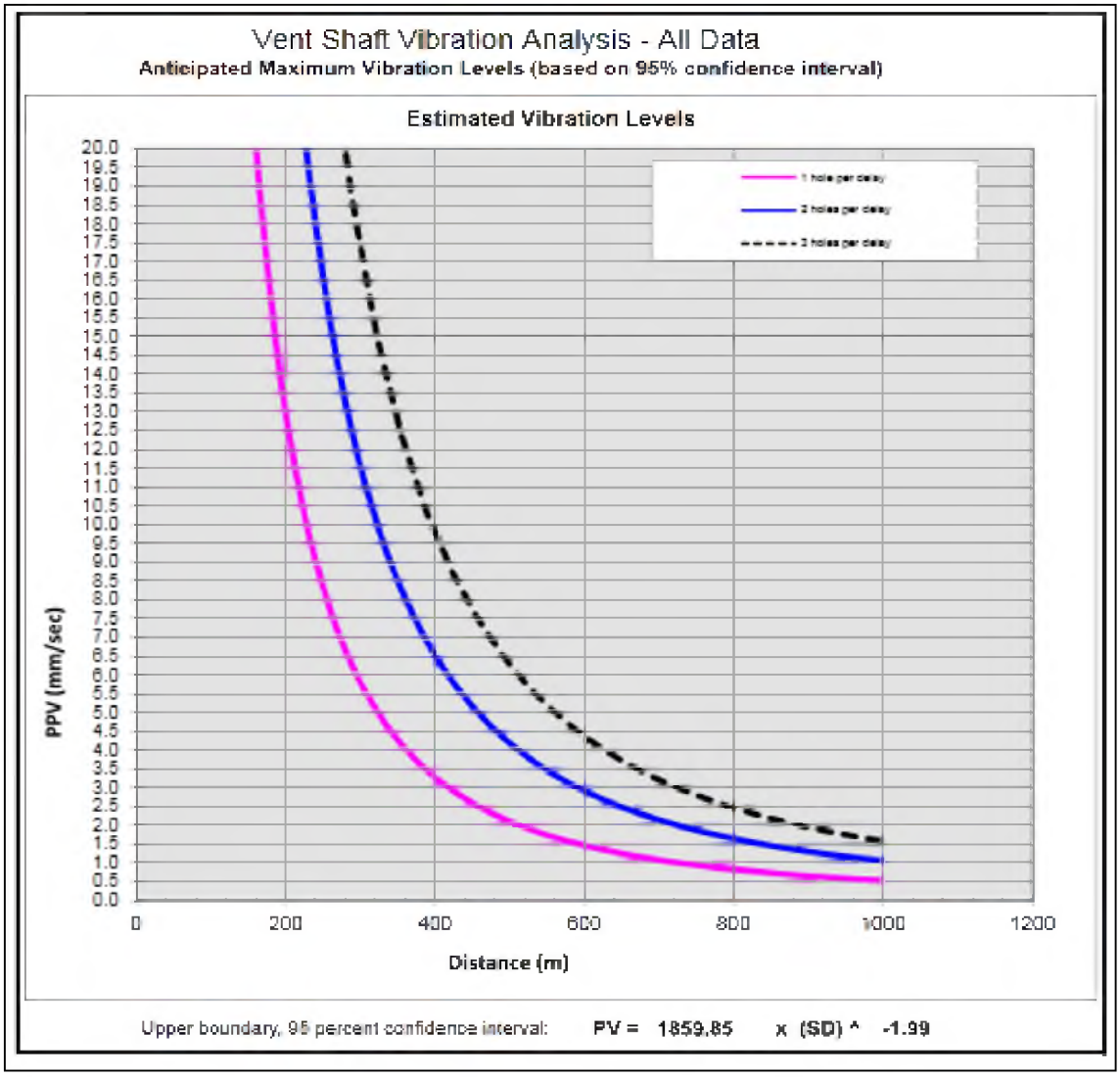

Figure 4-3 PPV versus distance graph

defined by Equation 4.3.

$$SD_2 = R / \sqrt{W} \qquad \textit{(Equation 4.3)}$$

where:

SD_2 = *scale distance, m/kg$^{1/2}$ (ft/lb$^{1/2}$)*

R = Distance to point of interest, m (ft)

W = maximum charge weight per 8-ms delay, kg (lb)

The square root scaled distance method allows the comparison of blasts with different distances and charge weights as a way to incorporate the charge weight. Then, the results are plotted in a log-log scale graph to take the form of a linear relation. The U.S. Bureau of Mines recommends the following limiting criteria for scale distance:

- 0-91 m away- Minimum allowable SD_2 is 22.6 $m/kg^{1/2}$ (50 $ft/lb^{1/2}$)
- 91-305 m away – Minimum allowable SD_2 is 24.9 $m/kg^{1/2}$ (55 $ft/lb^{1/2}$)
- Over 305 m away – Minimum allowable SD_2 is 29.4 $m/kg^{1/2}$ (65 $ft/lb^{1/2}$)

Example 4.1

If a blast is to be fired at 244 m (800 ft) from a house, the required scaled distance is 24.5 $m/kg^{1/2}$. Each hole is charged with 181 kg (400 lb) of ammonium nitrate (NH_4NO_3) fuel oil (FO) or ANFO, and is fired on a single delay. Is the charge enough to comply with U.S. Bureau of Mines criteria?

Ans: **$W = (244/24.9)^2 = 96$ kg (212 lb) per delay.**

No. The explosives charge of 181 kg (400 lbs) per delay exceeds the maximum allowable charge of 96 kg (211 lb) per delay

Factors that influence blast vibration are many, but some of them are within the blast engineer's control. They are defined from less significant to more significant, and the most significant ones include charge weight per delay, timing, delay interval and charge confinement (ISEE 2012).

4.4 Ground Vibration Prediction

When combining the scaled distance with measured vibration amplitude, the seismic characteristics of a site can be defined. It is possible to predict the ground vibration by plotting in a log-log scale plot the PPV against the SD obtained by Equation 4.3. In this plot, the relationship is no longer exponential; therefore a straight line may be fitted with an equation describing the trend. This empirical analysis can be made by obtaining geological information of the site, monitoring and measuring the vibration levels. Currently in the industry, seismographs are used

to monitor ground vibration, by using statistical methods, data can be interpreted as the resulting response of rock to ground motion and can be expressed by Equation 4.4.

$$PPV = A\ SD_2^{-B} \qquad \textit{(Equation 4.4)}$$

where

PPV = peak particle velocity, mm/sec (in./sec)

SD_2 = scaled distance, m/kg$^{1/2}$ (ft/lb$^{1/2}$)

A = site constant (intercept of line at SD value of 1)

B = slope of the line (negative)

4.5 Air Overpressure

Air overpressure is also importance in blasting. Air in the atmosphere is a fluid that propagates particle motions in the same manner as water. These vibrations are pressure waves travelling through the atmosphere like compressional or P-waves in the ground. No shear or S-waves exist in the atmosphere since fluids have no shear strength. If air overpressures reach a certain level, it could cause some damage.

Air vibrations are audible to the human ear at frequencies above 20 Hz and are referred to as “sound “or “noise.“ Air vibrations with frequencies less than 20 Hz are inaudible and are often called “airblast” (ISEE 2012).

Air overpressure travels at speed of sound. At sea level, the velocity of sound in air is approximately 335 m/sec (1,100 ft/sec) at 7^{o}C (45^{o}F) and no wind. As the temperature and wind velocity increase, the sonic velocity increases. The sonic velocity affects the arrival time of air overpressures in relation to ground motion.

Air overpressures are pressure waves that create a compression or positive pressure (push) followed by a dilatation or negative pressure (pull) effect. The amplitudes are measured in pascals (Pa), millibars (mb) or pounds/inch^2 (psi) above the ambient pressure. The pressures are reported as time histories. Blasting air overpressure may also be reported as the sound equivalent in decibels (db) and is calculated from measured pressures by Equation 4.5.

$$Ps = 20 \times \log (P/P_o) \qquad \text{(Equation 4.5)}$$

where

Ps = pressure level, db (psi)

P = measured pressure, pascals (psi)

P_o = Reference pressure, typically $2x10^{-5}$ pascals (psi)

The methodology to estimate air overpressure and ground vibration is similar. Both present the same limitations. Air overpressure is plotted against the cube root scale distance using a log-log graph as shown in Figure 4-4 and the air overpressure is determined by the statistical methods as in ground vibration. Then, the cube root scaled distance SD_3 is used to evaluate air pressure attenuation using Equation 4.6.

$$SD_3 = (R/W^{1/3}) \qquad \text{(Equation 4.6)}$$

And the best fit line to estimate the air overpressure from scaled distance, as defined for ground vibration, is determined by Equation 4.7.

$$P = A\,(SD)^{-B} \qquad \text{(Equation 4.7)}$$

where

P = air overpressure, db (psi)

SD_3 = cube root scaled distance, $m/kg^{1/3}$ ($ft/lb^{1/3}$)

A = site constant (intercept of line at SD_3 value of 1)

B = slope of the line (Note that the slope is negative)

As with ground vibrations, airblast can produce structure rattling and, in extreme cases, cracking and other damages. The U.S. Bureau of Mines has also conducted extensive research on this regard and results are summarized in the airblast report RI 8485. This report includes plots of residential structures responses to airblast for a variety of measurement methods. Table 4-1 (ISEE 2012) provides typical air overpressure criteria for structural damage. Since air blast is measured in decibels, pressures can be plotted in a log-log scale graph versus cube-root scaled distance. Air overpressure can be monitored to determine full waveform as with ground vibrations.

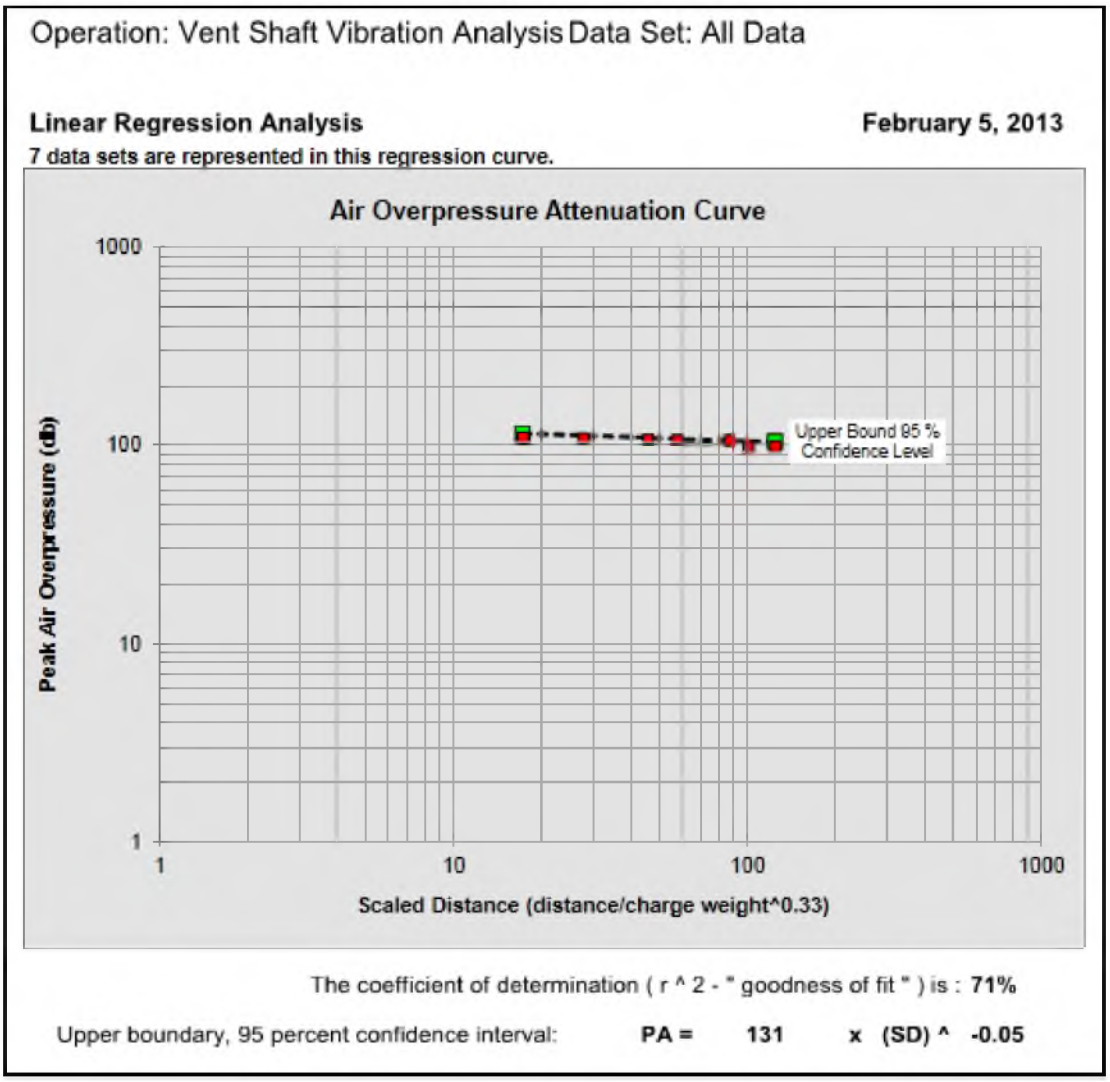

Figure 4-4 Air overpressure versus cube root scaled distance

Table 4-1 Typical air overpressure damage criteria

Potential Damage	Air Overpressure level	
	(Kpa)	db
Structural damage	20.7	180
General window (Oriard 1999)	6.9	171
Occasional window breakage (Oriard 1999)	0.69	151
Damage threshold at high frequencies (RI 8485)	0.25	140
No damage at low frequencies (RI 8485)Jointed Granite	0.010	134

Adapted from ISEE 2012

5. CASE STUDY

When a push back or expansion is required in a surface operation, generally there are no geometric constraints as long as property limits and permit boundaries are respected, and the slope design, operability, and stripping ratio allow the proper development of planning and production goals. The operation must also meet or exceed safety criteria and economic feasibility constraints. However, challenges are increased above those in typical mining practices when the operation involves surface and underground workings adjacent to each other.

The case study involves a hard rock mine operation located on the Carlin trend. As aforementioned, this operation was chosen as the open pit adjacent to underground workings. At this particular mine in the northwest area of the pit, exploration diamond drilling was conducted and a high grade deposit was identified. The resource estimate indicated that an expansion to the current northwest wall was profitable. The expansion will involve a push back design on the northwest area of the pit. The grade estimation indicated that the upper portion was all waste and the profitable portion was at the bottom of the pit, at the 4200 level; whereas surface elevation was at the 5200 level. The issue with this design was the fact that the future crest would be set at the proximity of the ventilation exhaust system of the adjacent underground mine, as shown in Figures 5-1 and 5-2. The ventilation infrastructure consists of the shaft, the plenum, two surface fans and their associated evases. The concrete shaft cross sectional dimensions are 5 m (15 ft) by 5 m (15 ft) with a 0.91 m (3 ft) thick wall and extends underground 380 m (1245 ft). The fan operates in normal conditions at 18,000 rpm and moves at an air flow rate Q of 70,800 m^3/sec (2.5×10^6 ft^3/min).

The initial concerns with this expansion were mainly the blasting near the concrete shaft of the vent system and repeated blasting as the sequential push back advanced. The initial blasting sequence would expose the face of the concrete shaft to significant levels of vibration

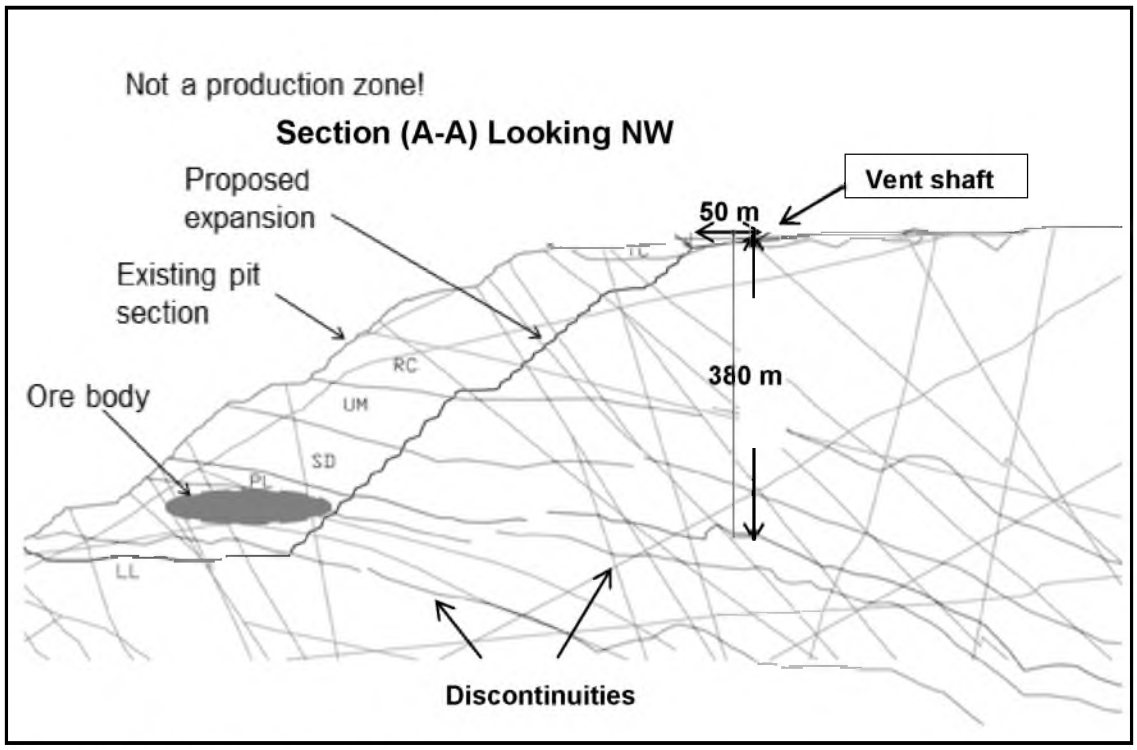

Figure 5-1 Push back section A-A

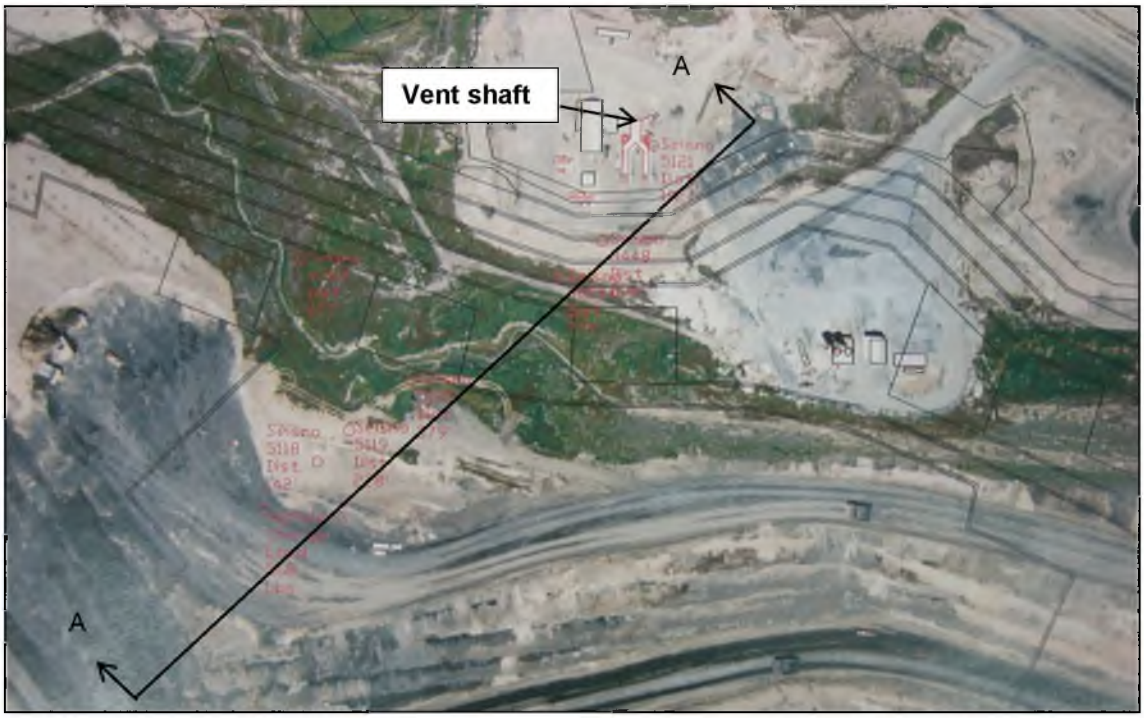

Figure 5-2 Push back plan view

and therefore could compromise the integrity of the concrete shaft structure. This would lead to significant delays to both surface and underground operations since the shaft is the main exhaust ventilation of the ventilation system.

The repeated successive downwards blasting was also a concern since the cumulative vibration could affect stability in deep sections of the shaft. The presence of considerable geological discontinuities also represents risk due to the uncertainty on their response to ground motion. They could act as conduits in which pressure of expanding gases can easily travel while they may reflect rather than transmit seismic waves.

It was decided to investigate whether current level of vibration used in regular production blasting might have an impact in the stability of the shaft once the push back begins. For this, vibrations were measured by conventional methods. Accuracy is very important so the blasting monitoring was conducted using seismographs deployed in the field according to “Field Practice Guidelines for Blasting Seismographs” (ISEE 2009).

Conducting vibration monitoring in an active mine is simple. Mine planning allows engineers to know where the next phase will be at a particular time. This fact provides a time frame to prepare and analyze the response of the ground to the level of vibration in that particular area.

As illustrated in Figure 5-1, the proposed expansion will get as close as 50 m (150 ft) to the shaft wall. The operation will involve sequential push back until the final layout is accomplished.

The concern about vibration generated by blasting was first validated. A set of monitoring devices was placed at different distances and vibration levels were recorded for both a regular production blast and signature blast.

5.1 Geological Considerations

In order to predict vibration levels at the site in question, knowledge of existing lithology is essential to understand the response of the ground to seismicity from blasting. As discussed earlier, blast design timing may influence ground vibration frequencies; however, vibration

frequency is affected primarily by the geology surrounding the blast site. For denser rock or soil, the seismic propagation velocities and associated frequencies will be high. In soft rock or where thick surface soils exist (alluvial valley floors or glacial tills), the seismic propagation velocities and frequencies will be slower (ISEE 2012). The seismicity of blasting involves different types of waves traveling through earth (i.e., body waves and surface waves). These waves travel at different velocities and frequencies and have different physical characteristics. The site geology determines which of these wave types dominate and in what form.

Another factor that can influence the response of the geology to the ground motion is acoustic impedance. Acoustic impedance is the resistance the energy encounters in moving from one medium to another. Rock properties such as acoustic velocities and densities can affect vibration in a similar way to confinement by the stemming used in a blasthole to fill in the space left between the top of the explosive column and surface. The stemming is usually bulk material like gravel or drill cuttings.

The geological characteristics of the site were obtained from a previous geological assessment. The lithological cross section, Figure 5-3, consists of 12 m (40 ft) of tertiary Carlin material, 200 m (650 ft) of bool material, 91 m (300 ft) of upper mud (UM), 61 m (200 ft) of soft deformation (SD), 46 m (150 ft) of planar, 122 m (400 ft) of wispy, and approximately 152 m (500 ft) of Limestone rock; this geological diversity may be of concern.

Before analyzing the case study, knowledge of earthquake engineering design provides useful guidelines to the problem of this thesis. A brief description of earthquake engineering design is given in “Seismic Design of Structures,” Chapter 6.

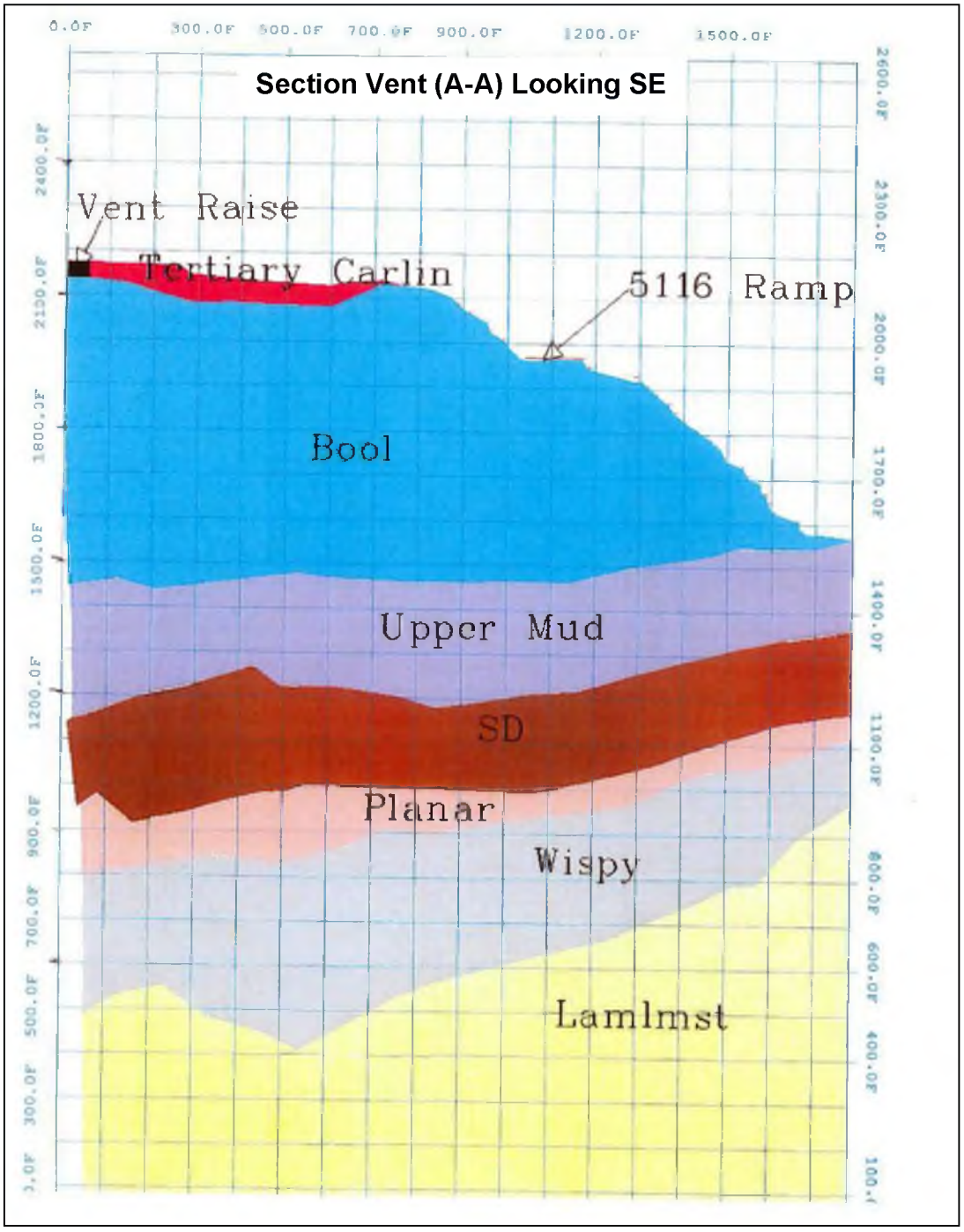

Figure 5-3 Lithology in the area of the case study

6. SEISMIC DESIGN OF STRUCTURES

In seismic design of buildings, bridges, and other structures, state regulations require the inclusion of the seismic load in the design. The ground vibration produced at a specific site by an earthquake is dependent on the proximity of the site to the source, on the site characteristics, and on the attenuation of the peak acceleration. To categorize the motion, the amplitude, frequency composition, and duration of vibrations are required and these are obtained at specific locations from strong motion accelerograms. The records are used to demarcate areas or zone with similar potential earthquake hazards taking into account frequency of occurrence, predication of the maximum earthquake magnitude, the probability of exceeding this magnitude, distance from the source, location of the source fault, and the geological details of the area. The U.S. Geological Survey keeps seismic hazard maps of the continental United States of America.

For design purposes, the basic ground motion is defined as the motion with a 10% probability of being exceeded in 50 years. This implies a recurrence interval of 475 years and the effective peak acceleration may be determined from a site-specific analysis or from the hazard map shown in Figure 6-1. The map of the USA is divided into five seismic zones with seismic Zone 4 corresponding to an effective peak acceleration of 0.4g and seismic Zone 1 corresponding to an effective peak acceleration of 0.075 g.

6.1 Structural Dynamic Analysis

The response of structures to dynamic loading is called structural dynamics and is produced by seismic forces. The member forces produced in a structure by gravity loads are static forces which are time independent. Seismic forces are produced in a structure by a variable

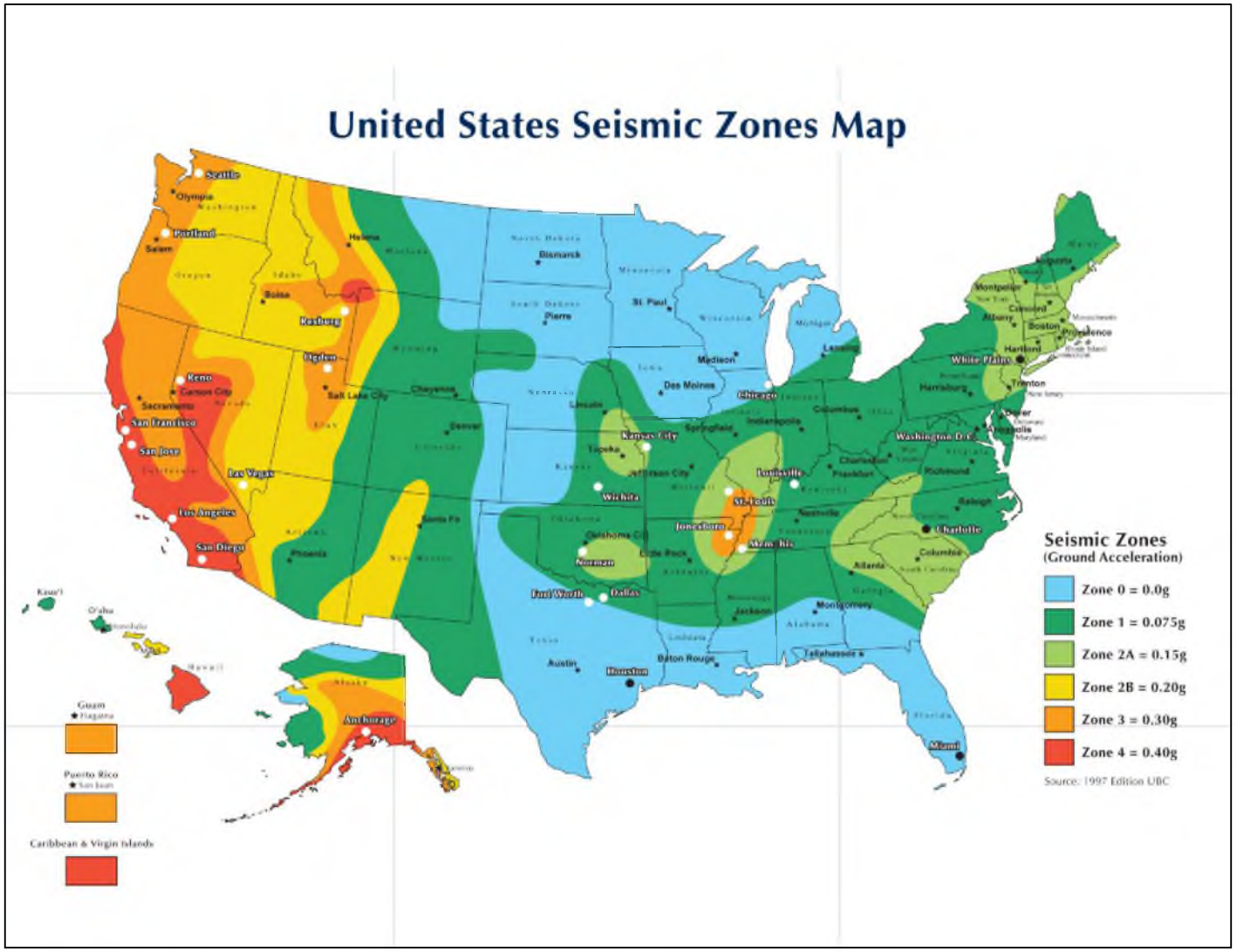

Courtesy of United States Geological Survey 2012
Figure 6-1 Seismic zone map of the United States

ground vibration, which causes a time dependent response in the structure. The response depends on the magnitude, duration, harmonic content of the excited ground motion, the dynamic properties of the structure, and the characteristics of the soil deposits at the site. Depending on the period of vibration *T,* the ground vibration is amplified in the structure to a greater or lesser extent. The damping effect, or frictional resistance of the structure to the imposed vibration, influences the magnitude and duration of the induced motion and a 5% damping is customarily assumed for normal buildings. The response spectrum is a graph of the maximum, or spectral response of a range of single-degree-of-freedom (SDOF) system to a particular motion as a function of the period or frequency of the vibration. The response may be expressed in terms of acceleration, velocity or displacement. The maximum values of each of these parameters depend only on the natural frequency and damping ratio of the SDOF. The maximum values of acceleration, velocity and displacement are referred to as *the* spectral acceleration *Sa*, spectral velocity *Sv,* spectral displacement *Sd,* respectively. The relationship between these functions may be determined by noting that when a node attains its maximum *Sd* the Sv is zero and the maximum inertial force equals the spring force (Williams 1997). Hence:

$$mSa = k\,Sd; \qquad \textit{(Equation 6.1)}$$

and since $w^2 = k/m$ *or* $\sqrt{k\ g/W}$;

$$Sa = \omega^2\,Sd \qquad \textit{(Equation 6.2)}$$

$$Sv = \omega\,Sd \qquad \textit{(Equation 6.3)}$$

where

Sa = spectral acceleration, g's

Sv = spectral velocity, m/sec (ft/sec)

Sd = spectral displacement, mm (in)

ω = *natural frequency, Hz*

k = stiffness, N/mm, (lbf/in)

6.1.1 Response Spectra

A response spectrum is a plot of the maximum S_d, S_a or S_v versus the natural period of a single degree of freedom system. The response spectra are a collection of response spectrum for varying damping ratios or soil types. This information can then be used by the structural engineer in the design of building structures. The increase in damping ratio "flattens out" the response curve. The more damping that is present, the lower the acceleration response will be for that particular structure's period.

6.1.2 Resonance

Resonance is a phenomenon that occurs when the dominant period of vibration (or frequency) of seismic events match the structure's natural period of vibration; when this happens, the intensity of the seismic event can be greatly amplified.

The Uniform Building Code (1997) allows for two basic design approaches to the earthquake-resistance of structures: a static approach in which the effects of ground motions are represented by lateral forces, and a dynamic approach in which ground motion is characterized by a design response spectra.

The static approach is only applicable to certain conditions of geometric regularity, occupancy and height. The static approach is based on determination of a design base shear, which is then distributed in a specified pattern over the height of the structure for structural analysis of lateral load resistance. The determination of lateral forces is based on the Newton's law, as written in Equation 6.4.

$$F = M \, x \, Sa = \left(\frac{W}{g}\right) Sa \qquad \textit{(Equation 6.4)}$$

the total design base shear V then, is given by Equation 6.5:

$$V = (Cv \, I \, / \, RT) \, W \qquad \textit{(Equation 6.5)}$$

where

C_v = velocity based ground response coefficient for a specific zone and soil profile

I = importance factor, 1.0 to 1.25

R = response modification factor, 2.2 to 8.5

T = structure's natural period, s

W= seismic Dead Load, N (lbf)

The above criteria are based on seismic coefficients that depend on proximity to active faults, site characteristics like local geology and soil characteristics, and the structures occupancy category, configuration, structural system (past performance and ductility) and height. The seismic coefficients C_a and C_v are dependent on soil type and effective peak acceleration, which represents the amplified acceleration as influenced by soil type.

The Uniform Building Code (1997) defines five soil profile types based on the average soil shear wave velocity, v_s, and a sixth type which requires a soil specific evaluation. The soil profiles are given in Table 6-1.

The first four classification soil profile types S_A, S_B, S_C, and S_D, are based on the average condition of the material that exists at the site from ground surface to a depth of 30 m (100 ft) in terms of shear wave velocity, standard penetration test $(N_1)_{60}$ values, and undrained shear strength. For the fifth soil type S_E, the classification is also based on engineering properties of the site but includes, in addition, sites that contain a clay layer thicker than 3 m (10 ft) having plasticity index > 20, water content ≥ 40%, and undrained shear strength < 24 Kpa (500 lb/ft^2).

Finally, sites with soil profile S_F are sites that require a site-specific evaluation and are vulnerable to potential failure or collapse under seismic loading such as liquefiable soil, quick and highly sensitive clays, and collapsible weakly cemented soils.

The dynamic approach is a thorough process that involves analyzing the structure response to ground motion with single and multiple degrees of freedom. The dynamic approach of the Uniform Building Code (1997) allows the response of the structure to be determined by a response spectrum analysis or by time history analysis.

Table 6-1 Soil profile type classification

Soil Profile	Description	Shear wave velocity m/sec (ft/sec)
S_A	Hard Rock	1524 (5000)
S_B	Rock	762 (2500) to 1524 (5000)
S_C	Soft Rock	365 (1200) to 762 (2500)
S_D	Stiff Rock	183 (600) to 1200 (365)
S_E	Soft Soil	<365 (600)
S_F	Site-specific evaluation required	

Adapted from the Uniform Building Code (1997)

The design response spectra can be determined in one of two ways: from site-specific ground response analyses or from smooth, normalized spectral shapes as shown in Figure 6-2.

The normalized spectral shapes account for frequency-dependent amplification of ground motion by different local site conditions (Williams 2003). These normalized spectra are presented for three subsurface profiles. As would be expected, the greater long-period spectral accelerations are associated with softer and deeper soil profiles, as shown in Figure 6-3. When the site is underlain by soft ground such as a soft clay or saturated clay deposit, there is an increase in peak ground acceleration and a longer period of vibration of the ground. The design response spectrum is obtained by determining the relevant response time T_s given by Equation 6.6.

$$Ts = C_v / 2.5\, C_a, \text{ if } Ts<T, \qquad \textit{(Equation 6.6)}$$

where

T_s = *relevant response time, sec*

C_a, C_v = *seismic coefficients*

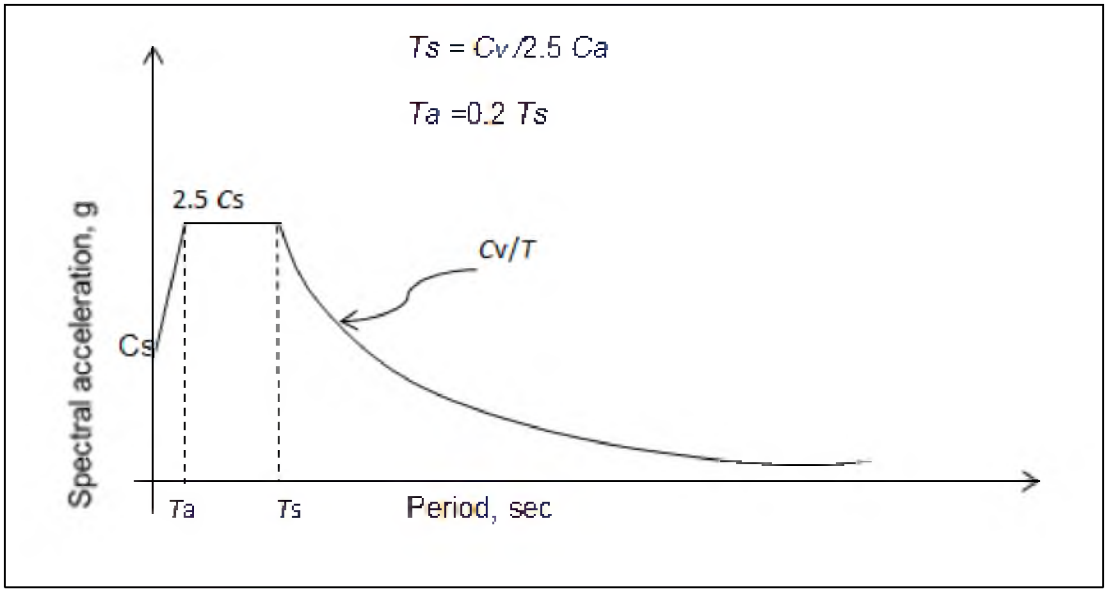

Adapted from the Uniform Building Code 1997
Figure 6-2 Response spectra

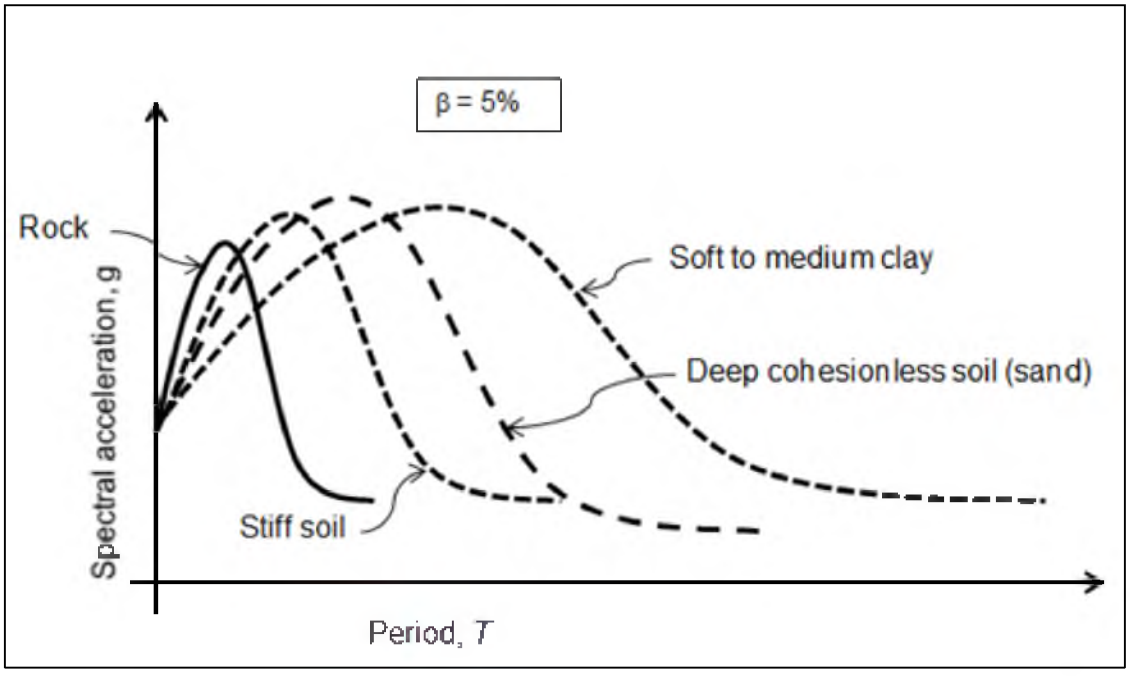

Adapted from Hiner 2002
Figure 6-3 Response spectra by soil type

This representation is important because it determines the level at which the structure is expected to respond elastically to ground motion based on the structure's fundamental period of vibration. For design purposes, the Uniform Building Code (1997) defines the procedure to construct the response spectra (shown in Figure 6-2). This technique uses the ground response coefficients C_a and C_v, which are dependent on the soil type. The coefficient C_a defines short period portion of the spectrum for structures with a fundamental period of less than $C_v/2.5\ C_a$. The velocity-related acceleration coefficient C_v defines the longer periods and constant-velocity portion of the spectrum. Both C_a and C_v equate to the effective peak acceleration for a structure on a foundation of soil profile S_B except for locations in seismic Zone 4 within 15 km (10 mi) from the source. Values of C_a and C_v, are given in Tables 16-Q and 16-R provided in the Uniform Building Code (1997). Figure 6-3 depicts characteristic curves for a site at Zone 4 and a distance no less than 15 km (10 mi) from an active fault, the response spectra provides curves for four different soil types. In seismic Zone 4, the near-source ground motion can significantly exceed motions some distance less than 15 km (10 mi) from the source. This is caused by a rapid progression of the fault rupture along the fault, which increases ground motion perpendicular to the fault.

In summary, the Uniform Building Code (1997) outlines an easy approach to prepare a response spectrum. First the seismic zone is determined, then the soil profile is determined and finally seismic coefficients C_a and C_v are determined. At a period of zero, the spectral acceleration is equal to C_a. The spectral acceleration then increases linearly to a value of 2.5 C_a. At a period of T_a, the spectral acceleration is constant until a period equal to T_s. For any period greater than T_s the spectral acceleration is equal to C_v/T where T equals the period of vibration on the horizontal axis as shown in Figure 6-2,

Once the response spectra are developed, a structure's period of vibration is used to determine in what region the structure will behave or whether the structure will respond elastically to ground motion, and the expected level of acceleration at which the structure will be subject to at a particular site for a given seismic event. Therefore the element that is key to a successful dynamic analysis consists of the knowledge of the structures fundamental period of vibration.

6.2 Structures Fundamental Period of Vibration, *T*

Determination of period of vibration in a structure is essential to protect the integrity of the structure when subject to ground motion. When building structures are subject to ground motion, their elements will produce a concentration of torsional stresses. The structures period *T* represents the elastic fundamental period of vibration in the direction under consideration. As described in "Structural Dynamic Analysis," section 6.1, the response spectra helps to determine the acceleration at which a structure will be subject to depending on site and seismic event characteristics. Therefore, the next step is to obtain the structure's period of vibration *T*. The Uniform Building Code (1997) defines two methods to obtain the period of vibration: Method A and Method B.

6.2.1 Method A

For all buildings, the value of *T* may be approximated from Equation 6.7.

$$T = Ct(h_n)^3 \qquad \textit{(Equation 6.7)}$$

where

Ct = 0.035 for steel MRF

Ct = 0.030 for reinforced concrete MRF or steel EBF's

Ct = 0.020 for all other building

h_n *= height of the building, m (ft)*

6.2.2 Method B

The fundamental period of vibration *T* may be calculated using the structural properties and deformation characteristics of the resisting elements in a properly substantiated analysis. The value of *T* may be computed from Equation 6.8.

$$T = 2\pi \sqrt{\frac{\sum wi\ \delta i^2}{g \sum fi * \delta i}} \qquad \textit{(Equation 6.8)}$$

where

$wi =$ *dead load at level i, N (lbf)*

$\delta_i =$ *elastic deflection for applied force f, mm (in)*

$f_i =$ *lateral force at level I, N (kips)*

$g =$ *acceleration due to gravity, mm/sec^2 (in./sec^2)*

The lateral force *fi* represents any lateral force distribution on the structure that increases with height. If only the fundamental mode shape is considered, the lateral force at level x is then given by Equation 6.9 (Uniform Building Code 1997).

$$Fx = \frac{(V-Ft)wihx}{\Sigma wihi} \qquad \textit{(Equation 6.9)}$$

where

Fx = *lateral force at level x, N (lbf)*

$hi =$ *height at level i, m (ft)*

wi = *dead load at level i, N (lbf)*

V = *Base shear, N (lbf)*

Ft = *Force at top of level, N (lbf)*

hx = *height above the base to level x, m (ft)*

The Recommended Lateral Forces Requirements and Commentary (SEAC 1999) defines rigid-nonbuilding structures as structural systems with a period of vibration in the order of 0.06 seconds. In terms of frequency, this value equals 16.67 Hz. This is of importance in the case study. If an assumption is made that the structure-rock system will behave as a rigid structure, then the resulting period of vibration equals 0.06 seconds, so the natural frequency of the structure-rock is approximately 16.67 Hz. Therefore, resonance can be expected at this frequency level. If resonance occurs, the amplitude of the seismic event can be greatly amplified as explained in “Resonance”, section 6.1.2.

Similarly, the case study may use a similar approach to the one presented by the Uniform Building Code (1997). This could be done by assuming the earthquake force is the actual force generated by the blast and the dynamic response of the shaft to the vibration can be analyzed by calculating the period of vibration of the shaft structure and the corresponding acceleration corresponding to that vibration mode. However, it would be necessary to create a response spectrum of the shaft structure that would determine at what elastic region the structure is expected to behave. Furthermore, the interaction between the shaft and the surrounding soil or rock needs to be taken into consideration.

In blasting, it is possible to determine the period of vibration generated by a blast, a peak particle velocity and response spectra by monitoring blasting operations.

As mentioned in “Seismic Design of Structures,” Chapter 6 the most important factor in the design of a structure is its ability to withstand ground movement. This design can be accomplished by accurately choosing the structure configuration by which lateral loads will eventually leave the structure. The Uniform Building Code (1997) defines structures as regular and irregular; irregular structures require special analysis or design features, and regular structures do not.

In the case study, the concrete shaft’s geometry is well defined. The fact that it is a long narrow structure makes it very difficult to classify as a standard type, but some assumptions can be made. For instance, if the structure is assumed to be rigid, forces of magnitude $f = ma$ would be generated in it, where m is the mass of the structure-rock system and its period would be 0.06 sec (rigid structures), the blasting frequencies would then need to be in the order of 17 Hz or greater to avoid resonance.

In summary, lateral force procedures for nonbuilding structures with structural systems similar to those of buildings should be based on appropriate ground motion representation, should be performed using accepted principles of dynamics as stated in the Uniform Building Code § 1630, and the load combination factors of stress design (SD) or load resistant factored design (LRFD), or the Uniform Building Code § 1612.3 for allowable stress design (ASD). The

fundamental period should be determined by rational methods such as Method B in “Seismic Design of Structures” or Uniform Building Code § 1630.2.

7. DATA ANALYSIS

The experiment consisted of two blasts, a signature blast and a production blast. The signature blast involved a blasthole 12-m (40-ft) deep and 241 mm (9.5 in.) in diameter with 5.18 m (17 ft) of stemming loaded with 270 kg (596 lb) of ammonium nitrate (NH_4NO_3) fuel oil (FO) or ANFO explosive. The production blast consisted of a pattern design with 300 blastholes loaded with an equivalent maximum charge weight of 1632 kg (3600 lb) of ANFO per 8-ms delay. The delay timing included 17 ms between adjacent holes and 34 ms between rows with same blasthole dimensions as the signature blast in terms of diameter, depth, and confinement.

The experiment was successful and vibration levels were recorded with the installed monitoring devices spaced at 50 m (150 ft), 70 m (230 ft), 120 m (395 ft), 145 m (475 ft), 220 m (721 ft), 254 m (834 ft), and 313 m (1030 ft), respectively, and arranged radially from the blasthole to the vent shaft wall.

7.1 Monitoring Devices

The monitoring devices included industry accepted seismographs manufactured by White Industrial Seismology, Inc. Model Mini Seis III, as shown in Figure 7-1. These devices have waveform modes with sample rates of 1024, 2048 and 4096, dynamic seismic range from 0.25 mm/sec (0.005 in./sec) to 508 mm/sec (20 in/sec), dynamic linear acoustic range from 58 (0.02 millibars) to 160 db (20.48 millibars), and serial communication with serial baud rates up to 230400. The devices have a frequency range from 1-350 Hz, trigger levels of 0.127 mm/sec (0.005 in./sec) for seismic and 88 db (10.24 millibars) for acoustic, and a standard accuracy DIN 45669-1 that conforms with “Performance Specification for Blasting Seismographs” (ISEE 2009).The units can store up to 1000 records ranging from 1 to 60 seconds duration.

Figure 7-1 Seismographs

7.2 Data Acquisition

The data was downloaded from each monitoring device by connecting the devices to a computer and using the data analysis software, White Data Analysis V11 by White Industrial Seismology, Inc. The software calculates the PPV, and the radial, transverse, and longitudinal frequencies from the resulting waveforms. It uses the Fast Fourier Transform to obtain dominant frequencies, and produces a printable file with numerical and graphical results, as illustrated in Figure 7-2. The numerical values were then imported in an Excel spreadsheet, as listed in Table 7-1, and analyzed by statistical methods. The location of the seismographs in relation to the signature blast is shown in Figure 7-3.

7.3 Data Interpretation

The next step in analyzing the vibration levels was to obtain the site-specific prediction equation. The data were plotted in a log-log scale where the x-axis was the PPV and the y-axis the distance from the blast, as shown in Figure7-4.

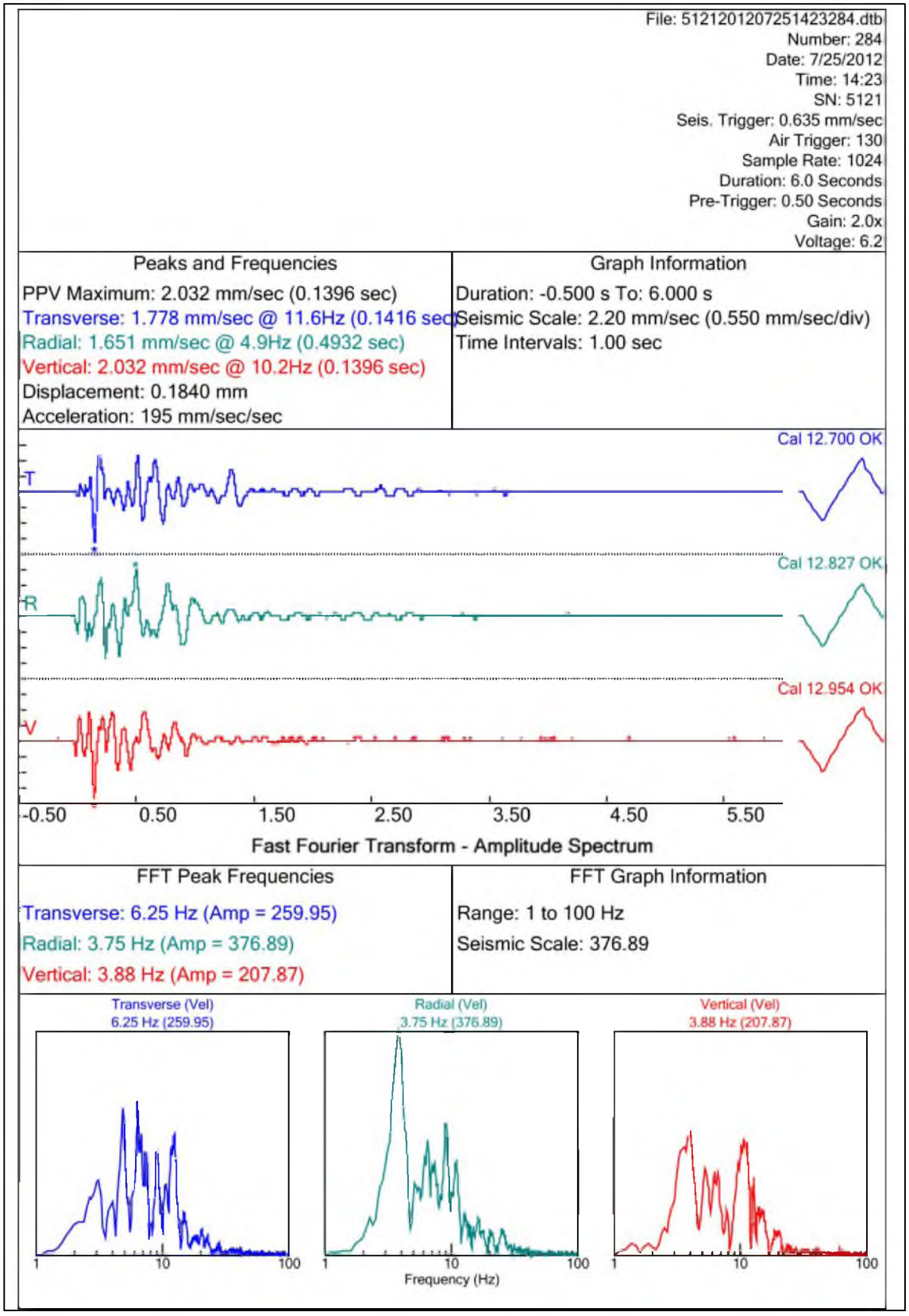

Figure 7-2 Typical output file

Table 7-1 Vibration data

Seismograph ID	Distance from blast	SD	Radial PPV	Vertical PPV	Transverse PPV	Max PPV	Vector Sum	Dominant Radial frequency	Dominant Vertical frequency	Dominant Transverse frequency
	m	$m/lb^{1/2}$	mm/sec	mm/sec	mm/sec	mm/sec	mm/sec	Hz	Hz	Hz
5118	50	3	79	58	50	79	110	5	12	5
5119	70	4	48	22	39	48	65	5	9	7
5120	120	7	41	13	22	41	48	6	10	8
4263	145	9	15	14	13	15	25	6	6	5
3029	220	13	6	4	6	6	9	5	10	5
3448	254	15	4	3	3	4	6	4	6	5
5121	313	19	2	2	2	2	3	4	4	6

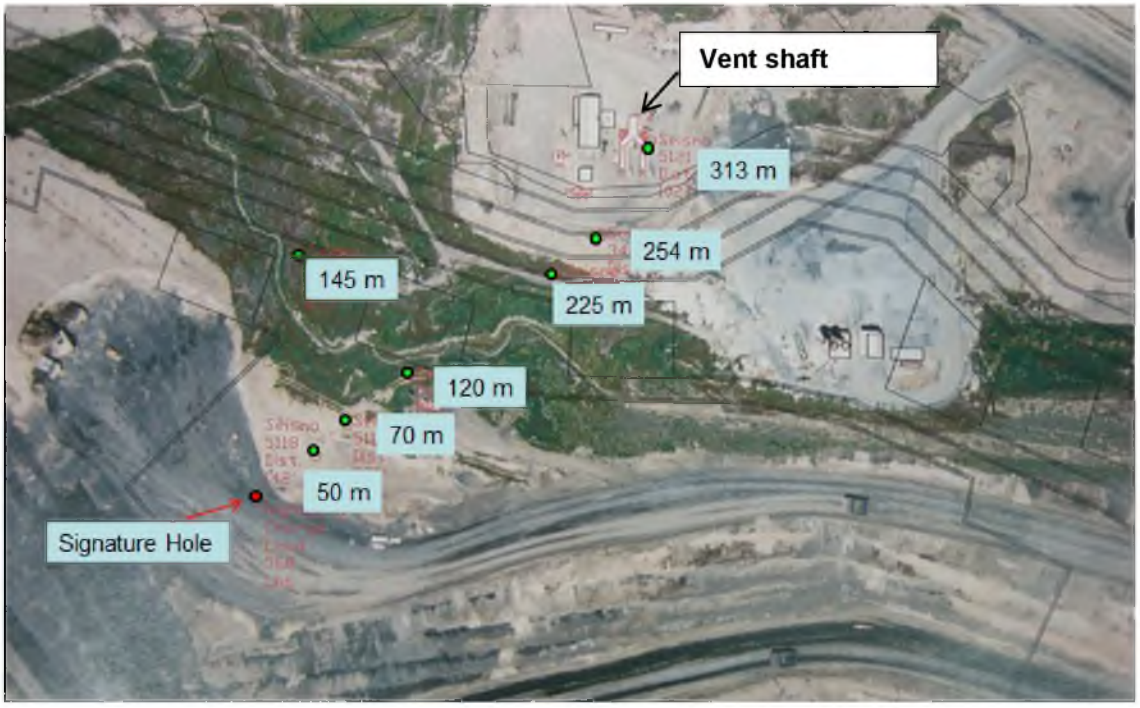

Figure 7-3 Signature blast and seismograph coordinates

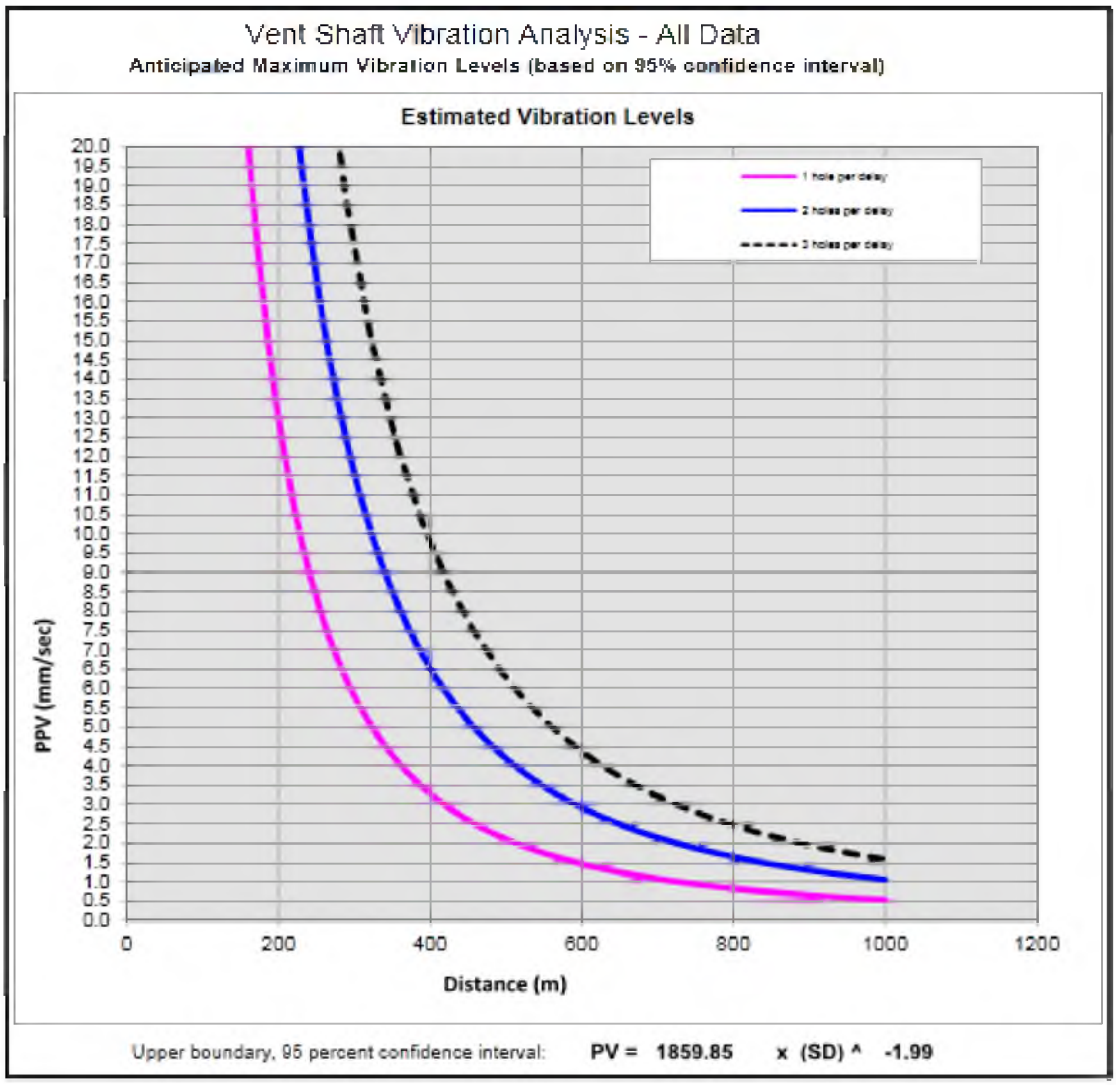

Figure 7-4 PPV versus distance plot for signature blast

As expected, the PPV decreased exponentially with distance. As an observation, the same would occur if the charge remained unchanged and the number of holes detonated within a delay period increased to two or three holes. Although this approach is useful, it is hard to explain the change in vibration if the charge weight is not included so a more realistic approach would be to normalize the distance. This was accomplished by including the charge weight using SD_2 obtained from Equation 7.1, and plotting the resulting SD_2 versus PPV in a log-log scale graph as illustrated in Figure 7-5. Since the curve is now in linear form and using statistical methods, prediction equations can be obtained with a certain level of confidence.

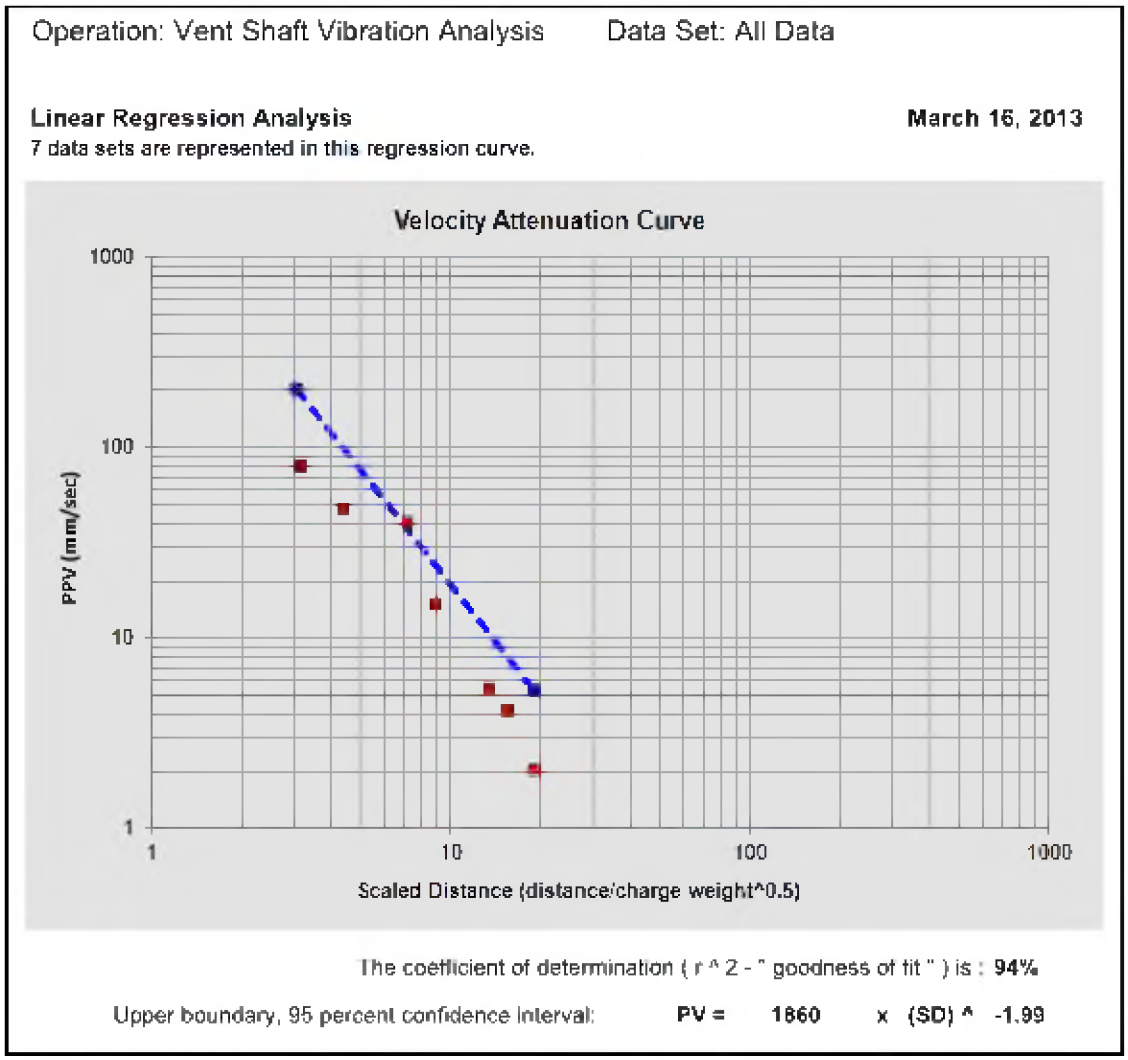

Figure 7-5 PPV versus scaled distance showing upper bound line

$$SD_2 = R / W^{1/2} \qquad \text{(Equation 7.1)}$$

The dashed line in Figure 7-5 is the upper bound of the 95% confidence level, fitted by linear regression. If a best fit curve is used, the line becomes the one shown in Figure 7-6, which is the average approximation (50% confidence level). The upper bound line is parallel to the best fit line. However, PPV predictions made with the equation of the upper bound line will be higher than predictions made by the best fit equation. It is often recommended to use the upper bound line because it represents a more conservative design. In practice, however, predictions made with the upper bound line equation can become difficult to accomplish. They involve lowering the blast charge to levels that may not be adequate for other purposes such as energy distribution

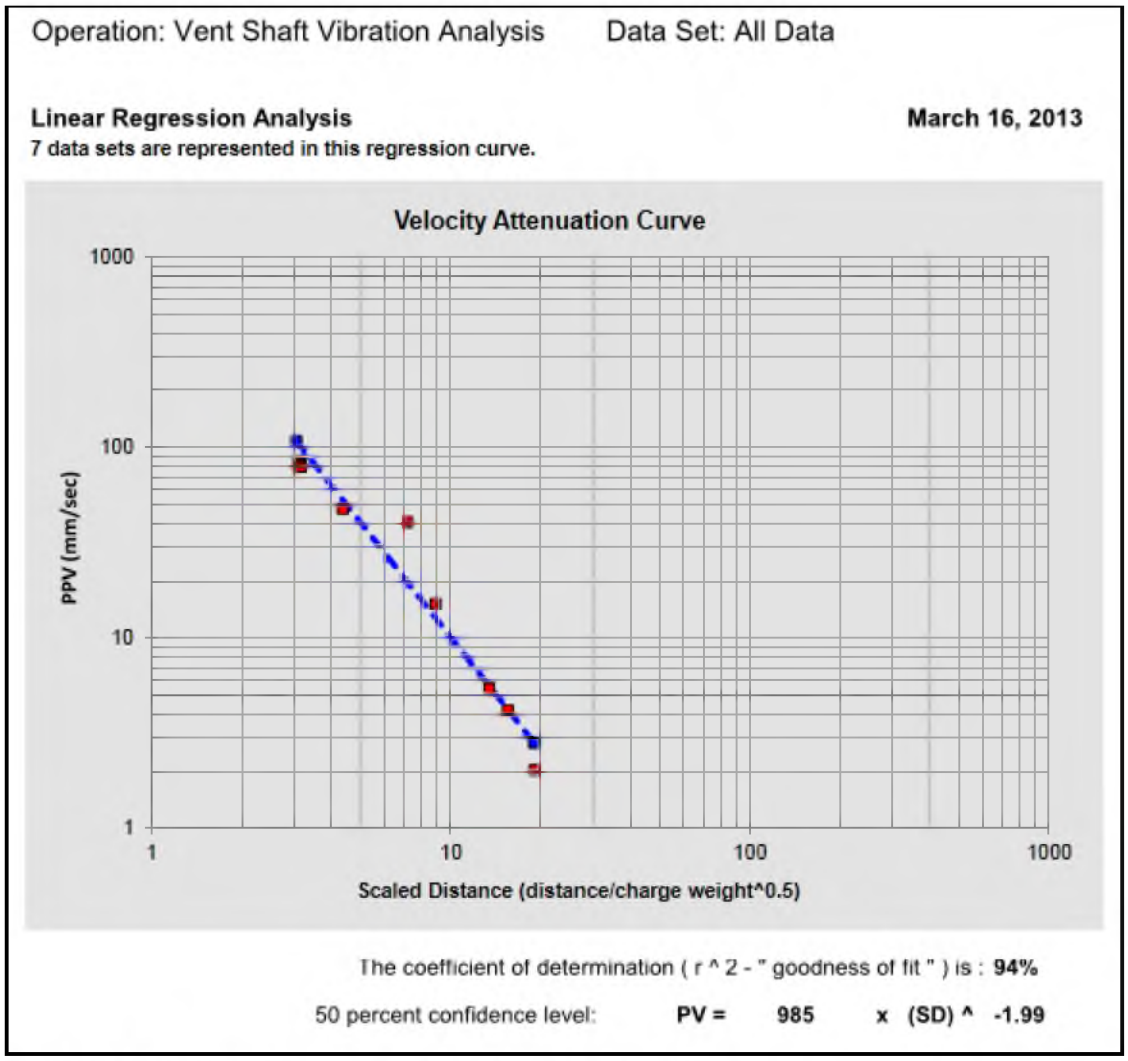

Figure 7-6 PPV versus scale distance showing best fit line

or fragmentation.

Similarly, the results of the production blast were also collected. The locations of the seismographs in relation to the signature blast are shown in Figure 7-7, and the resulting log-log PPV versus SD_2 graphs are shown in Figures 7-8 and 7-9 respectively. PPV Frequencies from the production blast were very low compared to those in the signature blast. This fact was mainly due to the proximity of the blast to the monitoring devices. The resulting attenuation equations are listed at the bottom of the log-log graphs of their respective figures.

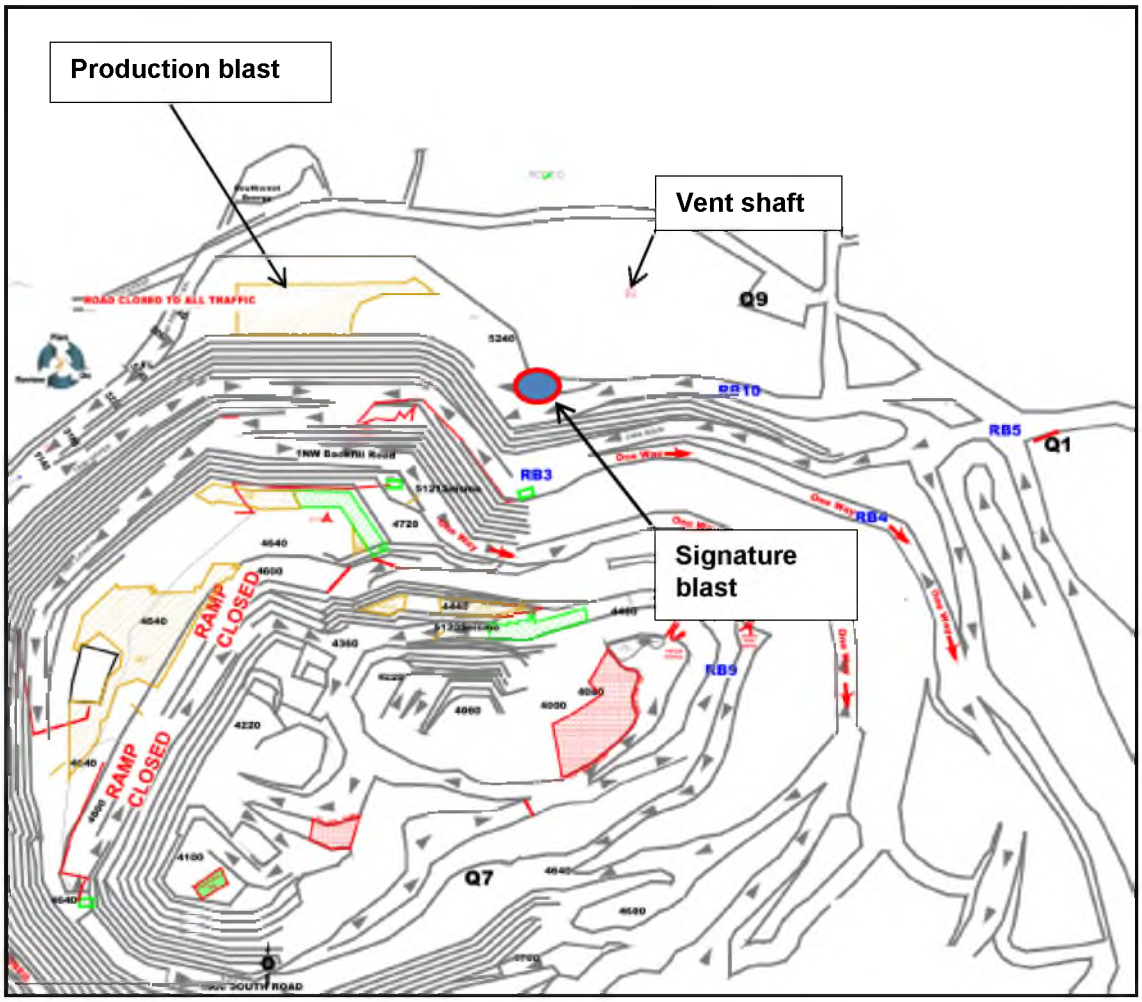

Figure 7-7 Production blast and signature blast map

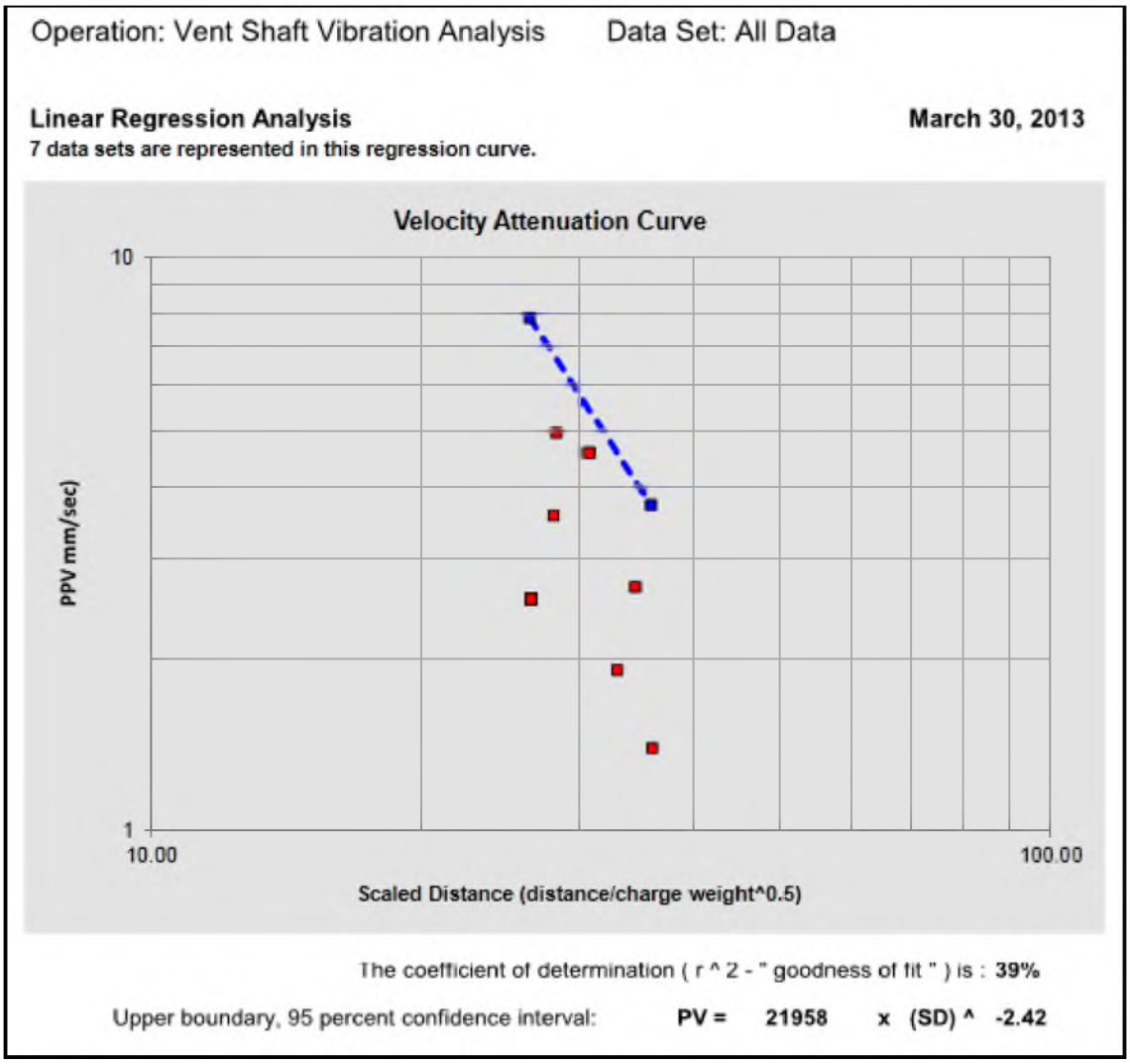

Figure 7-8 PPV versus scaled distance for production blast showing upper bound line

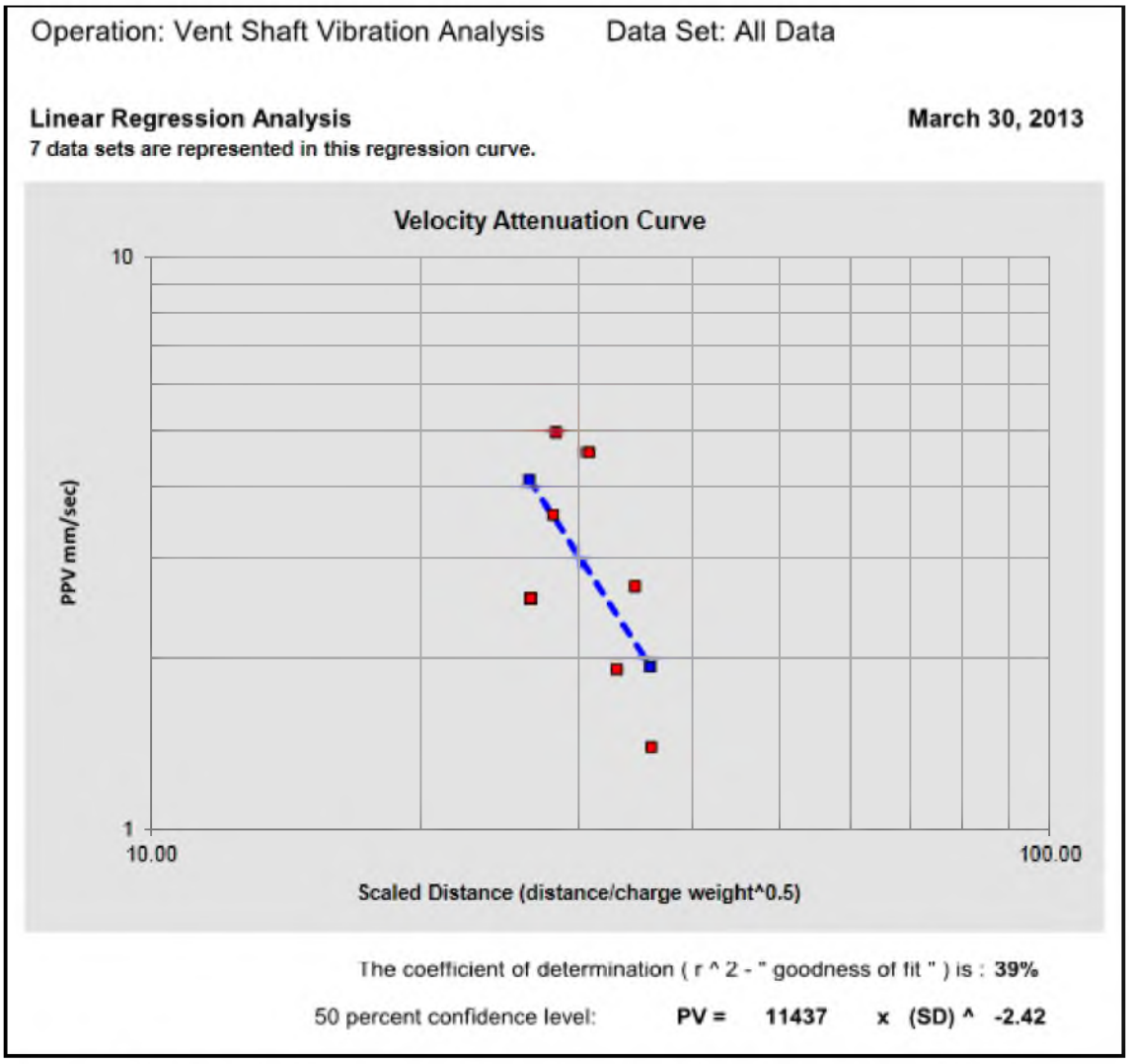

Figure 7-9 PPV versus scaled distance for production blast showing best fit line

8. ANALYSES OF RESULTS

Based on the results obtained from the signature blast, it can be inferred that the peak particle velocity does correlate well with respect to the proximity to the point of interest. For this data set, a regression analysis yielded the PPV attenuation equation that takes the form of Equation 8.1, where r^2 equals 0.94. Thus, scale distance is a good predictor of ground vibrations. This equation represents the upper bound of an envelope that encompasses 95% of the data set. The upper bound is parallel to the best fit line. Predictions made by the upper bound line should be higher than predictions made by the best fit equation.

$$PPV = 1860\ SD_2^{-1.99} \qquad \textit{(Equation 8.1)}$$

If the best fit line was used (50% confidence interval), the regression would yield Equation 8.2:

$$PPV = 985\ SD_2^{-1.99} \qquad \textit{(Equation 8.2)}$$

As expected, the predictions made by the upper bound line (Table 8-1) are higher than those of the best fit line (Table 8-2), and since the best fit line results in a lower confidence interval (50%), care must be taken if the best fit line is used in analysis. Thus, the upper bound line produces higher predictions than the best fit line, results from this equation will be used in the analysis.

Based on the results of the signature blast, the resulting PPV (mm/sec) is average and the frequencies values are significantly low. Therefore, there is a potential for structural damage if

Table 8-1 Maximum charge weight chart, upper bound line

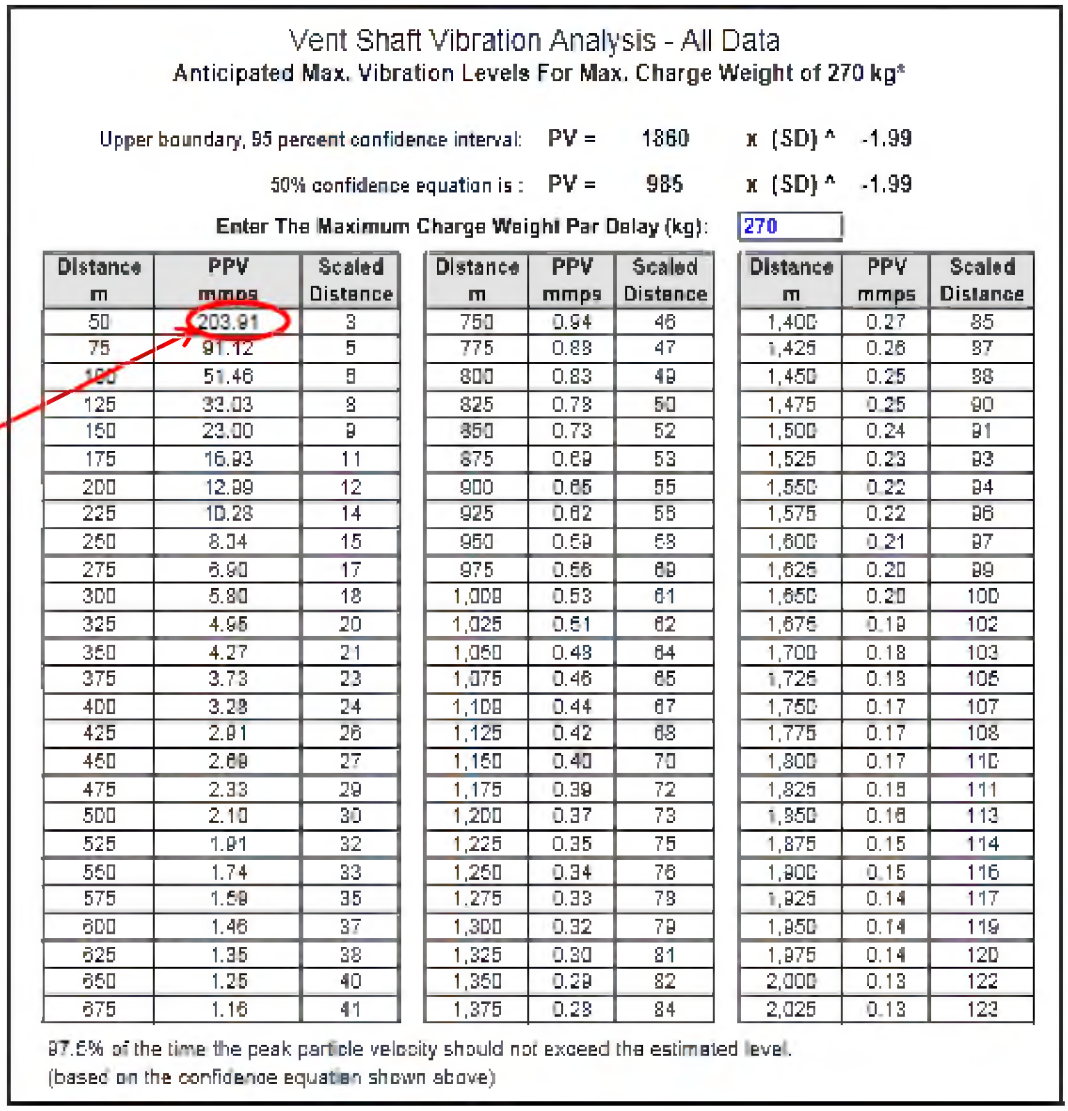

Vent Shaft Vibration Analysis - All Data

Anticipated Max. Vibration Levels For Max. Charge Weight of 270 kg*

Upper boundary, 95 percent confidence interval: PV = 1860 x (SD) ^ -1.99

50% confidence equation is : PV = 985 x (SD) ^ -1.99

Enter The Maximum Charge Weight Per Delay (kg): 270

Distance m	PPV mmps	Scaled Distance	Distance m	PPV mmps	Scaled Distance	Distance m	PPV mmps	Scaled Distance
50	203.91	3	750	0.94	46	1,400	0.27	85
75	91.12	5	775	0.88	47	1,425	0.26	87
100	51.46	6	800	0.83	49	1,450	0.25	88
125	33.03	8	825	0.78	50	1,475	0.25	90
150	23.00	9	850	0.73	52	1,500	0.24	91
175	16.93	11	875	0.69	53	1,525	0.23	93
200	12.99	12	900	0.65	55	1,550	0.22	94
225	10.28	14	925	0.62	56	1,575	0.22	96
250	8.34	15	950	0.59	58	1,600	0.21	97
275	6.90	17	975	0.56	59	1,625	0.20	99
300	5.80	18	1,000	0.53	61	1,650	0.20	100
325	4.95	20	1,025	0.51	62	1,675	0.19	102
350	4.27	21	1,050	0.48	64	1,700	0.18	103
375	3.73	23	1,075	0.46	65	1,725	0.18	105
400	3.28	24	1,100	0.44	67	1,750	0.17	107
425	2.91	26	1,125	0.42	68	1,775	0.17	108
450	2.60	27	1,150	0.40	70	1,800	0.17	110
475	2.33	29	1,175	0.39	72	1,825	0.16	111
500	2.10	30	1,200	0.37	73	1,850	0.16	113
525	1.91	32	1,225	0.35	75	1,875	0.15	114
550	1.74	33	1,250	0.34	76	1,900	0.15	116
575	1.59	35	1,275	0.33	78	1,925	0.14	117
600	1.46	37	1,300	0.32	79	1,950	0.14	119
625	1.35	38	1,325	0.30	81	1,975	0.14	120
650	1.25	40	1,350	0.29	82	2,000	0.13	122
675	1.16	41	1,375	0.28	84	2,025	0.13	123

97.5% of the time the peak particle velocity should not exceed the estimated level.
(based on the confidence equation shown above)

Table 8-2 Maximum charge weight, best fit line

Vent Shaft Vibration Analysis - All Data

Anticipated Max. Vibration Levels For Max. Charge Weight of 270 kg*

50 percent confidence level: PV = 985 x (SD) ^ -1.99

50% confidence equation is : PV = 985 x (SD) ^ -1.99

Enter The Maximum Charge Weight Per Delay (kg): 270

Distance m	PPV mmps	Scaled Distance	Distance m	PPV mmps	Scaled Distance	Distance m	PPV mmps	Scaled Distance
50	108.04	3	750	0.50	46	1,400	0.14	85
75	48.28	5	775	0.47	47	1,425	0.14	87
100	27.26	6	800	0.44	49	1,450	0.13	88
125	17.50	8	825	0.41	50	1,475	0.13	90
150	12.18	9	850	0.39	52	1,500	0.13	91
175	8.97	11	875	0.37	53	1,525	0.12	93
200	6.88	12	900	0.35	55	1,550	0.12	94
225	5.44	14	925	0.33	56	1,575	0.11	96
250	4.42	15	950	0.31	58	1,600	0.11	97
275	3.65	17	975	0.30	59	1,625	0.11	99
300	3.07	18	1,000	0.28	61	1,650	0.10	100
325	2.62	20	1,025	0.27	62	1,675	0.10	102
350	2.26	21	1,050	0.26	64	1,700	0.10	103
375	1.97	23	1,075	0.24	65	1,725	0.10	105
400	1.74	24	1,100	0.23	67	1,750	0.09	107
425	1.54	26	1,125	0.22	68	1,775	0.09	108
450	1.37	27	1,150	0.21	70	1,800	0.09	110
475	1.23	29	1,175	0.20	72	1,825	0.09	111
500	1.11	30	1,200	0.20	73	1,850	0.08	113
525	1.01	32	1,225	0.19	75	1,875	0.08	114
550	0.92	33	1,250	0.18	76	1,900	0.08	116
575	0.84	35	1,275	0.17	78	1,925	0.08	117
600	0.78	37	1,300	0.17	79	1,950	0.07	119
625	0.72	38	1,325	0.16	81	1,975	0.07	120
650	0.66	40	1,350	0.15	82	2,000	0.07	122
675	0.61	41	1,375	0.15	84	2,025	0.07	123

50% of the time the peak particle velocity should not exceed the estimated level.
(based on the confidence equation shown above)

the structure-rock system is assumed rigid. Furthermore, a dynamic analysis like the one mentioned in “Seismic Design” section of the Uniform Building Code (1997) is not applicable since the magnitude and time-histories of the blast are significantly smaller than that of an earthquake and the underlying rock is much stronger than soft-soils. Therefore, another approach to analyzing potential for structural damage is necessary. Thus, an analysis of concrete under dynamic loading is necessary to find out if there is a potential for damage to the shaft structure.

8.1 Damage Analysis

Damage will be observed once the ground vibration exceeds a certain level. Various investigators have associated damage to vibration levels close to the blast. Langefors and Kihlostrom (1973) proposed a PPV threshold of 610 mm/sec (24 in./sec) for formation of new cracks on rocks; Oriard (1982) proposed a threshold of 635 mm/sec (25 in./sec).

For hard rock, the peak particle velocity for the onset of cracking is close to 1000 mm/sec (39.37 in./sec). For fractured rockmasses, the maximum PPV is estimated one-fourth of what is calculated for intact rock (Calder and Larocque 1977).

In the case study, however, the criteria for determining damage thresholds must be defined based on the response of the concrete shaft structure to blasting and the interaction of the concrete and the surrounding media. In practice, an explosion adjacent to a concrete wall will cause a high-speed pressure wave to load the front face of the wall. A proportion of the energy will be reflected back and a significant proportion will propagate through the wall as a compressive stress wave. When this wave meets the back face of the wall there will be another reflection with some of the energy returning through the wall and some propagation into the rock. The reflection of the compressive stress wave within the concrete will give rise to a tension rebound from the back face. This could cause back face spalling as the concrete fails in tension and particles are ejected from the back surface at high speed.

Obviously, the flexural load exerted on the concrete wall face, as a result of the blast, is of particular importance in the case study, as Figure 8-1 illustrates. If spalling occurs, it could cause structural damage and expensive repairs to the underground operation. The ventilation system would have to be shut down and the whole underground mine crew evacuated to perform repairs, costing the mine significant downtime. Furthermore, based on attenuation Equation 8.1, the expected PPV at 50 m (150 ft) from the blast will result in 204 mm/sec (8 in./sec), circled in Table 8-1.

If the wave propagation velocity and the PPV are known, the ground strain can be estimated by differentiating the sinusoidal function that describes a simple harmonic wave. Since the blast wave is approximated as simple harmonic, the wave motion is defined by Equation 8.3.

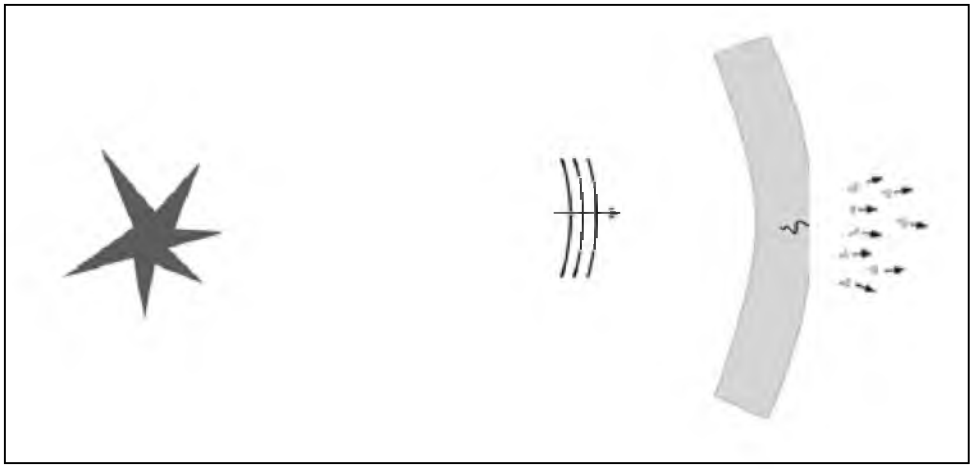

Figure 8-1 Backface spalling

$$u(x,t) = \sin(x-ct) \qquad \text{(Equation 8.3)}$$

Since *u* is the displacement of a particle in the parallel direction to propagation or movement, *x* the position, and *t* the time, the velocity is defined as the change of displacement with respect to time,

$$\dot{u} = \frac{du}{dt} = \frac{d(\sin(x-ct))}{dt} = -c\cos(x-ct) \qquad \text{(Equation 8.4)}$$

and the strain is defined as the change of displacement with respect to position,

$$\varepsilon = \frac{du}{dx} = \frac{d(\sin(x-ct))}{dx} = \cos(x-ct) \qquad \text{(Equation 8.5)}$$

by replacing Equation 8.5 in Equation 8.4, the ground strain, ε, can be expressed in terms of particle velocity and wave propagation velocity by Equation 8.6.

$$\varepsilon = \dot{u} / -c \qquad \text{(Equation 8.6)}$$

where

$\dot{u}$ = *particle velocity or PPV, m/sec (ft/sec)*

c = compressional p-wave propagation velocity or C_p*, m/sec (ft/sec)*

Propagation in the positive direction produces negative strains. As a result, the strain is compressive. Therefore, if the PPV of 204 mm/s (8 in./sec) and the compressional or P-wave propagation velocity of 1800 m/s (6000 ft/sec) are substituted in Equation 8.6, the ground strain, ε, equals 114 με. For simplicity the minus sign has been dropped.

$$\varepsilon = 204 / 1800 \times 10^3 = 114\ \mu\varepsilon$$

8.2 Strength and Serviceability

The basic criterion for strength design of concrete as indicated in ACI 9.1.1 (American Concrete Institute 2008) requires that all structural members and sections must be proportioned to meet demand under the most critical load combinations for all possible actions (flexural, axial, and shear):

Capacity ≥ Demand

Design Strength ≥ Required Strength

$$\emptyset M_n \geq M_u$$

Concrete properties are generally obtained from the applicable ASTM standards. The stress-strain relationship in the elastic region is defined by Hook's law, Equation 8.7.

$$\sigma = E\,\varepsilon \qquad \textit{(Equation 8.7)}$$

where

σ = *stress, Mpa (psi)*

E = Young's modulus, Gpa (ksi)

ε = *strain* (με)

For typical 20 Mpa concrete, Young's modulus is 22.5 x 10^3 Mpa. The concrete strength is 20 MPa in compression and 2.0 Mpa in tension. Since the Young's modulus of the rock is 22.6 x 10^3 Mpa, the ground vibration of 204 mm/s yields a wave stress, σ_{ppv}, of 2.58 Mpa. Hence:

$$\sigma_{ppv} = 22.6 \times 10^3 \times 114 \times 10^{-6} = 2.58\ \text{MPa}$$

This stress level does not exceed the allowable concrete compressive strength of 20 Mpa. However, it does exceed the allowable concrete tensile strength of 2.0 Mpa.

Based on this approach, the above analysis suggests threshold values in order to avoid exceeding the tensile strength of concrete. For example: there should be a maximum ground vibration of 158 mm/sec (6.22 in./sec) to avoid damage. This translates to a ground strain = 158 /1800x10^3 = 88 με to stay below 2.0 Mpa. Hence:

$$\sigma = 22.6 \times 10^3 \times 88 \times 10^{-6} = 1.98 \text{ Mpa} < 2.0 \text{ Mpa}$$

Alternatively, if the quasi-static tensile strain at peak, and assuming linear behavior, is given by ε_s (American Concrete Institute 2008):

$$\varepsilon_s = \sigma_t / E = 6.5\sqrt{f'c} / 57000\sqrt{f'c} = 114 \text{ με} \qquad \textit{(Equation 8.8)}$$

where

ε_s = *quasi-static strain,* με

σ_t = *quasi-static tensile strength, 2- 5 Mpa (290- 725 psi)*

E = concrete Young's modulus, 20-40 Gpa (3000 – 6000 ksi)

f'c = concrete compressive strength, 20-69 Mpa (3000 -8000 psi)

Although the quasi-static strain, ε_s, would not be exceeded by the ground strain, ε, of 114 με generated by the PPV = 204 mm/sec, some cracking would start to develop under static loading conditions. Obviously this conclusion is not valid since the ground strain is dynamic. Therefore, an analysis of ground strain under dynamic loading conditions is deemed necessary.

8.3 Dynamic Properties of Concrete

Before studying the properties of concrete under dynamic loading, it is necessary to understand its properties under static (or quasi-static) loading. The ASTM C496 tensile splitting test recommends a loading rate of 0.7-1.4 Mpa/min (100 -200 psi/min) for concrete of tensile strength in the range of 2-5 Mpa (300–700 psi), or 90–420 seconds, to fail. This is based on the

strain at peak of 114 με as seen in Equation 8.8 above. As a result, the quasi-static strain rate will be in the range of $0.26 \times 10^{-6}\ s^{-1}$ and $1.26 \times 10^{-6}\ s^{-1}$. For simplicity, the quasi-static tensile strain rate is assumed to be $1 \times 10^{-6}\ s^{-1}$.

Some studies have indicated that concrete capacity under dynamic loading conditions is different than under static (or quasi-static) loading conditions. When reinforced concrete structures are subject to blast loading, both concrete and steel are subjected to very high strain rates ranging from $10^{2}\ s^{-1}$ to $10^{3}\ s^{-1}$. Current studies have shown that these materials increase their strength significantly under dynamic conditions. In fact, they increase by more than 50% for reinforcing steel, by more than 100% for concrete in compression, and by more than 600% for concrete in tension (Malvar and Ross 1998).

The Defense Special Weapons Agency (DSWA 1997) has sponsored the numerical study of the response of reinforced concrete structures subject to blast loading. The most comprehensive model for strain rate enhancement, both in tension and compression, was presented by the Comite Euro-International du Beton (CEB 1993). For this research, the data of 46 impact tests on plain concrete at strain rates between $3 \times 10^{-6}\ s^{-1}$ and $300\ s^{-1}$ were plotted and the Dynamic Increase Factor (DIF) for both compression and tension was developed. The DIF is the ratio between the dynamic to static strength versus strain rate on a log-log scale. According to this research, the curves have a discontinuity in their slope at a strain rate of $30\ s^{-1}$, and the curve expression is valid up to a strain rate of $300\ s^{-1}$, where the DIF factor is 3.9 for 30 MPa (4350 psi) concrete.

Data by Malvar and Ross (1998) provided additional insights in the tensile range that was not previously available. The DIF varied from 1 to 7 at strain rates from $10^{-6}\ s^{-1}$ to $157\ s^{-1}$, with no increase for strain rates below 10^{-6} and a slope change at strain rate of $1\ s^{-1}$ that was proportional to $\dot{\varepsilon}^{1/3}$ (a straight line of slope 1/3 in a log-log plot). The results are illustrated in Figure 8-2 in a log-log scale. The data supports the DIF as a bilinear function of strain rate in the log-log plot, with no increase for strain rates below $10^{-6}\ s^{-1}$ instead of $30^{-6}\ s^{-1}$, as assumed by CEB (1993), and with a slope change at a strain rate of $1\ s^{-1}$ instead of at $30\ s^{-1}$, as also assumed by CEB (1993).

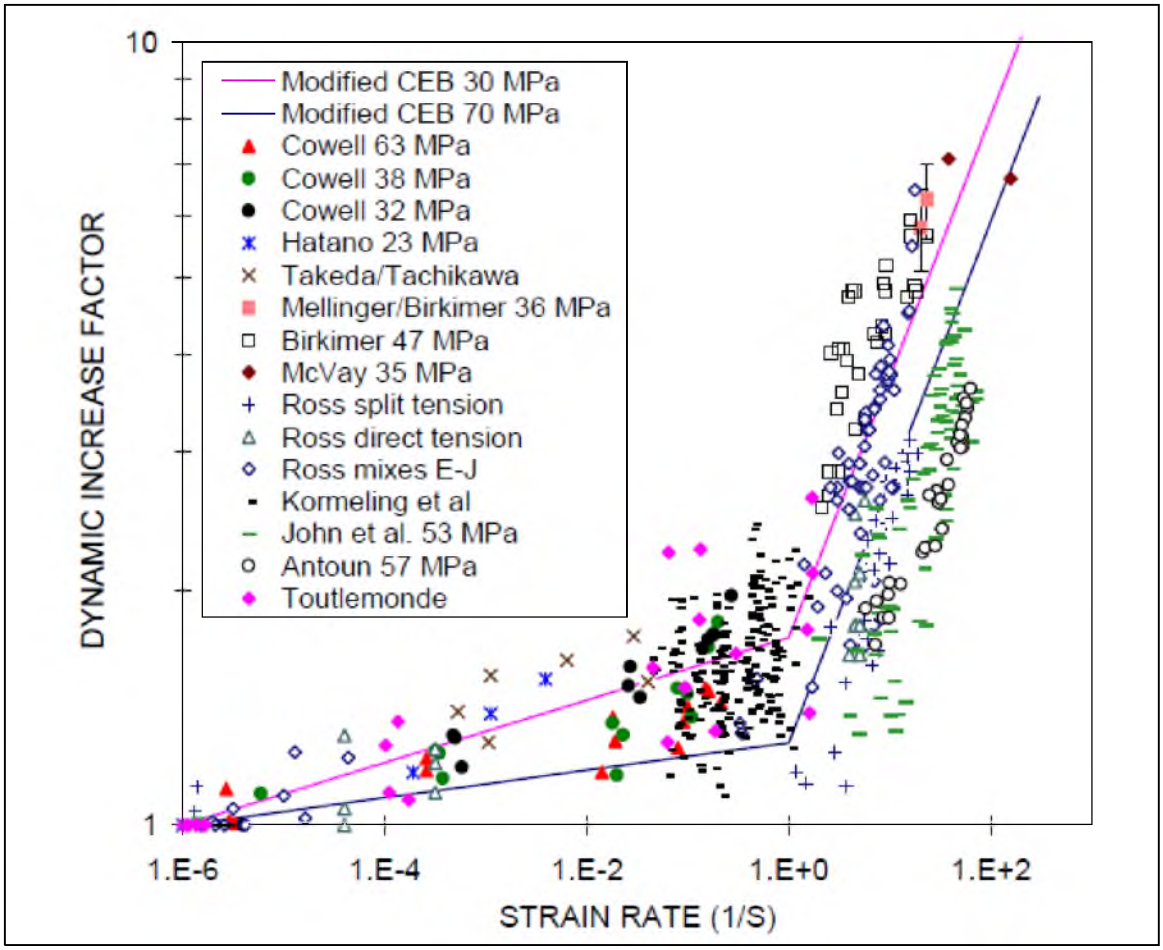

Adapted from Malvar and Ross 1998
Figure 8-2 Dynamic increase factor versus strain rate

Based on these studies, the concrete response under dynamic loading conditions resulted in a much higher capacity than under static loading conditions. The equations developed from Malvar and Ross (1998) produced a modified formulation for tensile DIF described by Equation 8.9.

$$\sigma_{dyn} / \sigma_{ts} = \left(\frac{\dot{\varepsilon}}{\dot{\varepsilon}_S}\right)^{\delta} \quad \text{for } \dot{\varepsilon} \leq 1\ s^{-1} \qquad \textit{(Equation 8.9)}$$

$$= \beta \left(\frac{\dot{\varepsilon}}{\dot{\varepsilon}_S}\right)^{1/3} \quad \text{for } \dot{\varepsilon} \geq 1\ s^{-1}$$

where

σ_{dyn} = *dynamic tensile strength at* $\dot{\varepsilon}$

σ_{ts} = *static tensile strength at* $\dot{\varepsilon}_s$

$\dot{\varepsilon}_s$ = *quasi-static strain rate,* $1x10^{-6}\ s^{-1}$

$\dot{\varepsilon}$ = *strain rate in the range of* 10^{-6} *to* $160\ s^{-1}$

$\log \beta = 6\delta - 2$

$\delta = 1/(1+8f'_c/f'_{co})$

f'_c = *static compressive strength, 30 – 70 Mpa (4350-10150 psi)*

f'_{co} = *10 Mpa (1450 psi)*

Table 8-3 shows the approximate ranges of strain rates associated with different types of loads. It can be seen that the ordinary quasi-static strain rate ranges from 10^{-6} to 10^{-5} s^{-1}, the seismic strain rate ranges from 10^{-3} to 10^{-1}, the impact strain rate ranges from 10^{0} to 10^{2}, while blast pressures yield loads associated with strain rates in the range of 10^{2} to 10^{4} s^{-1} (Ngo et al. 2007).

If the quasi-static concrete tensile strength, σ_{ts}, is 2.0 Mpa, the strain rate of the blast, $\dot{\varepsilon}$, is 10^{2} s^{-1} (Table 8-3), the corresponding DIF from Figure 8-2 (or Equation 8.9) would be approximately 4. By increasing the quasi-static concrete tensile strength four times, the dynamic tensile strength becomes 8.0 Mpa. Hence:

$$\sigma_{dyn} = 4 \times 2.0\ Mpa = 8.0\ Mpa \geq \sigma_{ppv} = 2.58\ Mpa\ (wave\ stress)$$

Therefore, the wave stress generated by the PPV of 204 mm/sec will not exceed the compressive nor the tensile strength of concrete. In fact, the maximum PPV can be as high as 630 mm/sec (24.8 in./sec) or, in terms of ground strain, 350 με for damage to occur. This result is consistent with Langefors and Kihlostrom (1973), and Oriard (1999). Similarly, Oriard and Coulsen (1980) defined a minimum PPV of 510 mm/sec (20.1 in./sec) required to crack mass concrete when blasting takes place outside the boundaries of the concrete, at a distance between 0 and 15 m

Table 8-3 Strain rates associated with the different types of loads

Load Type	Strain Rate, s^{-1}
Quasi-static	10^{-6}-10^{-4}
Earthquake	10^{-3}-10^{-1}
Impact	10^{0}-10^{2}
Blast	10^{2}-10^{4}

Adapted from Ngo, Mendis, Gupta, and Ramsay 2007

(50 ft). These specifications were included in the "Tennesse Valley Authority Vibration Specifications for Mass Concrete." (Oriard 1999). When blasting takes place within the concrete, it can be treated as manmade rock, and the required PPV to generate cracks is 9525 mm/sec (375 in./sec) to 15240 mm/sec (600 in./sec) (Oriard 1999).

For lined tunnels, Dowding (1984) suggested an incipient stress equivalent to a PPV of 1000 mm/sec (28.85 in./sec) to crack tunnel linings. Rein and Thomas (1985) suggested a threshold PPV value of 760 mm/sec (29.92 in./sec) for structural damage to develop, as discussed in "Reducing Blasting Damage by Increasing Delay Timing, " Chapter 2, section 2.1.

If this rationale were implemented in the case study, the maximum charge per delay at 50 m (150 ft.) from the shaft can be increased to 840 kg (1851 lb). This charge increase could be accomplished by having the following charge sequences:

- 840 kg (1851 lbs.) charge (1-hole per delay);
- 420 kg (926 lbs.) charge (2-holes per delay); or
- 280 kg (617 lbs.) charge (3- holes per delay).

As a result, up to two additional blastholes could be fired per delay time producing the same PPV of 630 mm/sec (24.8 in./sec) at 50 m (150 ft) from the shaft. No damage would be expected.

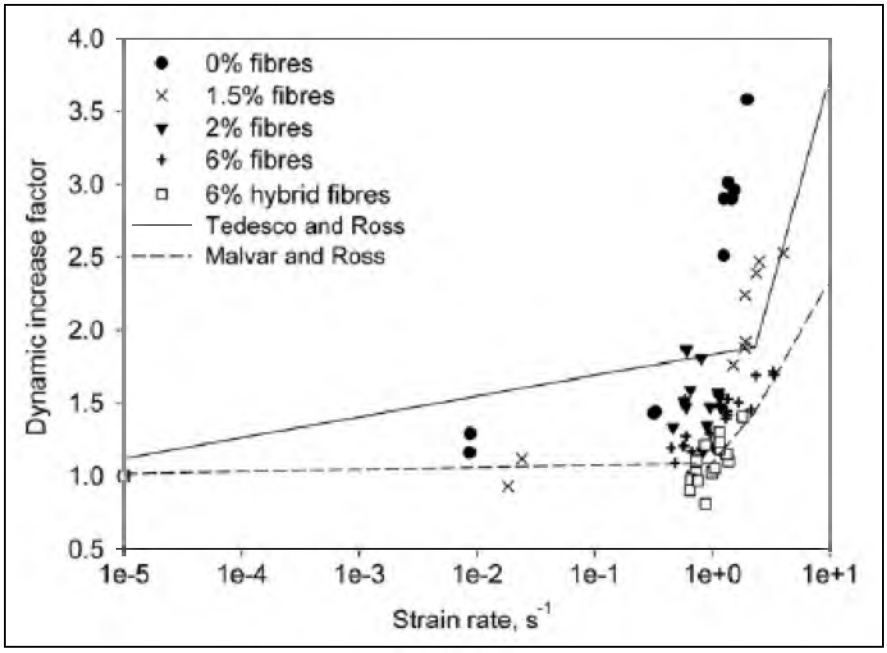

Adapted from Millard, Molyneaux, and Barnett 2010
Figure 8-3 Dynamic increase factor versus strain rate for reinforced concrete

Millar and Mollyneaux (2009) also studied dynamic properties of concrete under high strain rates. They studied two independent projects in which a drop hammer technique was used to investigate the DIF under both flexural and shear high-speed loading of new ultra high performance reinforced blast-resistant concrete. The results of both studies showed that for flexural strength, a DIF of the tensile strength rising from 1 at 1 s^{-1} on a one-third slope, on a log (strain rate) versus log (DIF), can be used for design purposes. At a strain rate of 1 s^{-1}, the DIF ratio becomes larger than 1 and can increase up to 4 (on certain cases 6), Figure 8-3. As a result, the concrete capacity under dynamic conditions increases up to about 400%. The results also showed that no DIF should be used to increase shear strength at high loading rates. These results are consistent with Malvar and Ross (1998), modified CEB (1993), John et al. (1991), and Pantelides (2013).

In conclusion, all data above the strain rate of 1 s^{-1} obtained from various tests devices and procedures show the same trend. The data collected by Malvar and Ross (1998) were obtained using two different sized, split Hopkinson pressure bars (SHPB), three different specimen sizes, six different concrete mixes, and two different types of tensile specimens.

Data collected by John et al. (1991) were obtained by independent SHPB tests. Data by Millar and Mollyneaux (2009) and Pantelides (2013) were obtained using a drop hammer technique. In all cases, very high dynamic tensile strengths were observed when compared to the quasi-static strength of concrete for strain rates above 1 s^{-1}.Therefore, an equation can be developed to estimate safe PPV levels when blasting takes place near underground concrete structures.

$$PPV = DIF^* \sigma_t / E * C_p \qquad \text{(Equation 8.10)}$$

where

$PPV_=$ peak particle velocity, mm/sec (in./sec)

C_p = p-wave propagation velocity in the rock, m/sec (ft/sec)

σ_t *= quasi-static tensile strength of concrete, Mpa (psi)*

E = Young's modulus of concrete, GPa (ksi)

DIF = dynamic increase factor from Figure 8-2 or Equation 8.9.

9. VIBRATION CONTROL TECHNIQUES

Thus far, the site-specific level of vibration is known and some idea of threshold values that could damage concrete damage can be inferred. Now the question is, “how to control vibration?”

The results indicate that knowledge of the site geology, peak particle, frequency and velocity, proximity to blast, blast charge, and overall vibration generated by the blast is essential to predict and prevent damage.

Research conducted by the U.S. Bureau of Mines indicates that some factors within the blasters control could help control vibration levels. Some suggest that increasing delay time may increase the frequency of vibration. For example, if the production blast design used in the case study is modified by increasing delay time intervals from 17 ms to 44 ms between holes and from 34 ms to 88 ms between rows, the overall dominant frequencies should increase. This was verified by modifying the blast record of seismograph 5118 using the Alpha-Blast V11 software by White Industrial Seismology, Inc. The software allows the modification of certain parameters (such as timing configuration) on an existing blast record stored in the Seismograph Data Analysis V11, and simulates the resulting PPV and frequency spectra. As a result, the original dominant frequency was increased from 5-12 Hz range to 22–23 Hz range, as illustrated in Figure 9-1. Thus, by expanding the delay times, the dominant peak frequency was increased to approximately 23 Hz. This is consistent with the discussion in “Reducing Blasting Damage by Expanding Delay Timing”, Chapter 2, section 2.1.

Some vibration control techniques currently used in the industry involve the use of initiation systems that can electronically control the release of energy in a productive and safe sequence. They time the sequence of detonation of multiple explosive charges in a blast to control breakage, rock movement, adverse noise, and flyrock.

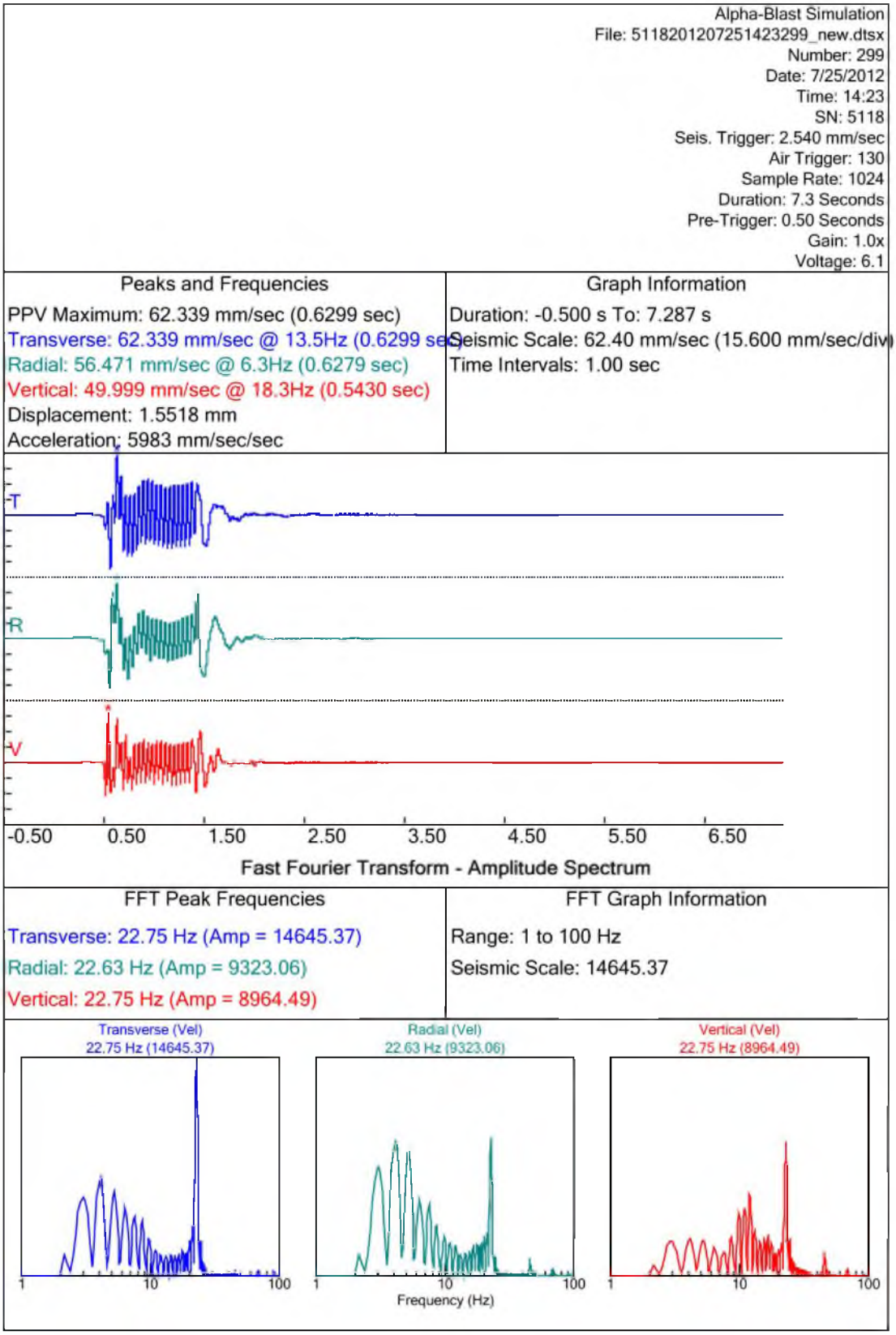

Figure 9-1 Simulation

The various systems available transmit a signal from blasthole to blasthole or from charge to charge with varying timing accuracy in short time intervals. This interval can vary from milliseconds to seconds. The use of electronic detonators facilitates this task by allowing the timing to be set very accurately at whatever range is required (ISEE 2012). Since part of the scope of this thesis is to obtain adequate levels of vibration to avoid damage to structures, the following section will define a set of techniques that may be used to accomplish such goal.

9.1 Timing

The electronic detonator is the most recent development in blasting initiation technology. One of the benefits of its use is the ability to have precise and accurate timing. Therefore, accuracy and precision are no longer a significant concern when using electronic detonators. The near absolute timing of electronic detonators has allowed significant improvements in control of fragmentation, vibration, and air blast. As shown in this research, increasing delay time will help decrease vibration level and will increase frequency of vibration. Obviously, timing will depend on the design goals of the blast. If fragmentation is the goal, one criterion could be used; if wall safety is the concern, a different approach may be implemented; and if vibration control is the goal, as in this research, expanding delay timing helps accomplish this goal. Suggestions for controlling vibrations by optimizing timing include:

- Find nominal delay times to shift the blast energy to high dominant frequencies while maintaining low PPV levels.
- Use longer row-to-row delay times to decrease levels of vibration.
- Initiating holes so that the vibration waves pass through the next hole before it is detonated to avoid constructive interference leading to excessive vibration.

10. CONCLUSIONS AND RECOMMENDATIONS

10.1 Conclusions

The results of the data analysis indicate that blasting near an underground structure would exceed the quasi-static tensile strength of the concrete shaft. However, based on the dynamic analysis of concrete under high strain rates, it is unlikely that the concrete shaft wall will fail in tension. This fact is based on the expected increased capacity under these dynamic conditions.

The data analysis suggests that vibration levels estimated on the basis of particle velocities can be decreased, and the frequency of vibration can be increased, by increasing delay intervals between blastholes, which is accomplished by:

- Finding nominal delay times to shift the blast energy to high dominant frequencies while maintaining low PPV levels.
- Using longer row-to-row delay times to decrease levels of vibration.
- To avoid constructive interference leading to excessive vibration, Initiate holes so that the vibration waves pass through the next hole before is detonated.

This approach allows reduction in vibration levels by creating phase shifts sufficient for destructive interference between vibrations. The resultant wave is not magnified by two adjacent waves and, therefore, constructive interference is avoided, and the same charge weight can be maintained.

The interaction between rock and concrete at the wall of the shaft is of particular importance, and it is imperative to conduct a site-specific ground response analysis to predict levels of vibration at a particular site. No two sites will produce the same response to ground motion.

A dynamic analysis of the structure is adequate to predict threshold level as means to estimate the allowable stress that a structure can experience both statically and dynamically.

The dynamic analysis approach presented in "Seismic Design" section of the Uniform Building Code (1997) is not applicable since the magnitude and time-history of the blast are significantly shorter than those of an earthquake and the underlying rock is considerably stronger than soil profiles S_A thru S_E. Furthermore, strain rates associated with seismic loading are much lower than of blast loading, as listed in Table 8-3. Therefore, concrete capacity enhancement under seismic loading is not expected.

10.2 Recommendations

The following criteria will help to decrease the level of vibration from blasting in mine operations:

- Implement a rigorous and extensive monitoring program of the production blasting and signature holes with single-charge detonations at the mine site. This is the basis for a balanced blast design and understanding of existing site conditions.
- Use Equation 8.10 to estimate PPV based on material properties. If lowering the PPV is needed, increase delay time between blastholes using electronic detonators and use at least 44 ms between holes and 88 ms between rows as described in Chapter 9. This timing design will produce a PPV approximately equal to 600 mm/sec (24 in./sec) and a frequency level of 23 Hz for this particular site.
- Based on the site-specific attenuation equation obtained in this study, the blast of 270 kg (596 lb) should be fired no closer than 50 m (165 ft).
- It is recommended to verify high strain rates associated with blasting by conducting in-mine testing or other empirical methods.

APPENDIX A

VIBRATION ANALYSIS

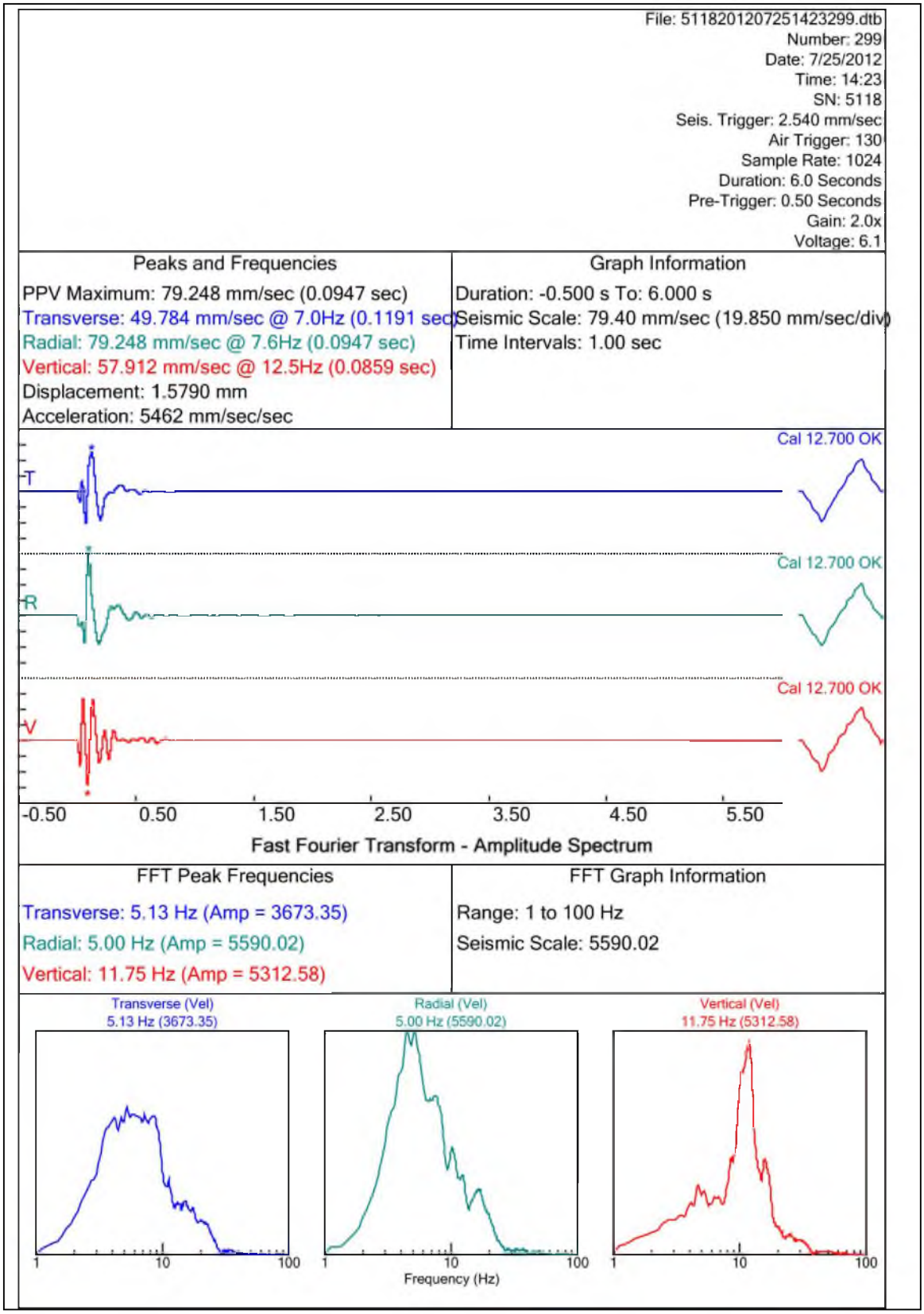

Figure A.1 Seismograph 5118 data

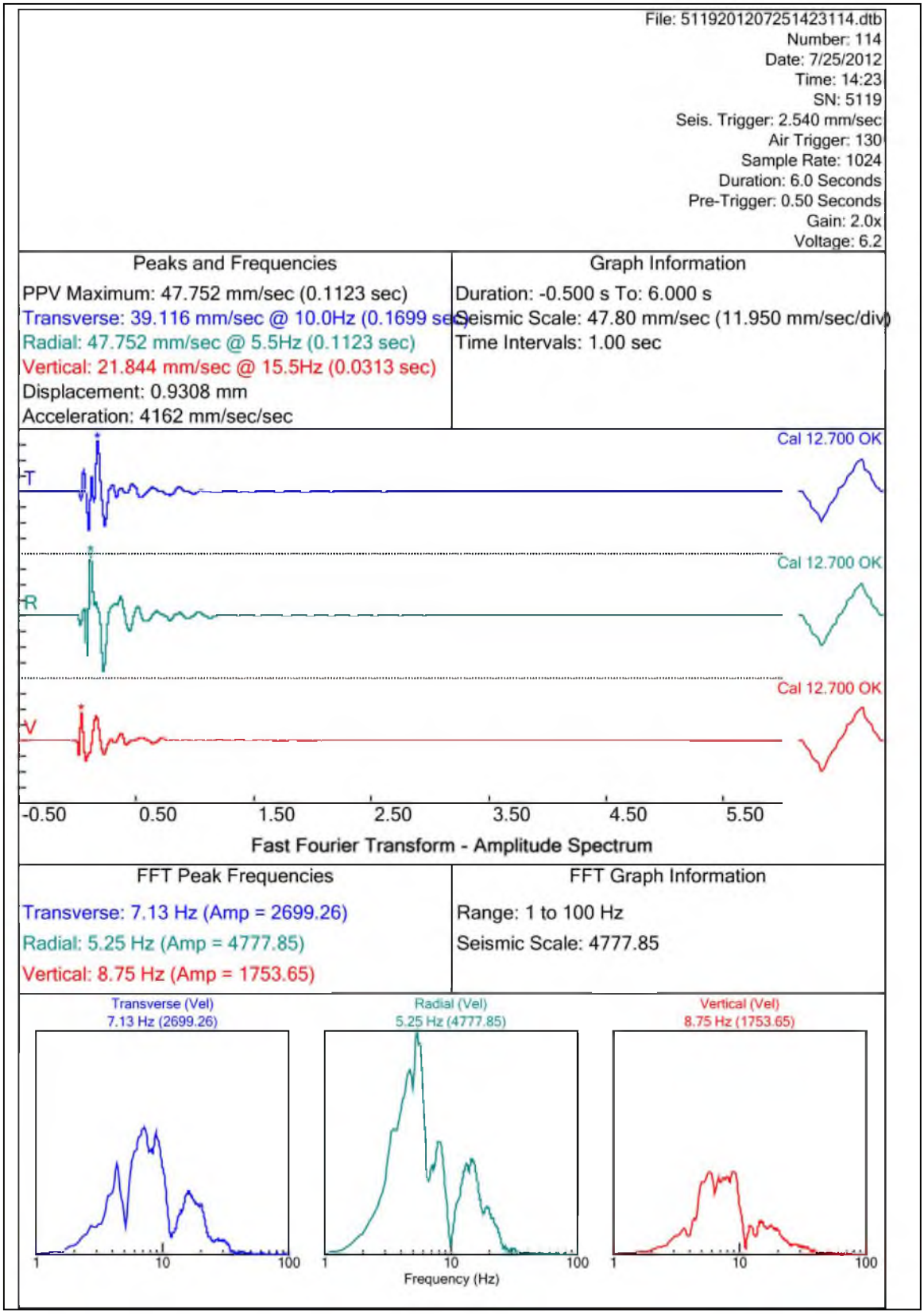

Figure A.2 Seimograph 5119 data

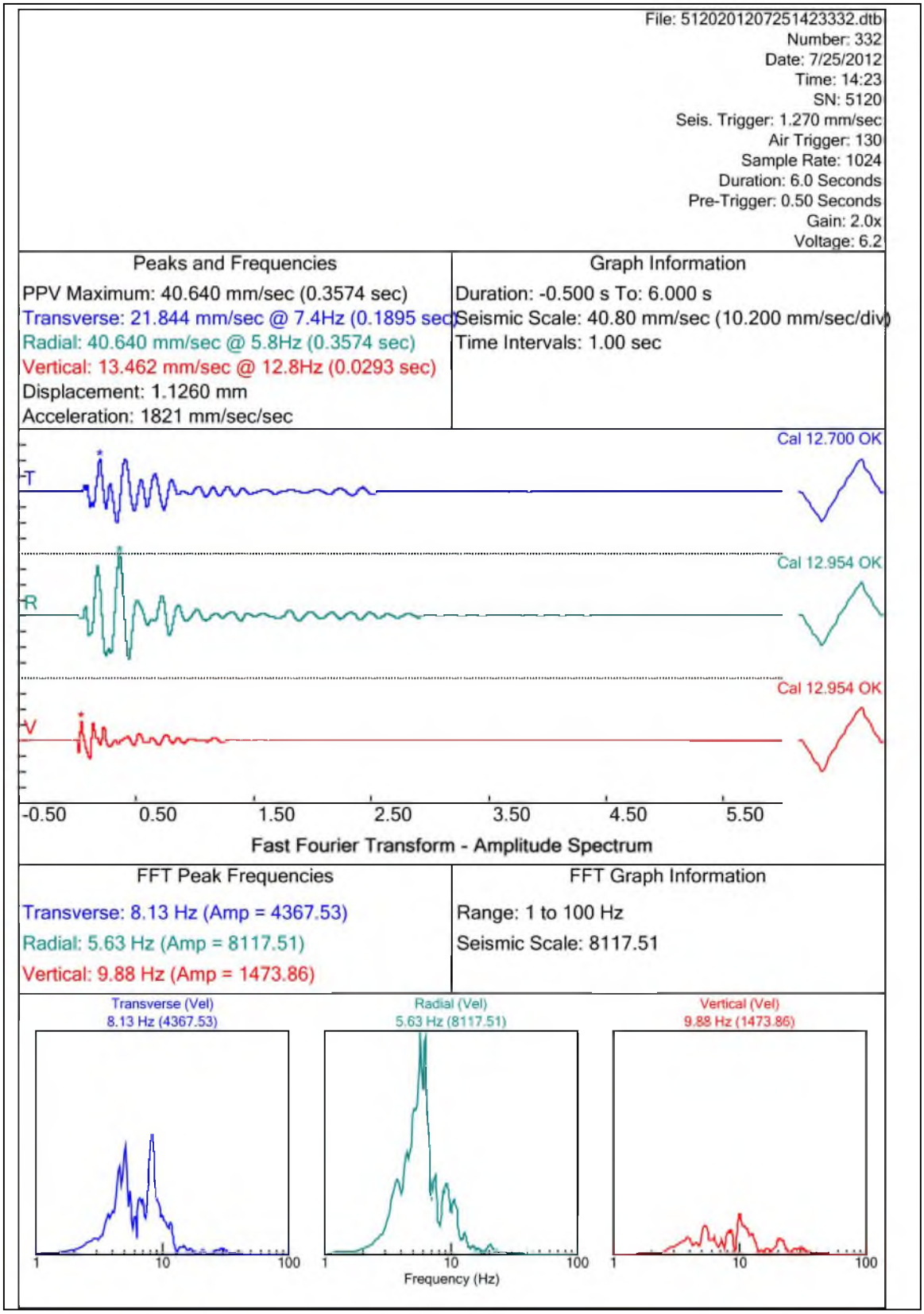

Figure A.3 Seismograph 5120 data

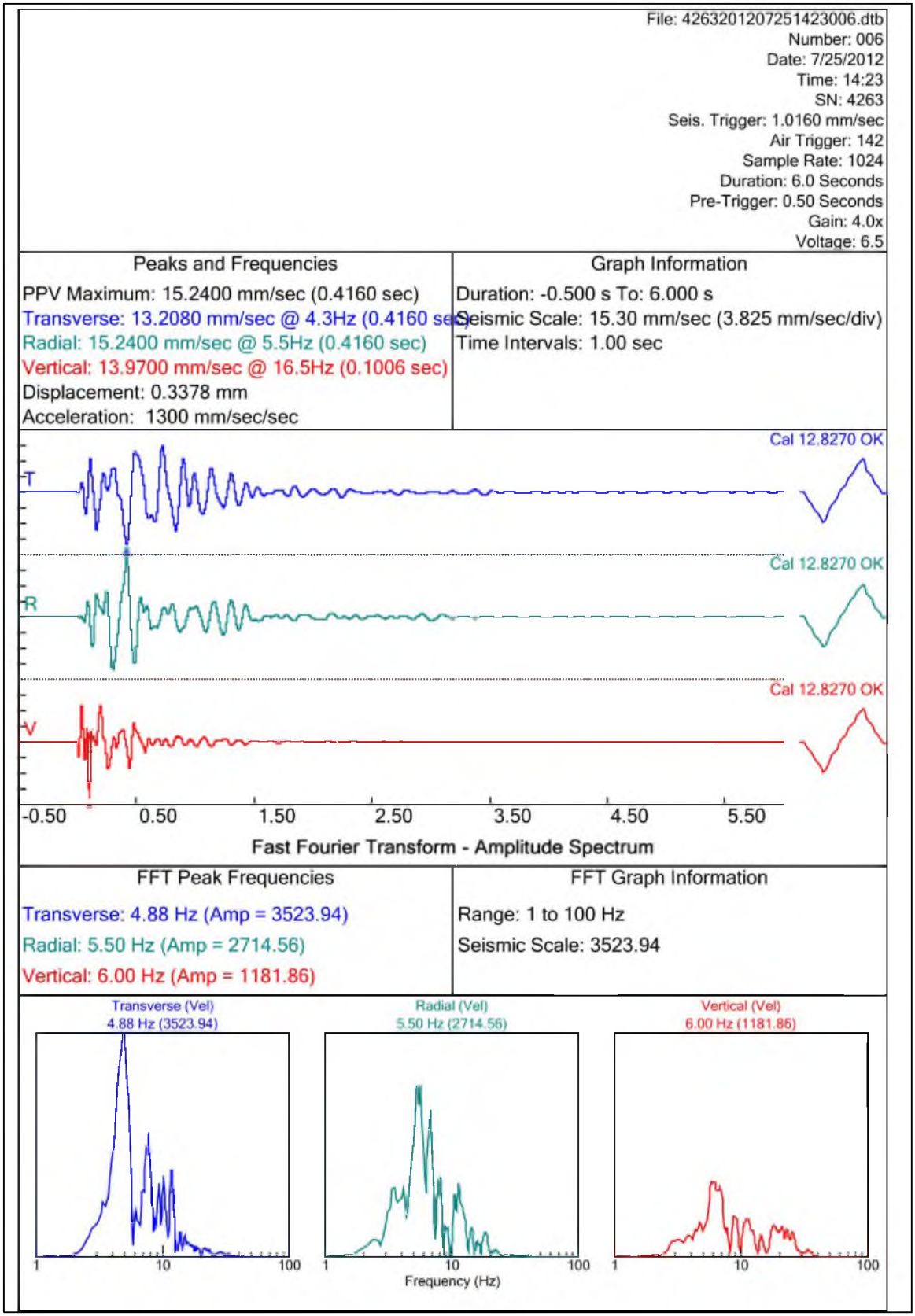

Figure A.4 Seismograph 4263 data

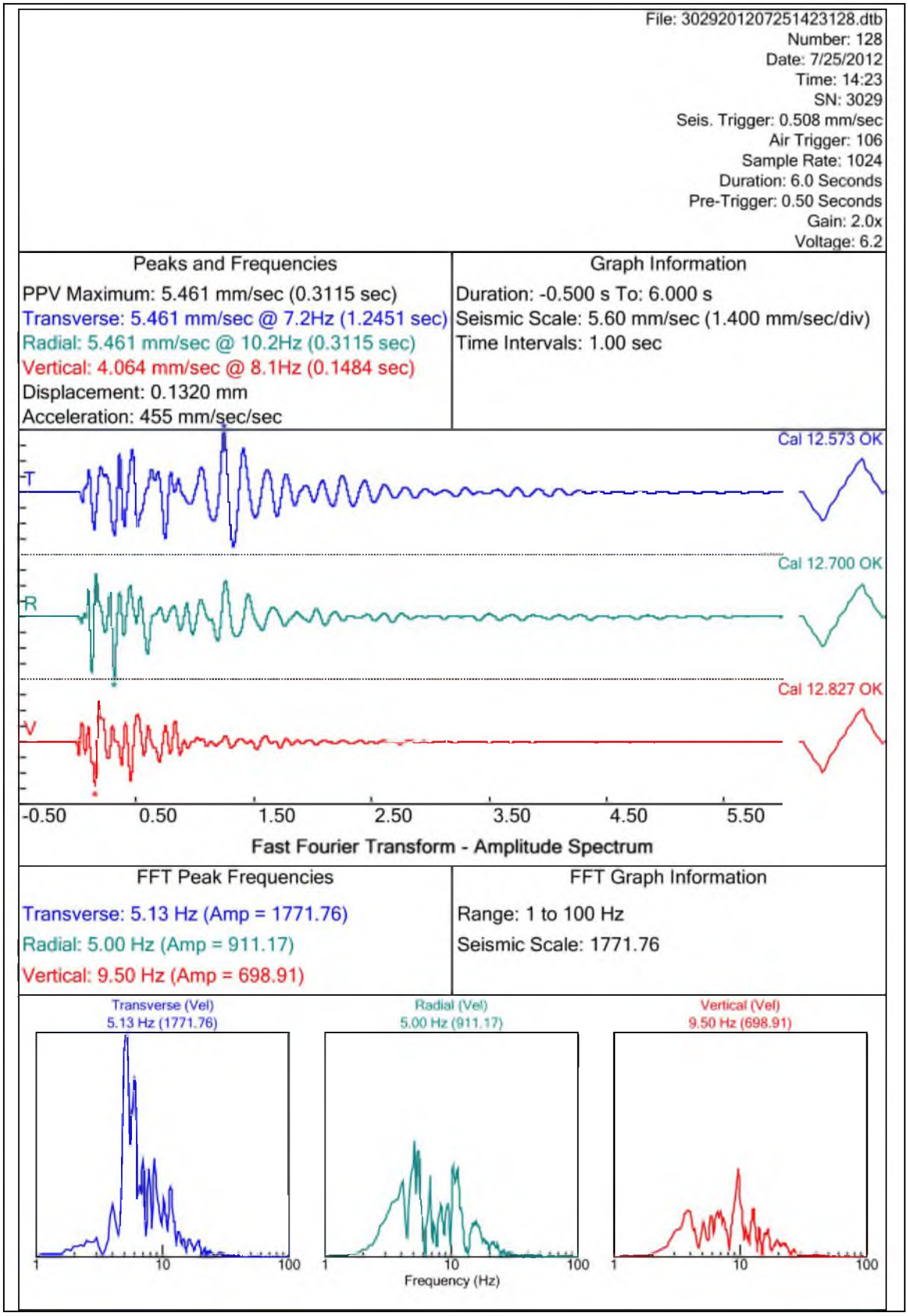

Figure A.5 Seismograph 3029 data

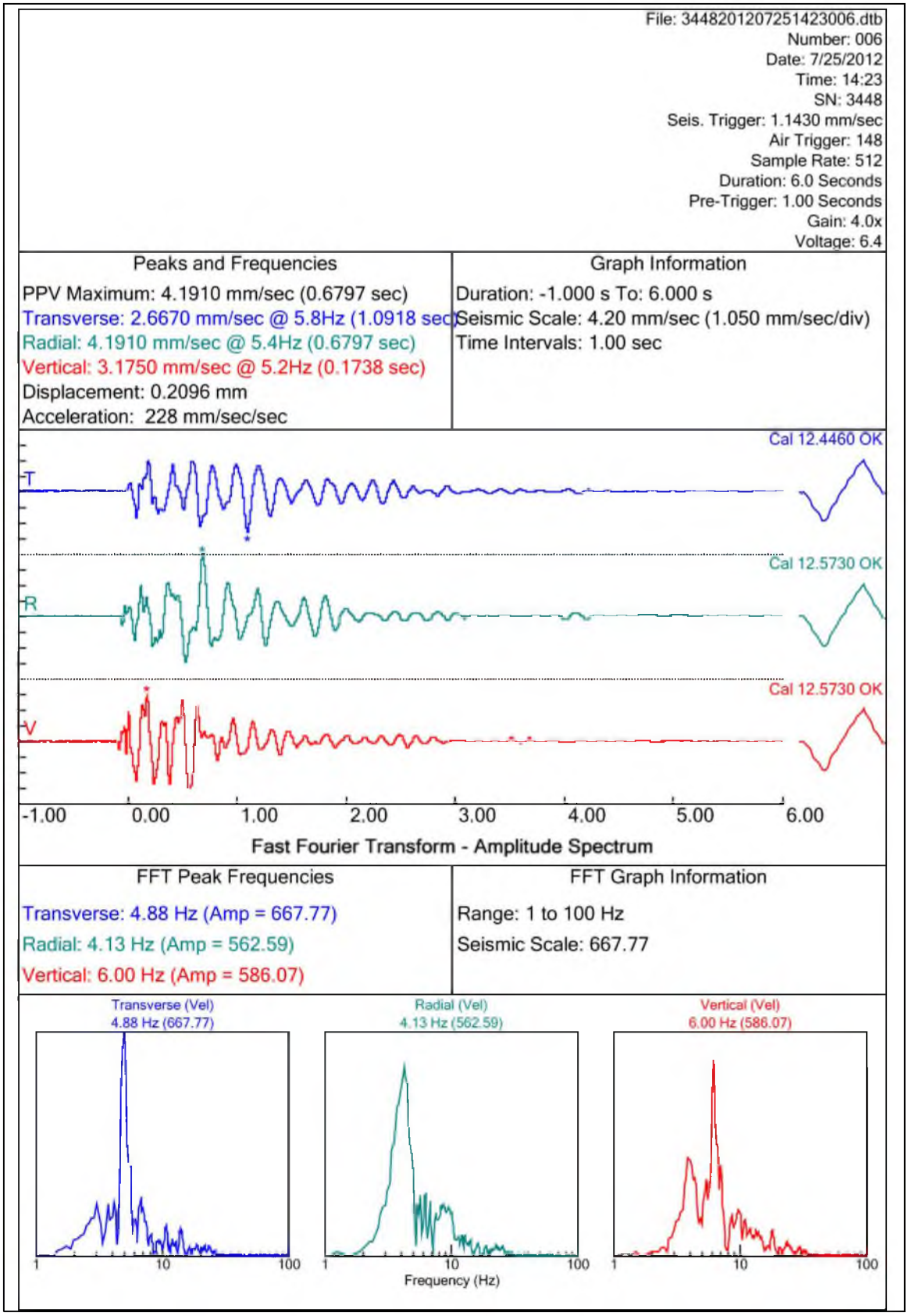

Figure A.6 Seismograph 3448 data

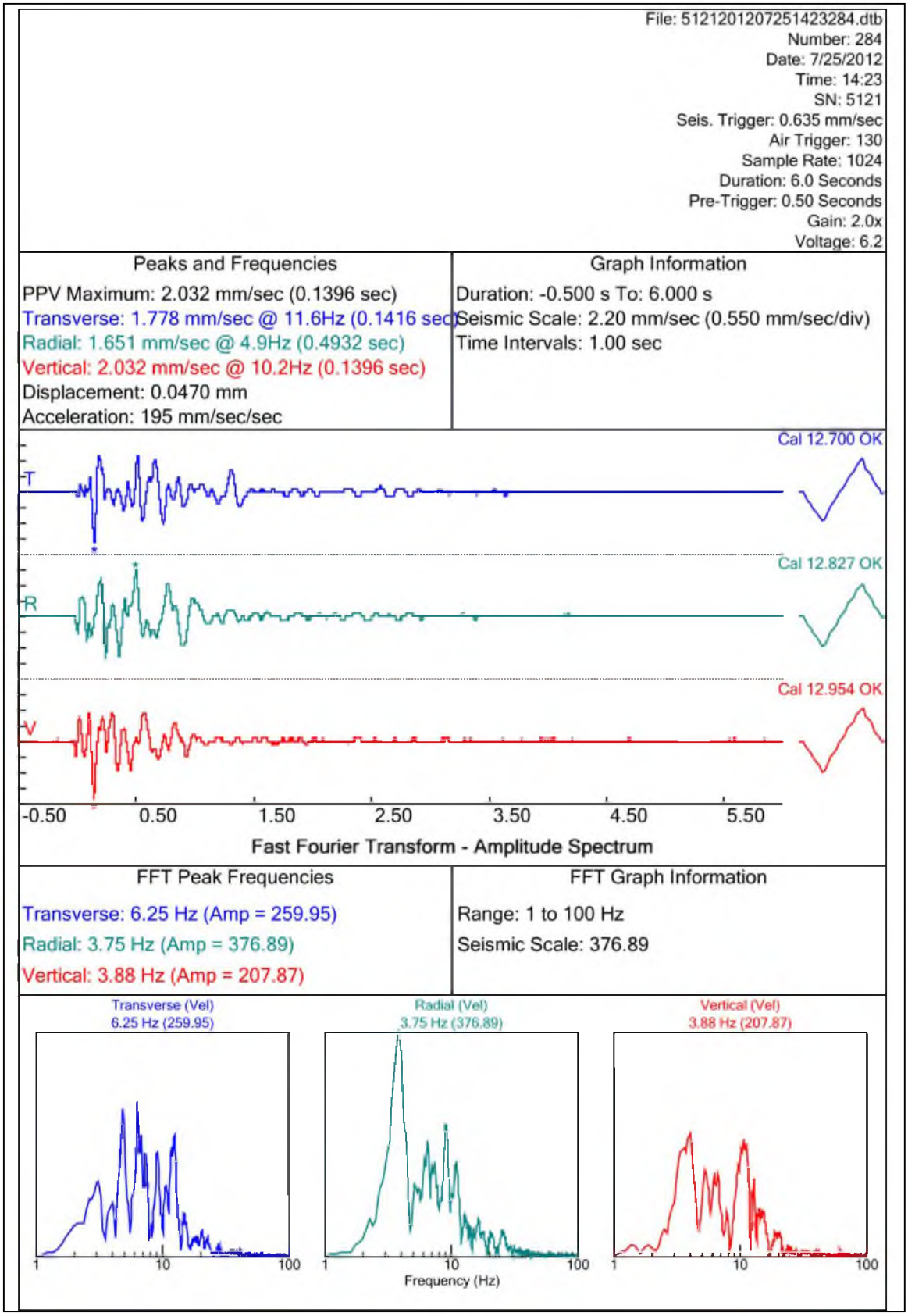

Figure A.7 Seismograph 5121 data

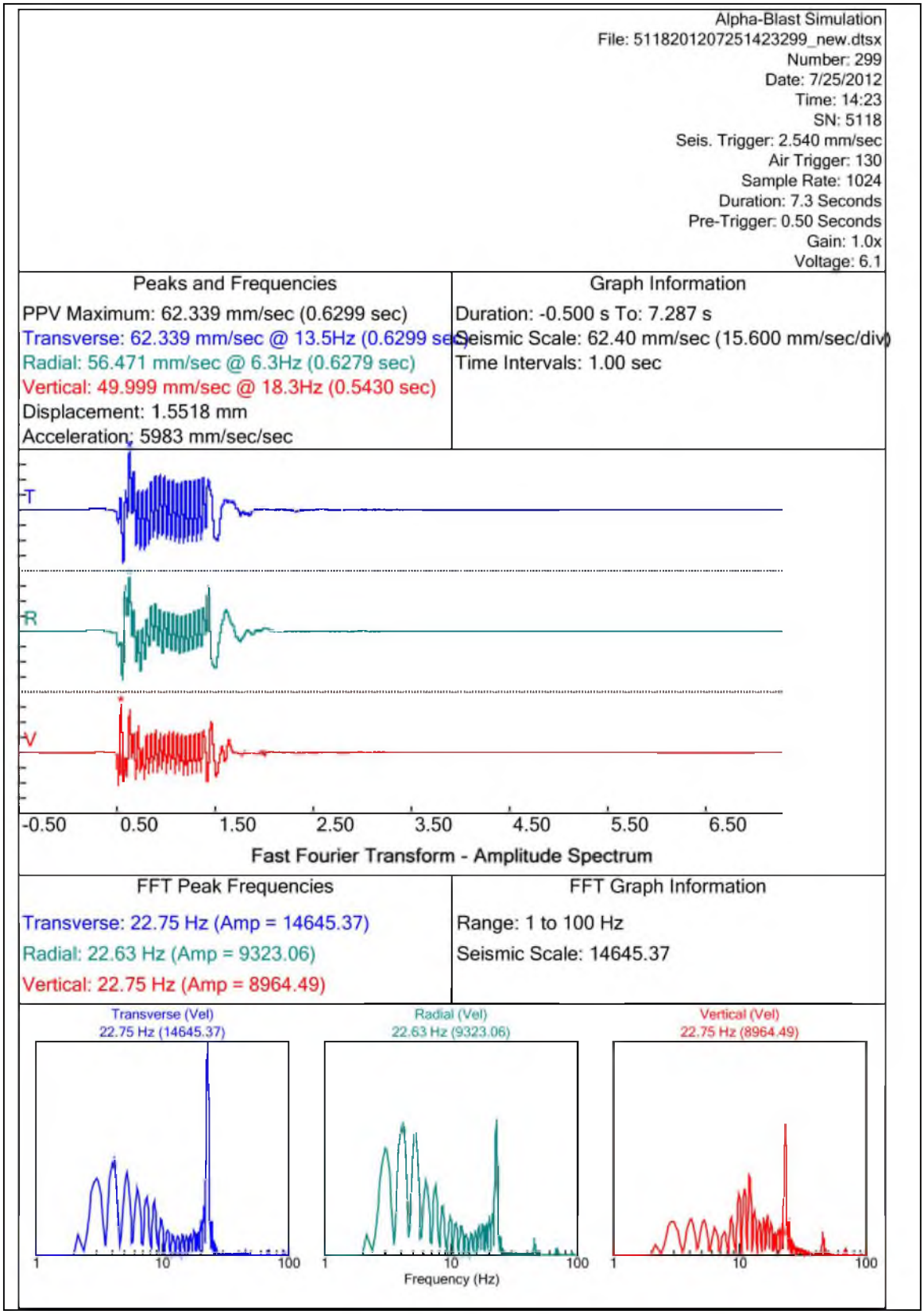

Figure A.8 Simulation data

APPENDIX B

PRODUCTION BLAST

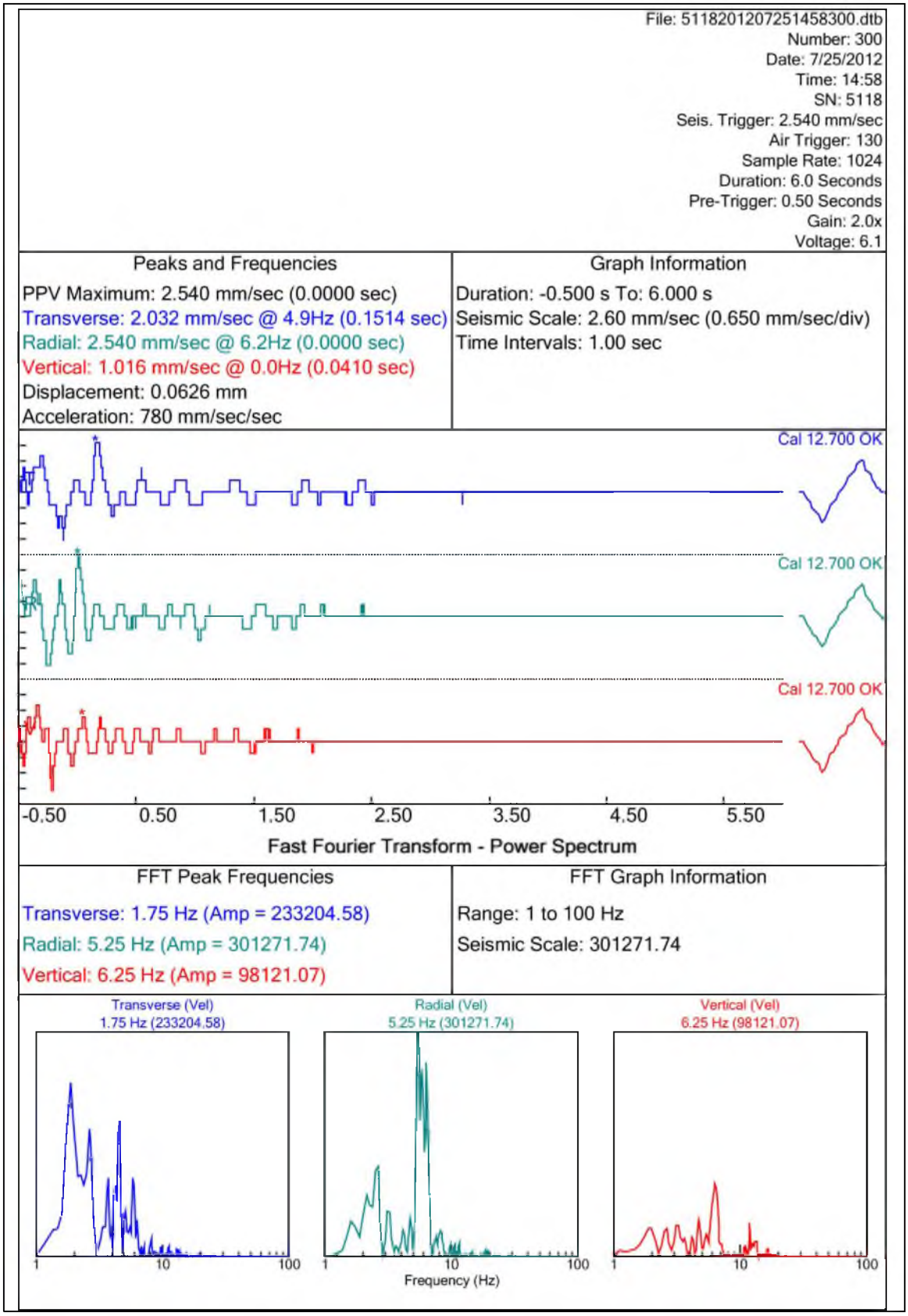

Figure B.1 Seismograph 5118 Prod blast

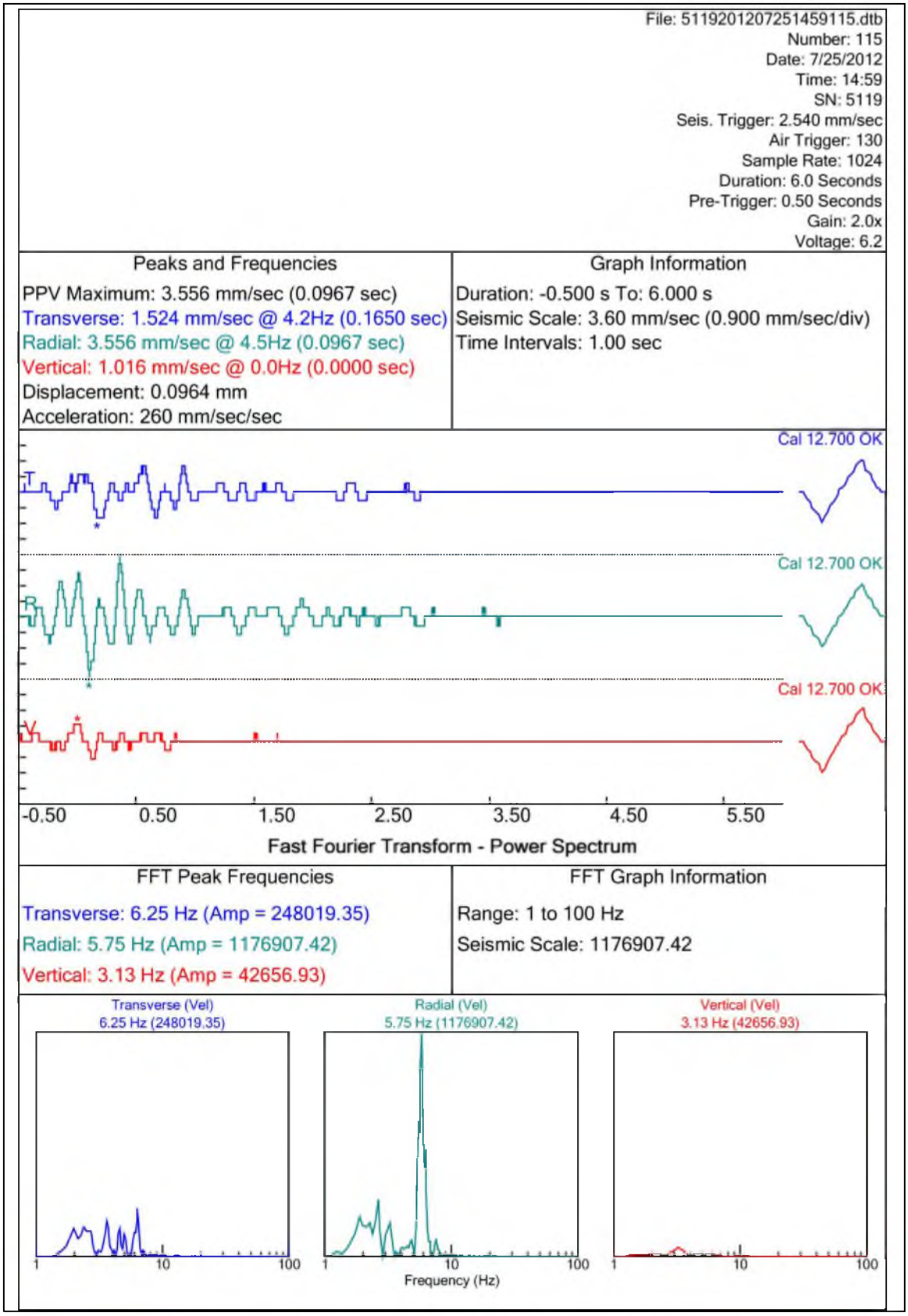

Figure B.2 Seismograph 5119 Prod blast

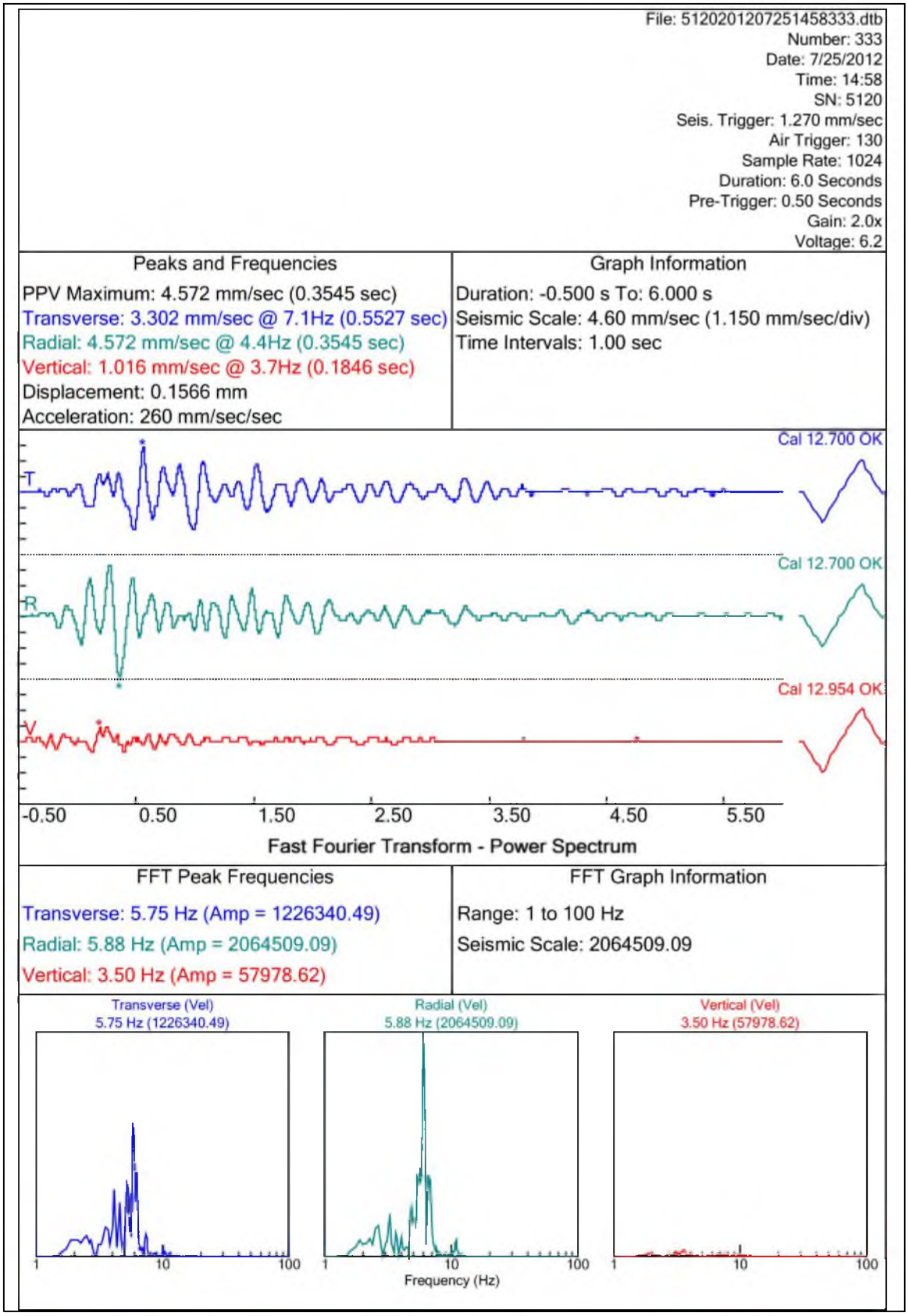

Figure B.3 Seismograph 5120 Prod blast

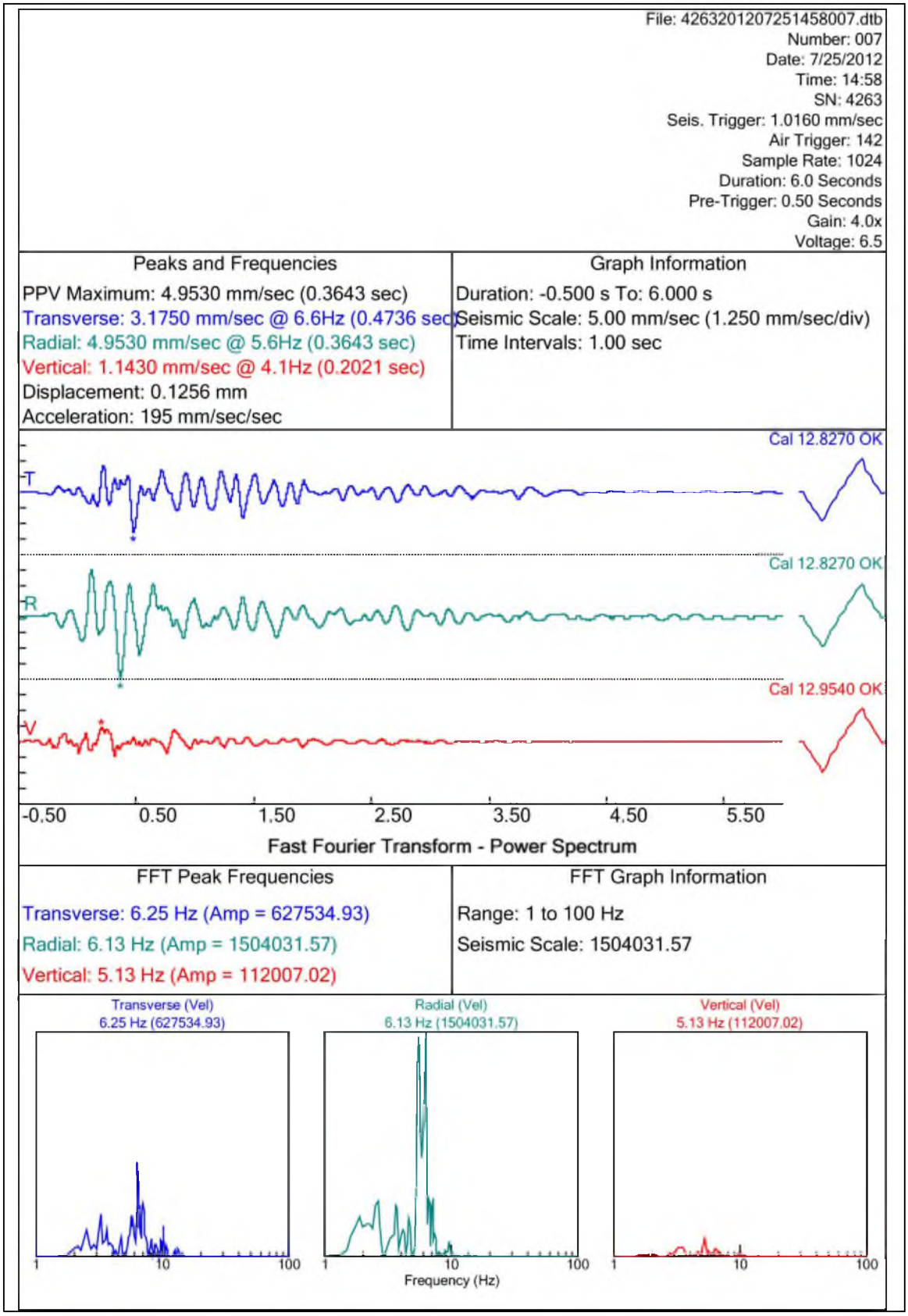

Figure B.4 Seismograph 4263 Prod blast

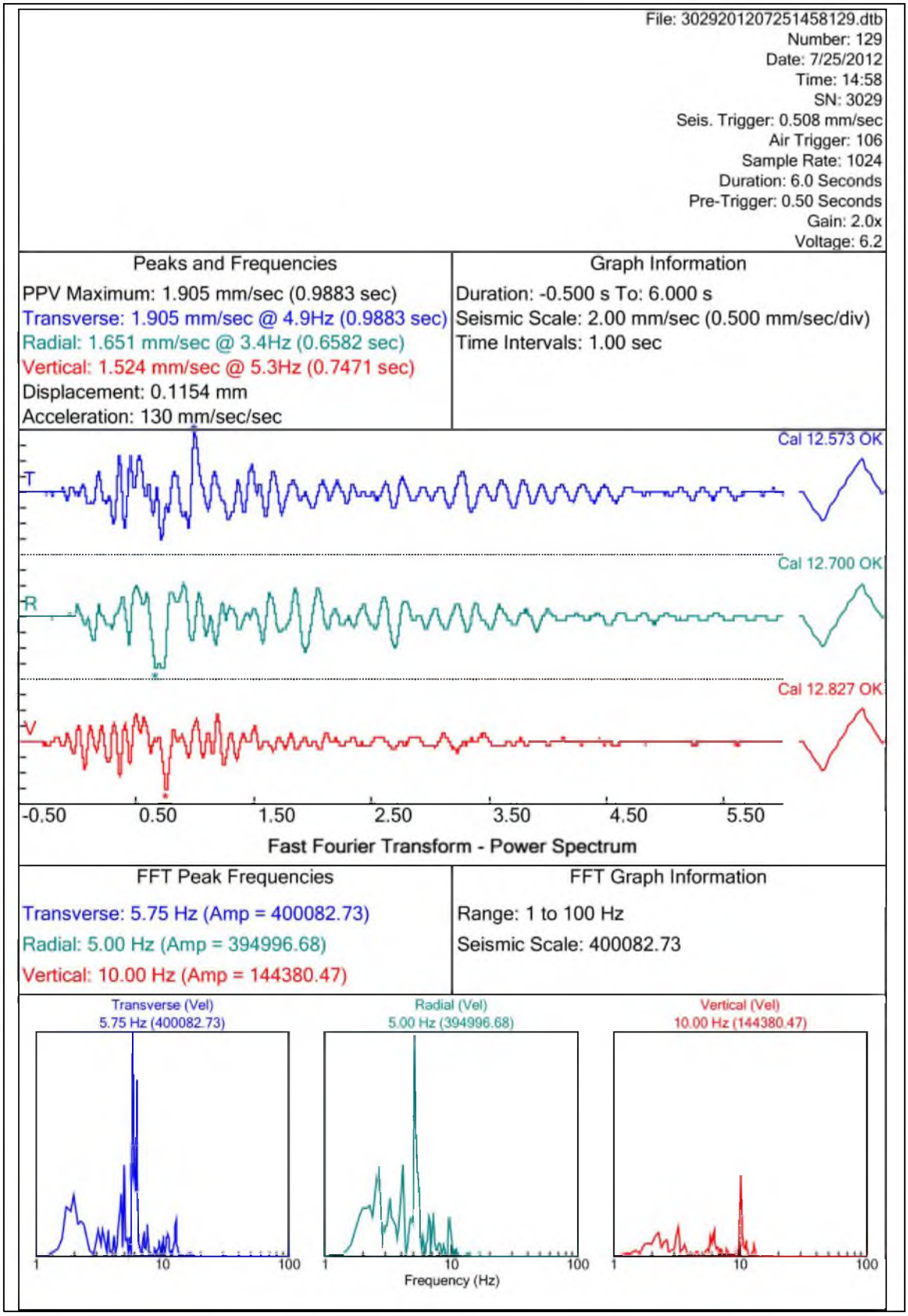

Figure B.5 Seismograph 3029 Prod blast

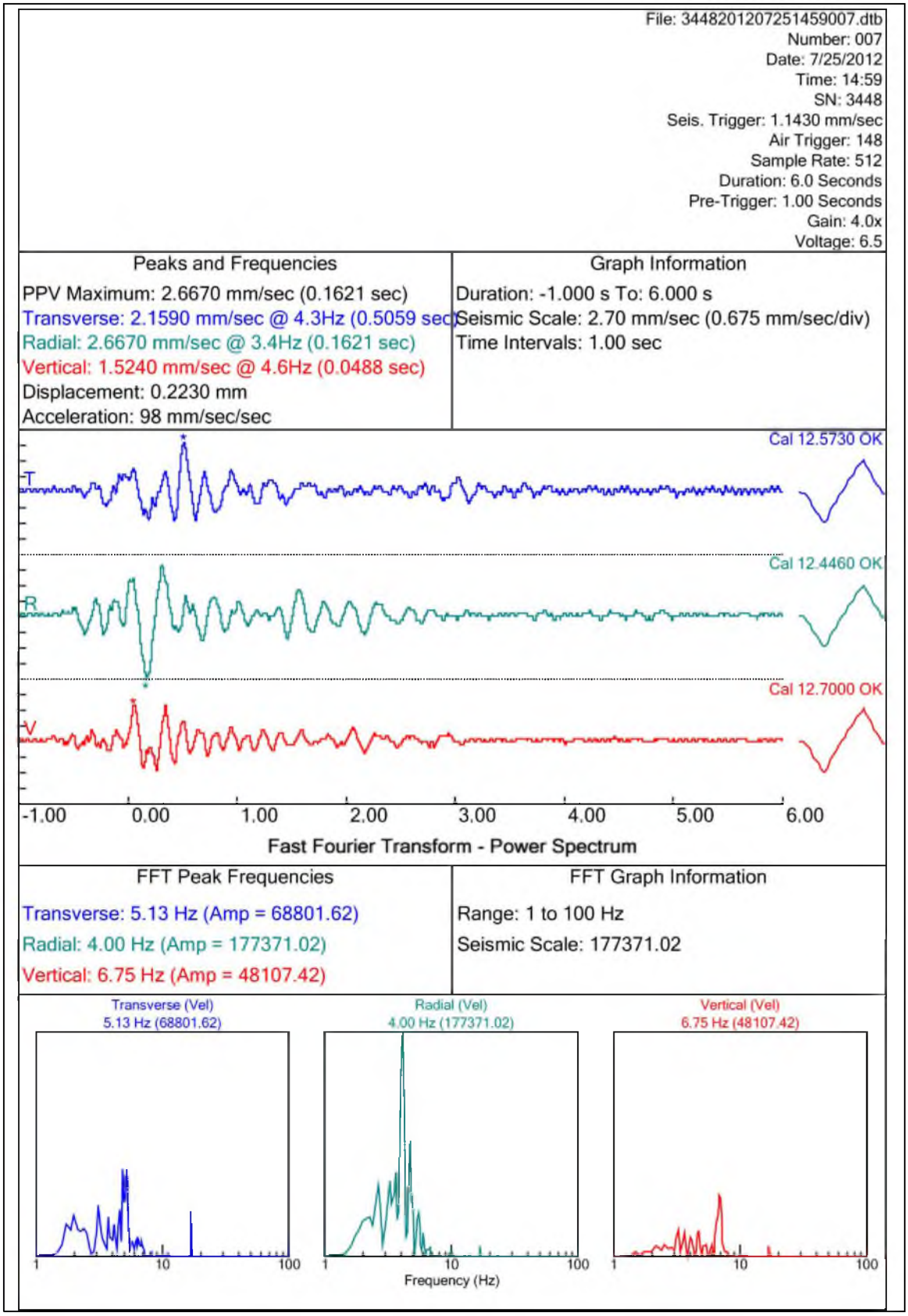

Figure B.6 Seismograph 3448 Prod blast

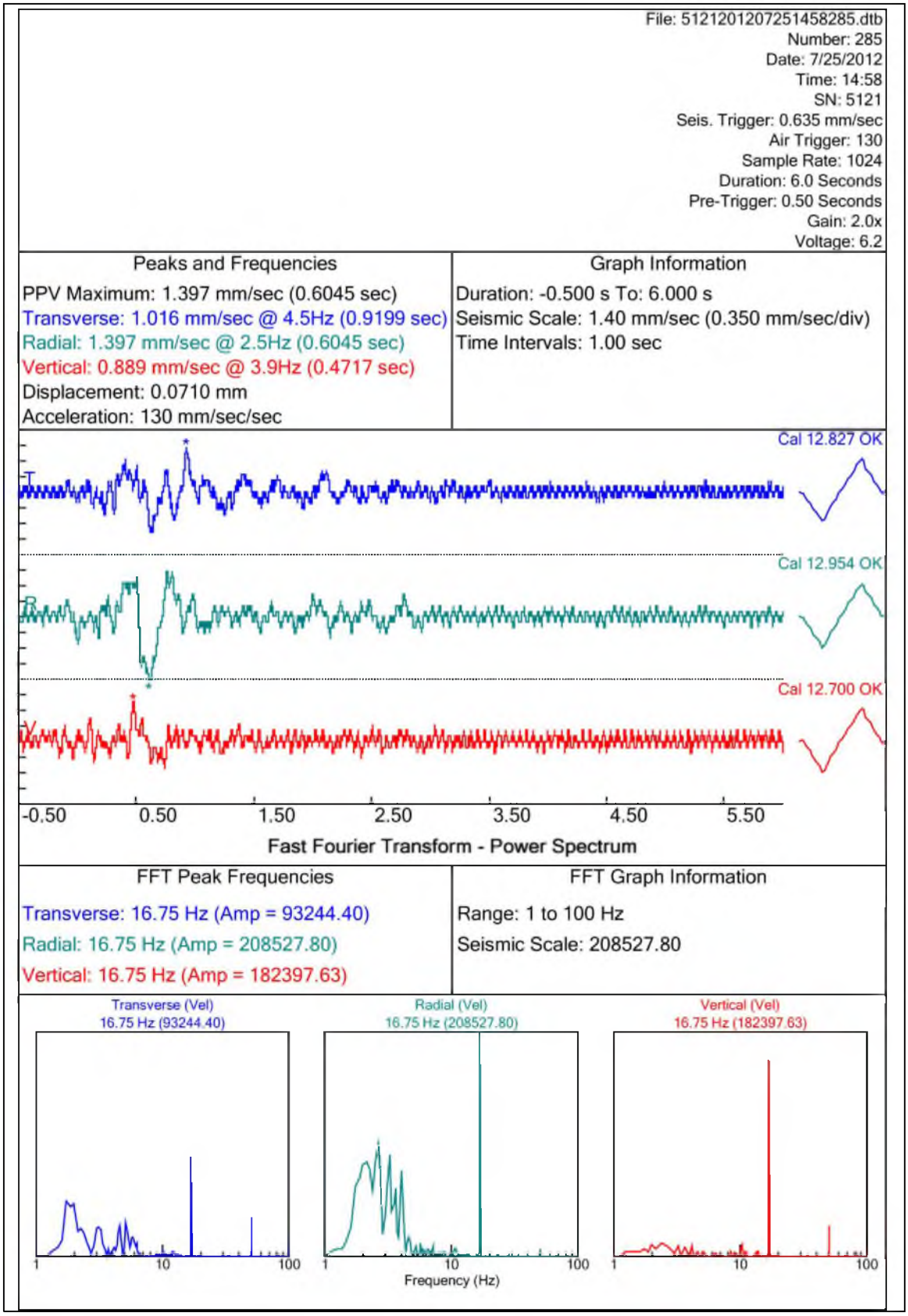

Figure B.7 Seismograph 5121 Prod blast

REFERENCES

ACI 318-08. 2008. *Building Code Requirements for Structural Concrete and Commentary.* American Concrete Institute. Farmington Hills, MI. Available from www.aci.org

ASTM C 496. 1996 *Standard Test Method for Splitting Tensile Strength of Cylindrical Concrete Specimens.* ASTM International. West Conshohocken, PA. Available from www.astm.org.

Avey, L. 1990. *Pre-split techniques and Practices at Gold fields Operating Co. Chimney Creek Mine*, *Proceedings Conference on Explosives and Blasting Technique, pp167-174*. '90 Society of Explosives Engineers, Orlando, FL.

Calder, P., and Larocque, G. 1977. *Perimeter Blasting,* Pit Slope Manual. Center for Mineral and Energy Technology. Ottawa, Canada.

Comite Euro-International du Beton. 1993. *CEB-FIP Model Code 1990*. Redwood Books.Trowbridge, Wiltshire.UK.

Defense Special Weapons Agency. 1997. *DAHS CWE Manual for the Design and Analysis of Hardened Structures under Conventional Weapon Effects*. DSWA. Volume I-II. Los Angeles, CA.

Dowding, C. H. 1984. *Estimating Earthquake Damage from Explosion Testing of Full-Scale Tunnels*. Adv Tunnel Technology and Subsurface Use. Pergamon Press, Ltd. UK. 4(2): pp113—114.

Dowding, C. H. 2008. *A Micrometer Crack Response*. Cleveland, OH. International Society of Explosive Engineers.

Hardy, H.R. 1972. *Acoustic Emission/Micro Seismic Activity. Principle, Techniques and Geotechnical Applications. Volume I and II.* University of Pennsylvania. Balkema Publishers. Tokyo, Japan.

Hiner, S.T. 2002. *Seismic Design Review Workbook for the California Civil Professional Engineer Examination.* http://home.pacbell.net/hiner Accessed in March 2002.

Hoek, E., and Bray, J.W. 1981. *Rock Slope Engineering*. Rev. 3rd Edition. Institution of

Mining and Metallurgy. London.

Humar, J.M., and Mahgoub, M.A. 2003. *Determination of Seismic Design Forces by Equivalent Static Load Method*. Canadian Journal of Civil Engineering. 30: 287–307.

ISEE. 2009. Blaster's Handbook. 17th Edition. International Society of Explosive Engineers, inc. Cleveland , OH.

ISEE. 2012. Blasters' Handbook. 18th Edition. International Society of Explosive Engineers, Inc. Cleveland, OH.

John, R., Antoun, T., and Rajendran, A.M. 1991. *Effect of Strain Rate and Size on Tensile Strength of Concrete.* Proceedings APS Topical Conference on Shock Compression of Condensed Matter. Elsevier Science Publishers. Williamsburg, VA

Konya, C.J. 1990. *Blast Design*. Montville, OH: Intercontinental Development Corp.

Langefors, U., and Kihlostrom, B. 1973. *The Modern Technique of Rock Blasting.* Wiley and Sons.
New York, NY.

Malvar, L.J., and Ross, C.A.1998. *Review of Strain Rate Effects for Concrete in Tension*. ACI Materials Journal, 95(6), 735-739.

McKenzie, C.K. 1999. *A review of the Influence of Gas Pressure on Block Stability during Rock Blasting*, AusIMM Expo '99 Conference, November, Kalgoorlie.

Millard, S.G., and Molyneaux, T.C.K. and Barnett, S.J. 2010, *Dynamic Enhancement of Blast resistant Ultra High Performance Fiber-reinforce Concrete under Flexural and Shear Loading.* International Journal of Impact Engineering, 37, 405-413.

Moore, A.J., and Richards, A.B. 2007. *Effects of Blasting on Infrastructure.* EXPLO Conference Wollongong, NSW.

Nagae, T., and Hayashi, S. 2004. *Seismic Response of Soft-First Story Buildings Supported byYielding Foundations.* 13th World Conference on Earthquake Engineering. Vancouver, B.C. Canada. Paper No. 3465.

Ngo, T., Mendis, P., Gupta, A., and Ramsay, J. 2007. *Blast Loading Effects on Structures.* University of Melbourne. EJSE. Melbourne, AU.

Oriard, L.L. 1999. *The Effects of Vibrations and Environmental Forces.* International Society of Explosives Engineers, Inc. Cleveland, OH.

Oriard, L.L., and Coulson, J.H. 1980. *TVA Criteria for Mass Concrete.* Proceeding of Conference American Society of Civil Engineers. Portland , OR.

Pantelides, C. (2013). University of Utah. Unpublished Work.

Raftoyiannis, I., Tassos, A., and Michaltsos, G. 2011. *A New Approach for Loads Moving on Infinite Beams Resting on Elastic Foundation.* Journal of Vibration Control. Sage http://jvc.sagepub.com/content/18/12/1828. Accessed in November 18, 2011.

Rein, R.D., Thomas, T.J. 1985. *Reducing Damage by Expanding Delay Timing.* Society of Mining Engineers, Caller No. D, Littleton, CO.

Siskind, D.E., Stagg, M.E., Kopp,J.W. and Dowding, C.H. 1980. *Structure Response and Damage Produced by Ground Vibration from Surface Mine Blasting.* U.S. Bureau of mines Report of Investigations 8507.

Shamsabadi, A., Sedarat, H., and Kozak, A. 1996. *Seismic Soil-Tunnel-Structure Interaction Analysis and Retrofit of the Posey-Webster Street Tunnels*. International Civil Engineering Consultants, Inc. Prepared for Caltrans, Contract No. 59X797.

Staatciouglu, M., and Humar, J. 2002. *Dynamic Analysis of Buildings for Earthquake-Resistant Design.* NRC Research Press Website, http://cice.nrc.ca. Accessed in November 2012.

ICBO. 1997. *The Uniform Building Code.* International Conference of Building Officials. Whittier, CA. Volume II.

ICBO 1997. *Recommended Lateral Force Requirements and Commentary.* International Conference of Building Officials. Whittier, CA.

Williams, A. 2003.*Seismic Design of Buildings and Bridges for Civil and Structural Engineers.* International Conference of Building Officials. Oxford University Pres, Inc. New York , NY.

Wolf, J.P. 1985. *Dynamic Soil-Structure Interaction*. N. Prentice Hall, Inc. Englewood Cliffs, CO.

Zhang, Y., and Toksoz, N. 2012. *Computation of Dynamic Seismic Responses to Viscous Fluid Of Digitized Three-Dimensional Berea Sandstones with a Couple Finite-Difference Method.* Acoustical Society of America. http://dx.doi.org/10.1121/1.47333545. Accessed in December 2012.